Author:
Bodart, Julien

Title:
Using gravimetry and meteorological data to assess the influence of El Nino-Southern Oscillation on Antarctica's mass balance

Using gravimetry and meteorological data to assess the influence of El Niño-Southern Oscillation on Antarctica's mass balance

Author: Julien Bodart

A dissertation submitted to the University of Bristol in accordance with the requirements for award of the degree of Master by Research - Section Glaciology - in the Faculty of Science.

School of Geographical Sciences - Bristol Glaciology Centre

Academic Years 2016-2018

Word count: 22,012

How to cite:

BODART, J. (2018). Using gravimetry and meteorological data to assess the influence of El Niño-Southern Oscillation on Antarctica's mass balance. *MScR Thesis*, *University of Bristol. September 2018.*

Author's declaration:

I declare that the work in this dissertation was carried out in accordance with the requirements of the University's *Regulations and Code of Practice for Research Degree Programmes* and that it has not been submitted for any other academic award. Except where indicated by specific reference in the text, the work is the candidate's own work. Work done in collaboration with, or with the assistance of, others, is indicated as such. Any views expressed in the dissertation are those of the author.

Usage Policy:

Signature:

Mr. Julien Bodart

Abstract

Given that the Antarctic Ice Sheet (AIS) has the potential to raise sea level by many tens of metres, it is crucial that we fully understand the factors controlling its mass balance and stability. Presently, much of the mass loss from the west AIS is being offset by accumulation over the East, such that the net AIS contribution to global mean sea level rise is not as great as it would otherwise be. This compensation is, however, sensitive to changing oceanic and atmospheric conditions including ocean warming, shifting winds and precipitation patterns. Previous research has shown that interannual variations in atmospheric conditions associated with El Niño-Southern Oscillation can alter surface-pressure distribution and moisture transport over Antarctica, potentially inducing mass balance changes over the ice sheet. This study makes use of the GRACE Mascons in combination with a range of auxiliary datasets, including atmospheric pressure, precipitation, sea surface temperature, and sea-ice, to investigate the relationship between El Niño and Antarctica's surface mass balance. In particular, the mass balance signature and associated response of the ice sheet to the very strong 2015 El Niño are elucidated and set within the context of the historical record. Our results show that the 2015 El Niño resulted in opposite response to the long-term secular trend of the ice sheet, with an increase (decrease) in the West (East). Strong similarities in atmospheric conditions were found between very strong events, mainly the 1997-98 and 2015-16, but little similarity was found with other previous events. We show that the Antarctic Peninsula and West Antarctica are particularly sensitive regions to El Niño variability, as well as Dronning Maud Land and Wilkes Land (East Antarctica). Overall, this study provides the first estimate of Antarctica's surface mass balance following an extreme El Niño event using gravimetry and contributes to our understanding of Antarctica's mass changes on interannual timescales.

Acknowledgements

I would like to acknowledge Rory Bingham for providing the guidelines for this research and for assisting in the programming part of this study. I would also like to thank the Alumni Foundation of the University of Bristol for providing funding to present my research at the International Glaciology Society (Lancaster, UK) and at the International Geodesy Society (Bonn, Germany) meetings in September 2017.

I would also like to acknowledge the numerous people in the Geography Postgraduate Office (Browns) for their continuous moral support and for making the office such a great and entertaining environment. More specifically, I would like to thank PhD student Jeison Sosa Moreno (University of Bristol) for his assistance in helping me overcome the many programming challenges I faced, and PhD student Laurence Hawker (University of Bristol) for proofreading this work.

Table of Contents

List of Figures

List of Tables

List of Supplementary Figures

List of Supplementary Tables

List of Acronyms

ABS: Amundsen and Bellingshausen Sea

ABSL: Amundsen and Bellingshausen Sea Low

ADP: Antarctic Dipole

AIS: Antarctic Ice Sheet

APIS: Antarctic Peninsula Ice Sheet

CAIS: Central Antarctic Ice Sheet

DOT: Delayed Oscillation Theory

EAIS: East Antarctic Ice Sheet

ECMWF: European Centre for Medium-Range Weather Forecasts

ENSO: El Niño-Southern Oscillation

EWT: Equivalent Water Thickness

GIA: Glacial Isostatic Adjustment

GRACE: Gravity Recovery and Climate Experiment

GRACE-FO: Gravity Recovery and Climate Experiment Follow-on

Gt: Gigatons

hPa: Hectopascals

ITCZ: Inter Tropical Convergence Zone

JPL: Jet Propulsion Laboratory

MSLP: Mean Sea Level Pressure

NOAA: National Oceanic and Atmospheric Administration

NOV15: November 2015

SAM: Southern Annual Mode

SAT: Surface Air Temperature

SIE: Sea Ice Extent

SMB: Surface Mass Balance

SOI: Southern Oscillation Index

SST: Sea Surface Temperature

TP: Total Precipitation

WAIS: West Antarctic Ice Sheet

WWE: Westerly Wind Event

1. Introduction

1.1. Background

The recent decrease in mass from glaciers and ice sheets has been one of the dominant drivers of global mean sea level rise since the mid-twentieth Century (Rignot and Kanagaratnam, 2006; Meier et al., 2007). Given that the two major ice sheets of Greenland and Antarctica have the potential to raise sea level by ~ 70 metres if completely melted (Church and Gregory, 2001; Alley et al., 2005), it is crucial that we fully understand the factors controlling their mass balance and stability. In this context, previous studies have focused on assessing Antarctica's mass balance and sea level rise contribution in the light of decadal changes in climatic conditions (Chen et al., 2009; Velicogna, 2009; King et al., 2012; Rignot et al., 2008; Shepherd et al., 2012; Sasgen et al., 2013). One of the most recent estimate of Antarctica's ice-mass discharge into the oceans shows a continent-wide mass loss of 69 ± 18 Gt/yr^{-1} (gigatons per year) between 2002 and 2010, the equivalent of +0.19 ± 0.05 mm/yr^{-1} of sea level contribution (King et al., 2012).

One of the remaining limitations when assessing the mass balance of the Antarctic Ice Sheet is that a considerable amount of research has focused on investigating changes on seasonal, annual, and multi-decadal timescales. However, less attention has been directed towards interannual changes in atmospheric conditions in relation to external tropical forcing, despite their potential to induce mass changes over the ice sheet (Boening et al., 2012). Whilst decadal changes in Antarctica's mass balance are dominated by ice-dynamical processes such as ice sheet thinning and changes in flow dynamics, short-term changes on interannual timescales have been shown to be dominated by changing atmospheric conditions (Boening et al., 2012; Lenaerts et al., 2012).

Previous research has shown that one factor affecting Antarctica's mass distribution on interannual timescales is known as El Niño-Southern Oscillation (ENSO), an irregularly periodic change in atmosphere-ocean interactions in the tropical Pacific Ocean (Welhouse et al., 2016;

Walker and Gardner, 2017). However, the complex set of teleconnections that exist between the Pacific and the Southern Hemisphere on interannual timescales have resulted in uncertainties regarding Antarctica's mass balance and sea level contribution. In this context, this study investigates the effect of El Niño-Southern Oscillation on the Antarctic Ice Sheet by taking advantage that, for the first time, we can combine satellite gravimetry with atmospheric datasets to assess the occurrence of a very strong El Niño event on the ice sheet.

Accumulation and mass loss rates are not uniform across the ice sheet and can vary on temporal and spatial scales. Indeed, presently much of the mass loss from West Antarctica is being offset by accumulation over the East, such that the net Antarctic Ice Sheet contribution to global sea level rise is not as great as it would otherwise be (Shepherd and Wingham, 2007; Hanna et al., 2013). It is therefore essential to apply a multi-level approach when assessing mass changes over Antarctica, particularly when considering that the effects of El Niño can be highly heterogeneous across the ice sheet (Gloersen, 1995; Welhouse et al., 2016, Paolo et al., 2018).

Efforts to estimate the net balance between mass loss and mass gain of glaciers and ice sheets have yet to reach a consensus (Shepherd and Wingham, 2007; Velicogna, 2009; Zwally and Giovinetto, 2011). However, quantifying the mass budget of the Antarctic Ice Sheet, represented by the sum of surface mass balance (primarily through snow deposition) and ice dynamics (i.e. changes in ice flow and ice-shelf collapse) is essential to our understanding of the past, present and future behaviour of the ice sheet and its contribution to global sea level rise (Boening et al., 2012). This research focuses on the surface mass balance aspect of the ice sheet's mass budget in relation to interannual variability. In other words, we assess how much mass is gained or lost on the surface of the ice sheet following ENSO events without considering ice-dynamical processes. This is achieved by comparing regional mass changes from GRACE Mascons with Surface Mass Balance estimates from cumulative precipitation rates to develop an understanding of the effects of these extreme events on the ice sheet. The results for the recent 2015-16 El Niño are then compared with historical records of atmospheric and ocean datasets following other ENSO events to assess the overall influence of El Niño on the Antarctic Ice Sheet.

1.2. Aims and Objectives

The overarching goal of this project is to quantify the impact of El Niño on the Antarctic Ice Sheet and surrounding ocean conditions using a suite of gravitational, meteorological, sea surface temperature and sea-ice analysis. For this, four research questions will be addressed:

1. How are atmospheric and ocean conditions around Antarctica affected by El Niño events?

2. Where and by how much do El Niño events impact Antarctica's Surface Mass Balance?

3. Are such changes proportional to the strength of El Niño and is the response symmetric or asymmetric with respect to the El Niño cycle?

4. How is sea-ice affected by El Niño and can ENSO events act as proxy for previous and future estimates of sea ice behaviour?

The main objectives of this research project are to:

1. Assess interannual mass changes by comparing the GRACE RL05M Mascon solutions (Jet Propulsion Laboratory) to Surface Mass Balance estimates from cumulative precipitation rates (ERA-Interim reanalysis products);

2. Relate interannual fluctuations in mass to changes in Mean Sea Level Pressure and Total Precipitation using ERA reanalysis products from the European Centre for Medium-Range Weather Forecast (ECMWF);

3. Assess interannual changes in ocean conditions using observational datasets of Sea Surface Temperature and Sea Ice Extent from the National Oceanic and Atmospheric Administration's (NOAA) Optimum Interpolation Sea Surface Temperature (OISST) V2;

4. Relate the above changes in atmospheric and ocean conditions to El Niño events using NOAA's Niño 3.4 index and identify whether the high latitude response is instantaneous or delayed to the onset of El Niño in the Pacific using lag analysis;

1.3. Thesis Outline

The second chapter of this thesis reviews the current literature that accounts for Antarctica's sea level contribution, justifying the scope of this study in terms of uncertainties over realistic mass balance and sea level rise estimates. A thorough review of the dynamics involved in the development of El Niño in the Pacific and its influence on global weather patterns is provided, along with a discussion of the complex set of teleconnections that enable the signal to reach the Southern Ocean. Lastly, this chapter investigate the effects of ENSO on the Antarctic Ice Sheet from an atmospheric and ocean perspective.

The third chapter of this thesis describes the datasets and methods used in this research. A particular focus is put on the newly-released GRACE Mascons and the key differences between this post-processing method and the more traditional spherical harmonics method. A description of the methods used to quantify mass changes for each sub-region and drainage basin is provided. Secondly, this chapter describes the post-processing methods used to obtain Surface Mass Balance estimates from the reanalysis precipitation fields, which are used here for comparison with the GRACE Mascons. Lastly, this chapter provides an account of the atmospheric and ocean indices used, along with the methods employed to process them.

The first part of Chapter 4 presents the results of the mass changes observed by GRACE following the 2015-16 El Niño event at a continental, regional and basin-scale level, and subsequently compares those to Surface Mass Balance estimates of cumulative precipitation rates. The results for the mass changes are then compared with atmospheric (Mean Sea Level Pressure and Total Precipitation) anomaly maps for the period 2015-16 to assess how the changes in atmospheric conditions related to the observed mass balance changes post-El Niño. The Surface Mass Balance time series for the 2015-16 El Niño are then compared with the other very strong El Niño event of 1997-98 to assess whether a typical ENSO-like signature is observed over the ice sheet following these two very strong events. Lastly, the anomaly maps for the most recent El Niño are compared with atmospheric conditions following previous events to detect whether an overall ENSO pattern can be observed over the ice sheet.

The second part of Chapter 4 reviews ocean conditions following the 2015-16 El Niño and compares those with ocean conditions following previous El Niño events to detect potential similarities in the response of Sea Surface Temperature and Sea Ice Extent to ENSO conditions.

The fifth chapter of this thesis discusses the results by linking the findings from this research to previous studies on the effect of El Niño on Antarctica. More specifically, this chapter discusses the differences between the mass changes observed by GRACE and the Surface Mass Balance time series and argues that the future availability of gravimetry data will be key in our understanding of the effect of future El Niño events on the ice sheet. This chapter also discusses the difference between the changes observed following the most recent El Niño and previous ENSO events and reflects on the results for the atmospheric and ocean datasets.

The final chapter of this thesis provides an overall summary of the key findings and offers suggestions for future studies that seek to improve further our understanding of El Niño's influence on the Antarctic Ice Sheet.

2. Literature Review

One of the most crucial challenges of our times lie in the threat that sea level rise poses to communities around the world. The effects of sea level rise on the environment and people have been widely discussed, amongst those are threats relating to the flooding of coastal habitats where both human population and fauna and flora have established (Nicholls and Cazenave, 2010), and risks to terrestrial and marine ecosystems (Harvell et al., 2002). In the light of these challenges, it has become increasingly important to monitor how much sea level rises and identify its primary contributors to improve our understanding of past, present and future sea level fluctuations.

Estimates of global mean sea level obtained from analysis of satellite altimetry and tide gauges show an increase of approximately 1.7 mm/yr^{-1} for the 20th century (Church and White, 2006; Holgate, 2007; Church and White, 2011), and it is predicted that sea level will increase by 0.5 to 1.4 metres above the 1990 level by 2100 (Rahmstorf, 2007). One of the main contributors to the global rise in sea level has been the input of meltwater from glaciers and ice sheets around the world (Rignot and Kanagaratnam, 2006; Bindoff et al., 2007; Meier et al., 2007). While most of the 20th Century sea level rise contribution from total land ice (glaciers and ice sheets) has been dominated by glaciers and ice caps outside of the two main ice sheets (Greenland and Antarctica), the vulnerability of the Antarctic Ice Sheet to changing ocean and atmospheric conditions represents one of the main concern for future sea level rise (Meier et al., 2007; Gardner et al., 2013; Deconto and Pollard, 2016). Rignot et al. (2011) showed that the acceleration in ice sheet loss over the Greenland and Antarctic Ice Sheet between 1992 and 2009 was 21.9 ± 1 Gt/yr^2 and 14.5 ± 2 Gt/yr^2 respectively, or a combined total of 36.3 ± 2 Gt/yr^2. This represents three times as much mass loss as the contribution from mountain glaciers and ice caps (12 ± 6 Gt/yr^2) (Rignot et al., 2011).

In this context, the major focus of past studies has been placed on understanding how Antarctica has changed on decadal timescales and how these changes impacted sea level rise (Zwally et al., 2005; Chen et al., 2009; King et al., 2012; Rignot et al., 2008; Sasgen et al., 2013;

Shepherd et al., 2012; Velicogna, 2009). One of the most recent estimate of Antarctica's ice-mass discharge into the oceans shows a continent-wide mass loss of 69 ± 18 Gt/yr^{-1}, equivalent to +0.19 ± 0.05 mm/yr^{-1} of sea level contribution between 2002 and 2010 (King et al., 2012). However, strong disparities exist between studies, with present-day estimates of Antarctica's ice-mass discharge ranging between 31 Gt/yr^{-1} (Zwally and Giovinetto, 2011) and 246 Gt/yr^{-1} (Velicogna, 2009).

Shepherd and Wingham (2007) showed that the large gap in the range of values for eustatic sea level estimates is larger than the estimated uncertainty range and associated this to the difference in methods and satellite instruments used. As a result, a more realistic estimate of mass balance and sea level contribution of the major ice sheets was provided by Shepherd et al. (2012) using a combination of satellite data; including altimetry, interferometry, and gravimetry data. This study allowed for a reconciliation of mass balance estimates by combining all available methods and reducing the disparities that exist between the various studies. Their results showed that between 1992 and 2011 the ice sheets of the Antarctic Peninsula, West Antarctica, and East Antarctica have changed in mass by -20 ± 14 Gt/yr^{-1}, -65 ± 26 Gt/yr^{-1}, and +14 ± 43 Gt/yr^{-1} respectively. These combined with a mass loss of -142 ± 49 Gt/yr^{-1} for the Greenland Ice Sheet represent an average increase in sea level rise of 0.59 ± 0.20 Gt/yr^{-1} since 1992. However, whilst this study provided a much more realistic estimate of eustatic sea level change in relation to mass changes on Greenland and Antarctica, there remains uncertainties regarding mass changes at regional level and the influence of interannual events on the ice sheet.

As shown by Shepherd and Wingham (2007) and Shepherd et al. (2012), much of the mass loss from West Antarctica is being offset by accumulation over the East, such that the net Antarctic Ice Sheet contribution to global sea level rise is not as great as it would otherwise be. Indeed, when estimating mass rates over individual regions, West Antarctica and the Antarctic Peninsula exhibit negative mass trends dominated by glacial discharge from melting and calving events (Thomas et al., 2004; Vaughan, 2006; Holland et al., 2010; Rignot et al., 2013), whereas East Antarctica has remained relatively stable and even experienced mass gains in recent years due in part to an increase in precipitation rates (Davis et al., 2005; Rignot et al.,

2008; Shepherd et al., 2012). This strong regional variability on decadal timescales, dominated by the large mass losses from particular ice streams such as Pine Island Glacier or Thwaites Glacier (Payne et al., 2004; Rignot et al., 2004; Favier et al., 2014), offsets the strong and location-dependent snowfall in the East (Davis et al., 2005). This results in large uncertainties for ice sheet mass balance. In contrast and when taken as a whole, future estimates of Antarctica's mass balance indicate an increase in mass dominated by an increase in precipitation (snowfall) throughout the 21st Century as a result of warming air temperatures (IPCC, 2013). Therefore, understanding the overall regime of precipitation over the Antarctic Ice Sheet represents one of the largest and most important challenges when assessing Antarctica's mass balance, mainly due to the role that snowfall plays in the mass balance cycle and for its influence on eustatic sea level change (Schlosser *et al.,* 2010).

One of the main focus when estimating changes in ice sheet mass budget as a result of ice-dynamics is the disappearance of ice shelves around Antarctica and their influence on sea level rise. Indeed, ice shelves act as important stabilisers for Antarctic ice streams by buttressing the flow of fast-moving glaciers on the continent (Thomas, 1979; Rignot et al., 2004; Dupont and Alley, 2005). For example, following the collapse of Larsen A Ice Shelf in 1995, Rott et al. (2002) reported that the terminus velocity of Drygalski glacier, the largest glacier in the area, increased threefold; while the flow of Hektoria, Green and Evans glacier increased eightfold following the break-off of Larsen B Ice Shelf in 2000 (Rignot et al., 2004).

The two main ablation processes responsible for ice mass loss on Antarctica are iceberg calving and basal melting (Jacobs et al., 1992; Pritchard et al., 2012; Depoorter et al., 2013; Arzeno et al., 2014). While ice mass loss is almost equally split between calving and basal melting on Antarctica as a whole (Depoorter et al., 2013), there are strong disparities between the different regions on the continent, especially within the ABS sector. For example, 30% of the total mass of icebergs produced in Antarctica are produce in the Weddell Sea, while only 3% are produced in the Bellingshausen Sea (Depoorter et al., 2013). Moreover, basal melting rates for the Ross Sea are estimated at 79 Gt/yr^{-1}, while they average 484 Gt/yr^{-1} in the Amundsen Sea sector (Depoorter et al., 2013). Altogether, basal melt rates in the ABS region approximate 70%, while they only account for 40% of the total mass loss over the whole continent

(Depoorter et al., 2013). Overall estimates of mass loss over the West Antarctic ice sheet for the year 2000 show a melting of approximately 106 ± 60 Gt/yr^{-1} (Rignot et al., 2008). According to Depoorter et al. (2013), the total basal melting and calving flux of all ice shelves on Antarctica is equivalent to 1454 ± 174 Gt/yr^{-1} and 1321 ± 144 Gt/yr^{-1} respectively, while Silva et al. (2006) estimate that the calving of giant icebergs (longer than 18.5 km) in Antarctica resulted in a total ice loss of 1089 ± 300 Gt/yr^{-1} for the period 1979-2003. Lastly, Pritchard et al. (2009) showed that the annual thinning of the major fastest-flowing glaciers feeding the Dotson and Crosson ice shelves in the Amundsen Sea Embayment exhibited a net volume loss of 57 ± 29 kg^{3}/yr^{-1} between 2004 and 2007.

Long-term changes in the Antarctic Ice Sheet, as dominated by changes in ice dynamics, have thus far dominated the scientific literature. On the contrary, less is known of short-term events affecting atmospheric circulation on interannual timescales, despite their potential to affect the ice sheet. One of the primary modes of atmospheric variability on interannual timescales over Antarctica is known as the El Niño-Southern Oscillation (ENSO) (Karoly, 1989; Harangozo, 2000; Stammerjohn et al., 2008). The influence of ENSO is considered to impact the Antarctic Ice Sheet on a significant level and result in anomalies in Sea Surface Temperature (SST), Sea Ice Extent (SIE), Total Precipitation (TP) and Mean Sea Level Pressure (MSLP) (Ledley and Huang, 1997; Harangozo, 2000). This in turn can lead to changes in precipitation rates and temperature over the ice sheet, which can ultimately result in mass changes. For instance, Cullather et al. (1996) found strong ENSO-related interannual variation in net precipitation rates between 1980 and 1990 that led to ± 1.2 – 1.5 mm/yr^{-1} maximum change in eustatic sea level contribution. Boening et al. (2012) also found that ENSO-related mass change over East Antarctica between 2009 and 2011 resulted in a positive anomaly totalling +350 Gt of cumulative mass gain, the equivalent of a decrease of 0.32 mm/yr in global mean sea level. This was also confirmed by King et al. (2012) and Shepherd et al. (2012) who also found similar results for Dronning Maud Land sector in East Antarctica following the 2009 El Niño.

Changes in the mass budget of the Antarctic Ice Sheet can therefore range from long-term processes to short-lived events. Ice-dynamical processes such as ice sheet thinning and changes in flow dynamics affect the ice sheet on longer timescales ranging from years to

decades (Payne et al., 2004; Jenkins et al., 2010), whereas short-term changes in precipitation influence the Surface Mass Balance of the ice sheet on interannual timescales (Lenaerts et al., 2012). Previous studies (Boening et al., 2012; Paolo et al., 2018) have suggested that the next step towards a comprehensive understanding of Antarctica's sea level contribution would be to assess the vulnerability of the ice sheet to interannual changes. Since changes in the flow dynamics of ice sheets occur on decadal timescales and that snowdrift has little effect on interannual timescales (Lenaerts et al., 2012), our hypothesis is that changes in the Surface Mass Balance of the ice sheet on short timescales must result from changes in atmospheric conditions.

2.1. The Southern Oscillation and the Walker Circulation

Essential to our understanding of the El Niño-Southern Oscillation and of its impact on the Antarctic Ice Sheet is our knowledge of the interactions that exist between the atmosphere and oceans and how these influence the development, frequency and intensity of ENSO events. One of the key atmospheric process inducing changes in Sea Surface Temperature in the tropical Pacific Ocean is known as the Southern Oscillation (SO), which was first defined by Walker (1924) as a tendency for surface pressure in the Pacific region to increase while surface pressure in the region of the Indian Ocean decreases. In particular, an important aspect of the Southern Oscillation when considering the effect of El Niño is the Walker Circulation, which plays a key role in the redistribution of atmospheric pressure across the equatorial Pacific. Whilst the SO is indicative of differences in atmospheric pressure along the complete circumference of the globe, the Walker Circulation is concentrated over a smaller area, with a pressure gradient that stretches from the Pacific coast of South America (high pressure zone) to the western equatorial Pacific (low pressure system) (Bjerknes, 1969).

First described by Bjerkness (1969), the Walker circulation is an east-west exchange of air circulation over the equatorial tropical Pacific on seasonal to interannual timescales. In its normal state (or in the absence of ENSO conditions), the thermally driven Walker Circulation cell acts as a conveyor in which moist and warm air present above the equatorial western

Pacific ascends and travels eastward via the upper troposphere, causing heavy precipitation over the western Pacific (Wang, 2002). This process is described by Bjerknes (1969) as the moist-adiabatic ascent. Once the air reaches the eastern boundary of the Pacific Ocean, it cools down and dries, resulting in the air sinking down. The cool air then returns toward the equatorial western Pacific in the lower troposphere to close the circulation (Wang, 2002). Commonly considered as the dominant force influencing the atmospheric overturning circulation over the Pacific Ocean (Tokinaga et al., 2012), the Walker Circulation results in near-global variations in circulation, clouds and precipitation and has been intimately linked with an east-west contrast in Sea Surface Temperature over the equatorial tropical Pacific (Julian and Chervin, 1978; Philander, 1983). Major changes in SSTs caused by wind-driven ocean dynamics over the equatorial Pacific Ocean can lead to large-scale disturbances of the normal Walker Cell circulation and thus alter ocean-atmosphere processes on an extremely irregular scale. This close association between atmospheric and ocean anomalies over the Pacific Ocean is known as the El Niño-Southern Oscillation.

2.2. The El Niño-Southern Oscillation

The El Niño-Southern Oscillation is a semi regular and extremely variable change in climate-ocean circulation patterns, which occurs on average every four years (with a periodic cycle of 3 to 6 years) in the central and east-central equatorial Pacific basin (Trenberth, 1997; Turner, 2004; Latif and Keenlyside, 2009) (Figure 1). It is widely regarded as the most influential ocean-atmosphere coupled mode in the tropical Pacific with the potential to alter weather patterns on a very large scale (Latif and Keenlyside, 2009; Chen et al., 2016).

The El Niño-Southern Oscillation is composed of two phases: the warm phase of ENSO, also known as El Niño, is characterised by warmer-than-usual SSTs in the eastern Pacific and a reduction in the ocean temperature gradient between the western and eastern Pacific (Figure 1).

This phase is often followed by a period of cooling of Sea Surface Temperatures and a change in climate-ocean interactions called La Niña (Grimm et al., 2000). According to Trenberth (1997), an El Niño event can be said to have occurred only if a 5-month running mean of sea surface temperature anomalies within the Niño 3.4 region (5° N – 5° S; 120° W – 170° W) exceeds the threshold of 0.5 °C for a period of six months or more. Consequently, past and present records show that El Niño occurred on average 31% of the time whilst La Niña occurred on 23% of occasions (Trenberth, 1997). The remaining 56% of the time are considered to be representing a normal state of atmospheric and ocean conditions (Turner, 2004).

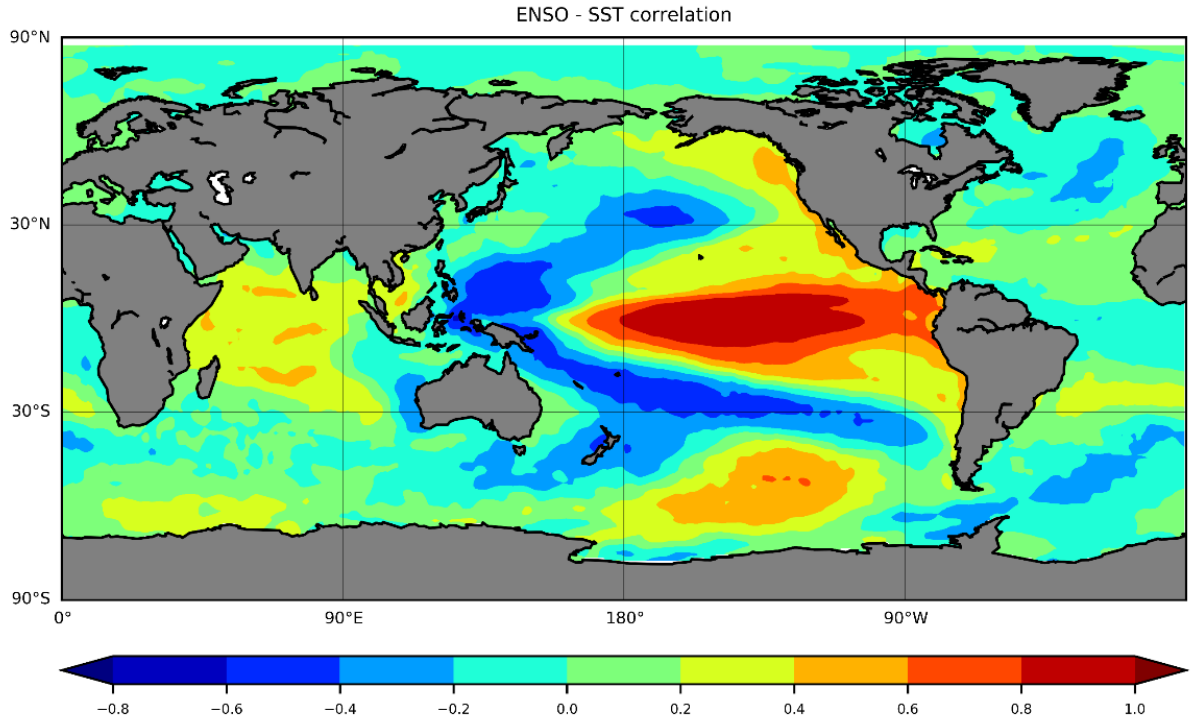

Figure 1. Correlation map showing the relationship between ENSO and Sea Surface Temperature across all ocean basins. Units are in correlation coefficient.

Rasmusson & Carpenter (1982) and Wang (2002) have demonstrated that the mature phase of almost all El Niño events since the second half of the 20th Century occurred during the calendar months of November to January. This is true for the seven major El Niño events between 1950 and 1999 (1957-58, 1965-66, 1972-73, 1982-83, 1986-87, 1991-92 and 1997-98) (Wang, 2002). Since 1999, almost all ENSO events (2002-03, 2009-10, 2015-16) have also seen their mature phase occur in the months of November to January (NOAA, 2016) (see Supplementary Table 2). This suggests a strong tendency for El Niño events to peak during the

end of the calendar year, which could represent a useful information in our understanding of the timing between ENSO phases and different regions of the world.

2.3. On ENSO Dynamics

Bjerknes (1969) was the first to hypothesise that ocean-atmosphere interactions have the potential to drive instabilities in the Pacific Ocean via a positive feedback loop (Philander, 1989b; Jin, 1997). His theory suggests that although the Pacific Ocean receives an equal amount of solar energy, Sea Surface Temperature in the tropics is zonally asymmetric and results in large interbasin SST contrasts (Jin, 1996). In particular, the process of upwelling of cold waters in the eastern part of the equatorial Pacific Ocean results in SST considerably colder than its western counterpart by 4 to 10 °C (Cane, 2005). Bjerkness (1969) found that the intensification of easterly trade winds above the equatorial Pacific Ocean drives the equatorial upwelling of cold waters at the surface via the thermocline.

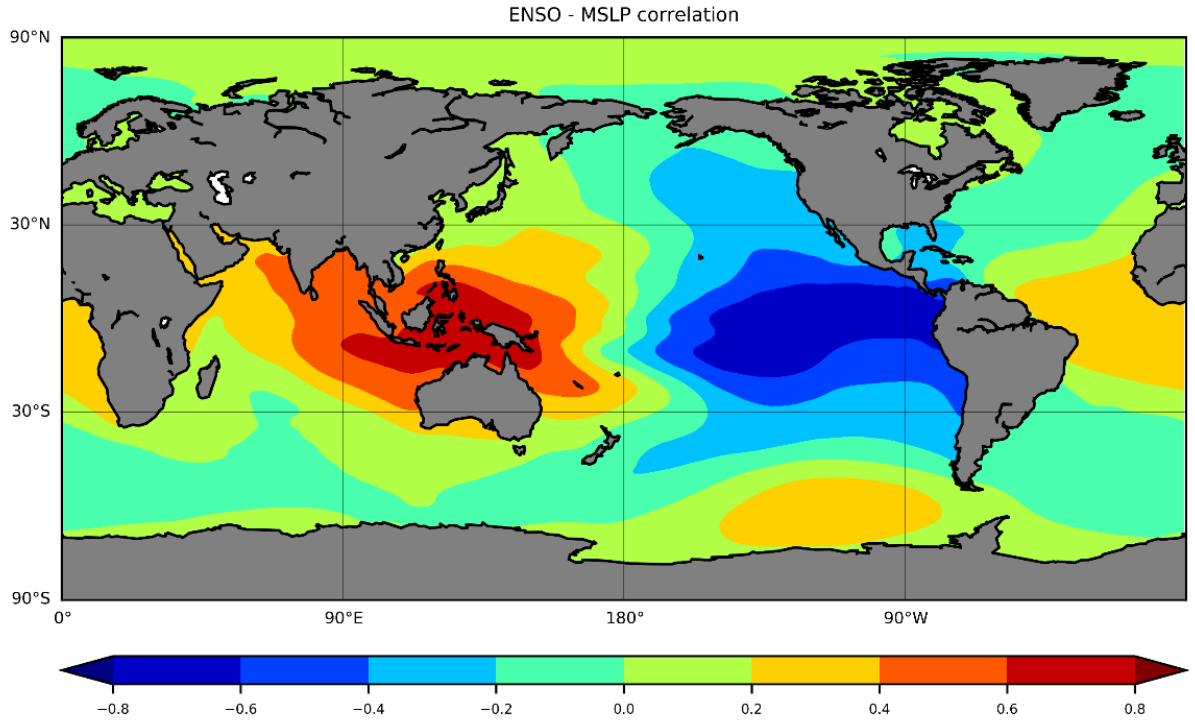

Figure 2. Correlation map showing the relationship between ENSO and Mean Sea Level Pressure (MSLP) across all ocean basins. Units are in correlation coefficient.

In doing so, trade winds create a contrast in Sea Surface Temperature between the east and the west, which together with the east-west gradient in atmospheric pressure (Figure 2) drive the equatorial Walker Circulation. Described by Bjerknes (1969) as a 'chain reaction', the Bjerknes theory states that under normal conditions, the strong Walker circulation drives the upwelling of cold water to the ocean surface in the eastern Pacific, intensifying in turn the easterly winds and the transport of cold water from east to west. This ultimately strengthens the thermocline budget and the SST gradient in the Pacific basin.

Bjerknes also shows that during abnormal conditions, such as during an ENSO event, this mechanism is reversed. He demonstrates that a decrease in trade winds as a result of warmer SSTs in the eastern Pacific leads to less warm surface water being transported westward and less cold water being upwelled at the surface in the east, reducing the east-west SST contrast and in turn supplying more heat to the atmosphere. Consequently, this opposite effect weakens the Walker Circulation and causes the convective zone of heavy precipitation to move eastward from the western Pacific towards the central-eastern Pacific (Rasmusson and Wallace, 1983; Philander, 1989a: 4; McPhaden et al., 1998). Additionally, Wang (2002) shows that during the development of previous El Niño phases, the circulation pattern of the Walker Circulation reverses sign, resulting in an anomalous ascending (descending) motion of air in the eastern (western) equatorial Pacific, as opposed to the western (eastern) equatorial Pacific in non-ENSO years (Figure 2). This shows that a strong connection exists between the ocean (eastern Pacific SSTs) and the atmosphere (Southern Oscillation) that essentially comes together to become a single mode: El Niño-Southern Oscillation (Cane, 2005). To this day, the Bjerknes feedback theory remains at the forefront of our understanding of ENSO dynamics even though Bjerknes was unable at the time to explain why the system was oscillating between warm and cold SST phases (Jin, 1996; Zebiak, 1989).

Previous studies (Harrison and Schopf, 1984; Weisberg and Wang, 1997; Vecchi and Harrison, 2000; Lengaigne et al., 2004; Kao and Yu, 2009) have shown that the westerly wind events (WWEs) over the equatorial western-central Pacific play an important part in the onset of El Niño events by generating a strong downwelling kelvin wave that causes a positive SST anomaly in the central-eastern Pacific. It has also been widely recognised that for an El Niño event to

develop, a precursory phase is first required (Philander, 1983). Several precursors have been identified as influencing the onset of the ENSO cycle and include: (1) the slow warming of the western Pacific Ocean as a result of strong trade winds, commonly known as the Delayed Oscillator Theory (Wyrtki, 1975); (2) an eastward displacement of the Walker Circulation over the eastern tropical Pacific (Rasmusson and Wallace, 1983; McPhaden et al., 1998); and (3) the equatorward expansion and intensification of a band of rising air within the Hadley Cell known as the Inter Tropical Convergence Zone (ITCZ) (Philander, 1983; Philander, 1989a: 249; Deser and Wallace, 1990; Cai et al., 2014).

2.4. The BWCZ Hypothesis

Wyrtki (1975) associated the Delayed Oscillator Theory (DOT) as the main precursor for the onset of an El Niño. This theory suggests that prior to an El Niño cycle, strong southeast trade winds and strong atmospheric pressure over the Pacific Ocean lead to a gradual build-up (recharge) of warm water in the western Pacific over several years, creating the conditions for an El Niño to develop (Quinn, 1974; Wyrtki, 1975; Wyrtki, 1985). Once the stress of trade winds decreases, downwelling equatorial waves (Kelvin waves) in the thermocline develop and discharge the warm water that was once confined in the Western Pacific to the rest of the Pacific basin, conveying warm and nutrient-poor waters eastward to the South American coast (Godfrey, 1975; Wyrtki, 1975; Yu and Rienecker, 1998). According to McPhaden (1999), the Kelvin waves observed during the 1997-98 El Niño spread from west to east across the Pacific basin in the space of two months, resulting in a 90-metre depression of the thermocline in the eastern Pacific in late 1997. According to Graham and White (1988), the Kelvin waves that spread from west to east along the equatorial Pacific average speeds of 2.5 m/s^{-1}.

As previously indicated, the feedback theory developed by Bjerknes (1969) was not sufficient to explain the dynamics that govern the phase transition mechanism between El Niño and La Niña. It is suggested that the key factor that was missing in Bjerknes' hypothesis was the depth of the thermocline during the ENSO cycle. According to Cane (2005), the changes observed in the depth of the warm layer of the thermocline as a result of ENSO are too important to be the

single result of heat exchanges with the atmosphere, but are rather the consequence of wind-driven ocean dynamics as described by Wyrtki (1975). Following Wyrtki's (1975) findings, Zebiak and Cane (1987) generated the first coupled model combining Bjerknes' feedback theory and Wyrtki's recharge-discharge theory to provide a full understanding of the ENSO cycle and its transition from warm El Niño to cold La Niña phases (Zebiak and Cane, 1987; Jin, 1997). The recharge/discharge mechanism of heat content in the western Pacific, which is out of phase with SST anomalies throughout the El Niño cycle was suggested to be the main driver of ENSO phase transitions (Zebiak and Cane, 1987; Cane, 2005). This led to the Bjerkness-Wyrtki-Cane-Zebiak (BWCZ) theory which demonstrated that the El Niño-Southern Oscillation is a naturally-occurring basin-wide oscillation in the tropical Pacific Ocean that combines both oceanic and atmospheric processes. Zebiak and Cane (1987) showed that their model successfully reproduced the build-up of warm water prior to the onset of El Niño and its discharge throughout the cycle, and concluded that the recharge-discharge theory was an essential component for the initiation of the ENSO cycle.

Despite the Delayed Oscillation Theory (DOT) being regarded as the main process influencing the onset of ENSO events, other wind-driven processes have been found to affect El Niño events in the past. Since the mid-20th Century, almost all El Niño events have been associated with high level of intraseasonal westerly wind forcing lasting for periods of one to three weeks prior to and during each El Niño phases (Luther et al., 1983; Cane, 2005). Previous El Niño events have also been associated with the Madden Julian Oscillation (MJO) (Lau and Chan, 1986), tropical cyclone formations (Keen, 1982), surges of cold air from mid and high latitude (i.e. from East Asia and Western North Pacific) (Yu and Rienecker, 1998), the North Pacific Oscillation (NPO; Vimont et al., 2003) and more recently the Arctic Oscillation (Chen et al., 2016). For example, McPhaden (1999) shows that although the DOT played an important role in the formation of the 1997-98 El Niño, the intensification of the Madden-Julian Oscillation was a major factor in the onset of this particular event. Therefore, despite evidence that global scale variability in atmospheric or oceanic circulation can influence the onset or the termination of ENSO events, there is still not consensus on the origins of ENSO's irregularities and on whether the ENSO cycle is triggered by an association of successive events at irregular intervals or by one single mechanism (Neelin et al., 1998).

2.5. The ENSO Phase Transition Mechanism

When the front of the downwelling Kelvin wave comes into contact with the eastern boundary of the ocean basin, some of its energy is reflected westward to become a slowly-moving Rossby wave and the remaining energy is deflected by the South American boundary and moves poleward to become a costal Kelvin front (Enfield and Allen, 1980; Harrison and Schopf, 1984; Wyrtki, 1985). The change in wind patterns also creates an upwelling equatorial Rossby wave that travels westward towards Indonesia and Papua-New Guinea (Wakata and Sarachik, 1991; Boulanger and Menkes, 1999). As the Rossby wave comes into contact with the western boundary of the Pacific basin, it is reflected as freely-propagating upwelling Kelvin waves moving eastward to elevate the thermocline in the eastern Pacific (Tziperman et al., 1994; McPhaden, 1999). This has the effect to weaken the downwelling Kelvin signal in the central and eastern Pacific, which in turn decreases SST anomalies and permits the transition from warm El Niño conditions to cool La Niña conditions (Wakata and Sarachik, 1991; Boulanger and Menkes, 1999). According to Battisti (1988), the transition mechanism between El Niño and La Niña is inherent to the Delayed Oscillator Theory which governs interactions between ocean-atmosphere feedback and large-scale equatorial ocean wave dynamics. As in the case of the 1997-98 El Niño, the return of the trade winds in the eastern Pacific in May 1998 and the reflection of Rossby waves at the western boundary allowed for the cold subsurface waters to upwell and cool down Pacific SSTs, marking an end to the El Niño conditions and the start of a La Niña phase (McPhaden, 1999). During La Niña years, a reversed ocean pattern occurs, in which an upwelling Kelvin wave front is emitted to the east and downwelling Rossby waves are emitted to the west (Wakata and Sarachik, 1991). Moreover, aside from the east-west equatorial exchange of heat, Cane et al. (1986) also suggest that a north-south circulation of heat exists at the equator during the peak phase of El Niño cycles which can considerably affect the discharge of the western equatorial reservoir during an El Niño and its recharge post El Niño. This anomalous heat transport can further influence the periodicity and length change between El Niño and La Niña conditions.

Once the heat reservoir of the western Pacific is empty and the strength of eastward Kelvin waves reduces, the thermocline in the eastern Pacific becomes shallower and allows for cold

water conditions to prevail over warm waters, thus leading to either the return of normal SST conditions (non-ENSO) or to lower-than-average SSTs associated with La Niña (Wang and Picaut, 2004). The presence of cold water in the vicinity of South America also allows for the return of easterly winds that lead to the slow recharge (build-up) of the warm water reservoir in the western Pacific (Cane et al., 1986; Jin, 1996; Wang and Picaut, 2004). Once enough warm water has built up in the reservoir and the trade winds weaken, the chain-reaction associated with the El Niño cycle initiates again (Wyrtki, 1985; Cane et al., 1986; Jin, 1997).

2.6. The Impact of ENSO on a Global Scale

ENSO events have wide-ranging effects on the global climate system (Latif and Keenlyside, 2009) and have been widely discussed in the scientific literature (Stenseth et al., 2002, 2003; van der Werf et al., 2004; Vecchi and Wittenberg, 2010). Special attention has been drawn onto the El Niño events of 1982-83 and 1997-98 which have been described as the strongest climatic disruptions of the 20th Century and were responsible for an extreme warming of the equatorial Pacific Ocean, reaching record-high SSTs well-above 28 °C (Philander and Seigel, 1985; McPhaden, 1999; Cai et al., 2014). The disruptions caused by those extreme ENSO events are often associated with increased stormy conditions, strong precipitation and temperature anomalies, and an increase in droughts, wildfires, and flooding across the world. These extreme events can in turn lead to a decline in both marine and terrestrial biodiversity, enhance greater glacier melting and result in negative socio-economic impacts

According to Philander (1989a: 40), the displacement of the ITCZ in late 1982 led to heavy rainfall in Ecuador and Peru that started before the usual onset of the wet season and that lasted longer than usual. Measurements taken at the time in Guayaquil (Ecuador) indicated a total rainfall record of 2636 mm between the El Niño months of November 1982 and April 1983, compared to 1670 mm during the relatively strong 1972 El Niño year (in comparison, normal average rainfall between the months of November and April for the period 1951-1960 are of the order of 942 mm) (Philander, 1989a: 40). Moreover, higher-than-normal Sea Surface Temperature during the 1982-83 El Niño event were associated with high coral mortality off

the Pacific coast of Panama (Glynn and D'croz, 1990; Glynn and De Weerdt, 1991), along with a shift in population distributions of many marine species (Pearcy and Schoener, 1987) and a decline in seabirds off the coast of the United States (Hodder and Graybill, 1985).

Conditions during the strong 1997-98 El Niño were also widely documented, with extremely high SSTs in the eastern Pacific exceeding 29 °C (McPhaden, 1999) and resulting in global weather disruptions. Extreme droughts in Northern China and the severe flood in the summer of 1997 south of the Yangtze River in Southern China damaged large areas of farmland leading to serious economic losses and cost the lives of thousands of people (Lau and Weng, 2001). Moreover, Indonesia, New Guinea, the Amazon Basin and Central America all experienced less-than-average rainfalls in the year 1997 (Bell and Halpert, 1998). These resulted in severe droughts and uncontrolled wildfires in forested peatlands of Indonesia between the months of June and December 1997, which led to large amounts of CO_2 being released into the atmosphere (Page et al., 2002). A deficit in precipitation rates over Bolivia and an increase in air temperature over Ecuador also affected glaciers in the outer and inner tropics of South America by reducing the albedo effect and therefore increasing ablation rates as in the case of Zongo Glacier in Bolivia (Wagnon et al., 2001) or Antizana 15 Glacier in Ecuador (Francou et al., 2004). Moreover, food shortages in New Guinea resulted in booming cases of malnutrition and starvation, affecting hundreds of thousands of people across the country (Bell and Halpert, 1998). Lastly, this extreme event also affected biodiversity on a very large scale. Ladah et al. (1999) and Edwards (2004) reports extremely high mortality rates amongst giant kelp populations found in the northeast Pacific which almost resulted in the mass extinction of kelp forests along Baja (Mexico) and Southern California. Vargas et al. (2007) also report a 60% decline in populations of Galápagos penguins following the two strong El Niño events of 1982-83 and 1997-98.

Although it is still early to examine its effects on global weather patterns, the 2015-16 El Niño event has already been associated with reduced summer precipitation in Asia, leading to abnormal dry weather and droughts in Central Inner Mongolia, the Yellow River region and the coastal areas of Bohai Bay in Northern China (Zhai et al., 2016). Moreover, Chen et al. (2016)

reported that a total of 21 storms had been observed over the North Pacific in 2015, exceeding the ENSO-related record of 17 storms reported by Chu (2004).

2.7. The Impact of ENSO on Antarctica

Anomalies in Sea Ice Extent and Surface Air temperature over Antarctica on interannual time scales have for a while remained relatively unexplained. Zwally et al. (1983: 4) reported a regional difference in SIE between 1973 and 1976 which resulted in lower SIE in the Weddell and Ross Seas compared to an increase in the Amundsen and Bellingshausen Seas.

Figure 3. Map of Antarctica showing the key places that will be discussed in this thesis. The regions are color-coded and are as follows: Yellow: Antarctic Peninsula Ice Sheet (APIS), Red: West Antarctic Ice Sheet (WAIS), Green: Central Antarctic Ice Sheet (CAIS), Blue: East Antarctic Ice Sheet (EAIS).

Subsequent work from Carleton (1988) revealed for the first time that reduced sea ice concentrations in the Weddell Sea was linked with the Southern Oscillation in the tropical Pacific. According to this study, sea-ice concentrations were lower during the austral summer months of December to January following an El Niño event compared with previous summers. Following Carleton's work, Jacobs and Comiso (1993) recorded low sea ice extent in the ABS region compared to relatively high sea ice extent in the Weddell Sea sector following the 1991-92 El Niño, in line with higher-than-normal southerly surface winds and record-high surface air temperatures on the west side of the Antarctic Peninsula after the 1986-88 El Niño. Similar to the results of Zwally et al. (1983), Jacobs and Comiso (1993) showed that a decrease in one sector of the Southern Ocean was balanced out by an increase in the opposite sector. However, they were unable to provide an accurate explanation for the relatively large difference in SIE between the Eastern and the Western sectors of the Antarctic Peninsula on interannual timescales. Numerous other studies (Smith and Stearns, 1993; Gloersen, 1995; Simmonds and Jacka, 1995; Ledley and Huang, 1997) also reported that the observed SIE and Surface Air Temperature (SAT) anomalies in Antarctica were linked with the ENSO signal from the equatorial Pacific. However, none of these could explain precisely the processes that allowed the ENSO signal to be transported to the high latitudes of the Southern Hemisphere.

Subsequent work from Yuan and Martinson (2000, 2001) allowed for a more accurate understanding of the ENSO processes on Antarctica. In particular, they were the first to associate interannual anomalies in Sea Ice Extent and Surface Air Temperature to the Antarctic Dipole (ADP). This quasi-stationary wave pattern, which forms in the western Amundsen Sea and with opposite polarity in the Weddell Sea is considered to be the dominant pattern of climate variability in the region and responds strongly to ENSO (Renwick, 2002; Yuan, 2004). This polarity brings positive (negative) temperature anomalies and negative (positive) SIE anomalies during El Niño (La Niña) events in the Pacific sector of the ADP, and opposite signs in the Atlantic side of the ADP (Liu et al., 2002) (Figure 4).

According to Yuan and Martinson (2000, 2001), an out-of-phase relationship exists between ice and temperature anomalies in West Antarctica and the central tropical Pacific that is transported via Rossby waves to the ADP. As opposed to previous studies which suggest that

SST, MSLP, and SST anomalies associated with ENSO are transported around Antarctica via a self-sustained eastward propagating wave known as the Antarctic Circumpolar Wave (ACW) (White and Peterson, 1996; Peterson and White, 1998; Cai and Baines, 2001), Yuan and Martinson (2000, 2001) showed that the teleconnections between the pacific and polar regions are expressed by a quasi-standing wave pattern that provides extrapolar climate variability to Antarctica on interannual timescales. The ENSO-related anomalies present in the ADP are then transported eastward via the Antarctic Circumpolar Current and communicated to the rest of the Southern Ocean (Christoph et al., 1998; Yuan, 2004).

Since then, improvements in our understanding of Antarctica's ocean circulation ruled out the role of the ACW for conveying ENSO's signal around Antarctica based on two main observations of the ACW circulation pattern. First of all, the strongest section of the ACW is found in the Weddell Gyre and eastern Pacific section of Antarctica where the ADP forms, implying that the relationship between ENSO and the ACW is primarily concentrated in the ADP region (Yuan and Martinson, 2001). Second of all, the ACW does not complete a full circle around Antarctica and its signal becomes weaker as it passes Drake Passage (Christoph et al., 1998), implying that the ACW is not the main source of climate variability around Antarctica as it is unable to transmit the ENSO signal across the entire Southern Ocean (Park et al., 2004). The Antarctic Dipole theory is also supported by Park et al. (2004) whose results show that the ACW represents only 25% of the total climate variability associated with El Niño in the Southern Ocean. This suggests that the ACW is not a self-sustained pattern of climate variability and cannot be considered as the distinct climate mode responsible for the distribution of interannual climate variability around Antarctica.

According to Liu et al. (2002) and Yuan and Li (2008), the anomalies in SAT and SIE recorded in the ADP region are the largest ENSO-related anomalies observed on Earth. Based on analysis of SAT anomalies between warm and cold phases of the ENSO cycle between 1970 and 2000, Liu et al. (2002) were amongst the first to provide an explanation for the mechanism that governs the teleconnections between ENSO and the ADP. Instead of the ENSO signal being transported slowly via oceanic processes and distributed around Antarctica through the ACW, Liu et al. (2002) showed that the strong ENSO-ADP signal propagates poleward at a much faster

rate during the ENSO cycle and that the rate at which the signal is transported from the tropics to the high latitude can only be the result of atmospheric processes.

The complex set of interactions between ocean and atmospheric processes originating in the equatorial tropical Pacific was further exposed by the modelling study of Rind et al. (2001) who further confirmed the strong relationship between ENSO and the Antarctic Dipole. This study, along with the work of Yuan (2004) revealed that the difference in polarity between the Pacific and the Atlantic sectors of the ADP results in a temperature gradient between the two regions. During El Niño, two opposite processes occur simultaneously between the Pacific and the Atlantic Ocean (Figure 4).

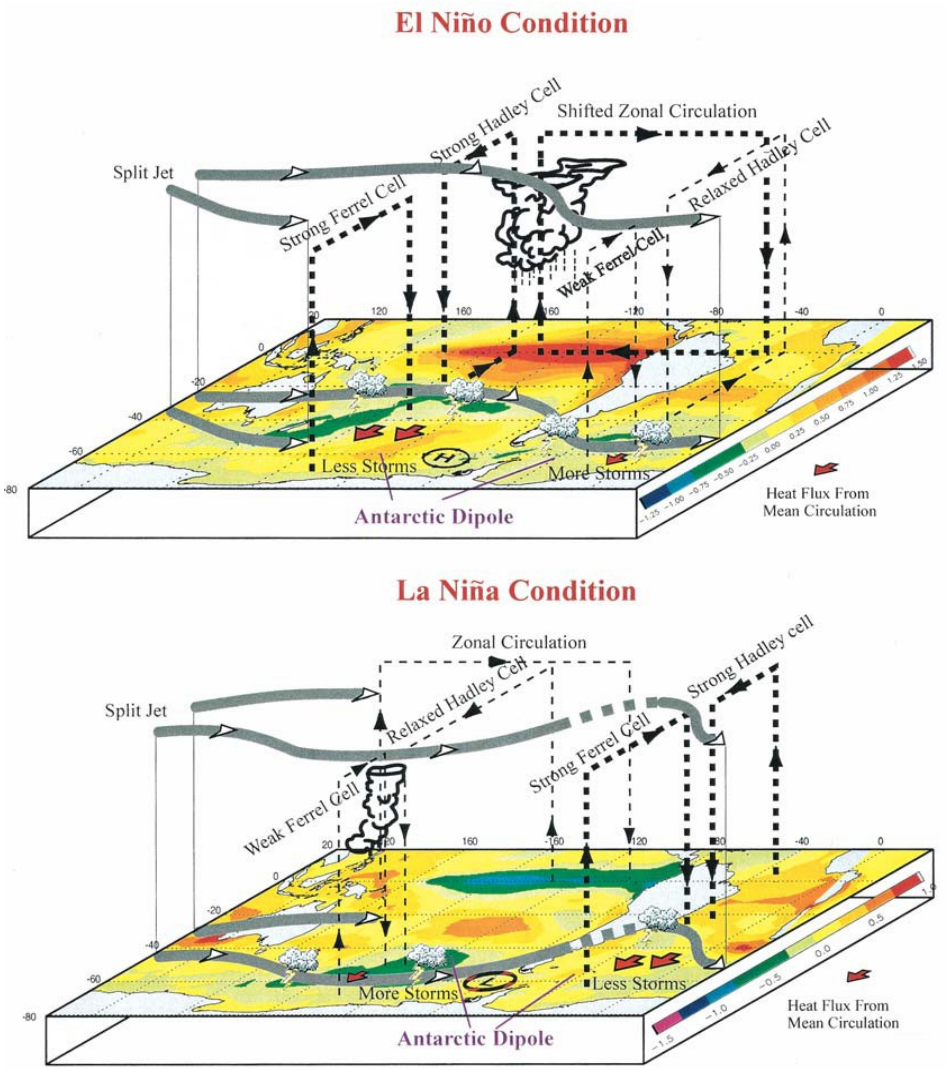

Figure 4. Patterns of atmospheric circulation in relation to El Niño (top) and La Niña (bottom) conditions superimposed on SST anomaly composites for each of the two ENSO phases (Yuan, 2004).

Firstly, the warm SSTs found in the tropical Pacific during El Niño events enhance tropical convection and increase the meridional temperature gradient between the equator and the polar latitudes (Yuan, 2004). This strengthens the Hadley Cell over the Pacific, which has the effect of increasing the equatorward shift of the storm track via stronger subtropical jets and as a consequence enhances the Ferrel Cell over the South Pacific. Secondly, the enhanced tropical convection in the tropical Pacific leads to the eastward displacement of the zonal circulation towards the Atlantic Ocean, weakening in turn the Hadley Cell over the Atlantic (Yuan, 2004). The weakening of the Hadley Cell and the poleward shift in jet streams push the storm tracks towards the southern high latitudes, which weakens the Ferrel Cell in the South Atlantic and results in a reduced transport of heat fluxes towards the Atlantic sector of the ADP. During La Niña conditions, these processes are reversed, leading to the westward displacement of the zonal circulation (towards the Pacific Ocean), along with an increase (decrease) in storm activity over the Pacific (Atlantic) sector of the ADP, and a weakening (strengthening) of the Hadley and Ferrel Cells over the Pacific (Atlantic) Ocean (Yuan, 2004) (Figure 4).

The increase in SSTs in the tropical Pacific during El Niño events also triggers the poleward displacement of Rossby wave trains that propagate the ENSO signal to the mid-high latitudes of the Southern Hemisphere (Hoskins and Karoly, 1981; Karoly, 1989; Harangozo, 2000). As a result, the excitement of Rossby waves creates a pattern of high-low-high atmospheric pressure anomalies known as the Pacific South American (PSA) mode (Karoly, 1989; Garreaud and Battisti, 1999; Yuan, 2004). The anomalous high-pressure centre of the PSA concentrates on the Pacific sector of the ADP during warm ENSO events, providing warm air from the equator towards the Amundsen and Bellingshausen Seas (Garreaud and Battisti, 1999; Yuan, 2004; Yuan and Li, 2008). The presence of the PSA over the South Pacific Ocean also creates a centre of low pressure over the Weddell Sea, bringing cold Antarctic air to the region of the South Atlantic Ocean (Yuan, 2004). Conversely, this high-low pressure centre eventually switches polarity when tropical Pacific SSTs shift from warm El Niño to cold La Niña states, and the high-low pressure centre intensifies over the Weddell Sea sector, bringing warm air to the South Atlantic sector of the ADP and cold air to the South Pacific (Yuan, 2004).

2.7.1. The Effect of El Niño on Antarctica's Atmospheric Circulation and Mass Changes

Numerous studies have demonstrated a strong link between ENSO and Antarctica's atmospheric circulation. In particular, the advection of warm (cold) air towards the continent following ENSO warm (cold) conditions has been shown to induce changes in precipitation rates (Cullather et al., 1996), increase surface melt events (Tedesco and Monaghan, 2009; Nicolas et al., 2017), lead to near-surface temperature anomalies (Yuan and Martinson, 2001; Kwok and Comiso, 2002), as well as resulting in atmospheric-driven SST anomalies (Walker and Gardner, 2017) and Sea Ice Extent anomalies (Kwok et al., 2016). More specifically, ENSO's response in the Southern Hemisphere's High Latitudes has been associated with blocking events induced by Rossby wave trains that alter surface-pressure distribution and moisture transport over the Amundsen Sea sector of the Antarctic Peninsula (Hoskins and Karoly, 1981; Harangozo, 2000). In consequence, precipitation anomalies during ENSO warm and cold conditions result in abnormal accumulation rates in both the Amundsen and Weddell sectors of the Antarctic Peninsula (Yuan, 2004; Yuan and Li, 2008).

One of the most recent account of ENSO-induced anomalies over the Antarctic Ice Sheet (AIS) was the large increase in precipitation that occurred over Dronning Maud Land in 2009, which resulted in mass increase over the East Antarctic Ice Sheet (EAIS) (Boening et al., 2012; King et al., 2012). According to Boening et al. (2012), the development of a high-pressure system over the EAIS following the moderate 2009 El Niño resulted in increased cloud formation and subsequent precipitation in this sector. Shepherd et al. (2012) report that this event resulted in an additional 200 gigatons of snow over this area, corresponding to the mean annual snow accumulation rate in this region. However, whilst these studies provide the first account of ENSO-related anomalies on Antarctica's mass balance, the strength of the 2009 El Niño was rather weak in comparison with other very strong El Niño events (i.e. 1982-83, 1997-98, 2015-16) (Figure 8). Thus, to this date, little is known of the effects of extreme El Niño events on the ice sheet.

2.7.2. The Effect of El Niño on Antarctica's Sea Surface Temperature and Sea Ice Extent

The Southern Hemisphere's sea ice cover has on average increased over the last 30 years at a rate of 1.5% per decade (Turner et al., 2015). However, this increase is not homogeneous across Antarctica, with most of the increase occurring in the Ross Sea and Indian Ocean, and some decrease in the Amundsen and Bellingshausen Sea sector (Parkinson and Cavalieri, 2012). As of yet, there are no consensus on the reason for this increase (Kwok et al., 2016), although various mechanisms have been suggested, including stratospheric ozone depletion (Turner et al., 2009), interannual variability in relation to the Southern Annular Mode and the Southern Oscillation (Kwok and Comiso, 2002; Stammerjohn et al., 2008), a strengthening of the Amundsen and Bellingshausen Sea Low (ABSL) (Purich et al., 2016), and an intensification of surface winds (Holland et al., 2012).

Previous studies have shown a strong connection between Sea Surface Temperature and Sea Ice Extent following ENSO conditions (Carleton, 1988; Ledley and Huang, 1997; Yuan, 2004; Kwok et al., 2016; Purich et al., 2016; Pope et al., 2017). In particular, the atmospheric bridge that transports the ENSO signals to the Southern high latitudes considerably affects climate and ocean dynamics in and around the Antarctic continent and can lead to extensive sea ice redistribution in the region of the ADP (Yuan and Li, 2008) (Figure 4). According to Liu et al. (2002), the increase of heat transport in (out of) the ABS region during El Niño (La Niña) years reduces (favours) sea ice growth, whilst the output (input) of heat in the Weddell region leads to increased (decreased) sea ice extent. They conclude that interannual variations in the mean meridional heat flux as a result of changes in the regional Ferrel Cell is closely linked with fluctuations in sea ice in the ADP region during ENSO years. The resulting SAT fluctuations associated with changes in the Mean Meridional Circulation reduce the air-sea temperature contrast in the ADP region, leading to less sensible heat being released from the ocean to the atmosphere. This in turn results in warmer SSTs and more anomalies in sea ice extent, with contrasting increases and decreases between the South Pacific and South Atlantic sectors of the dipole (Kwok and Comiso, 2002; Liu et al., 2002).

Later work showed that ENSO has been influencing Sea Surface Temperature and Sea Ice Extent in the Southern Ocean at different timescales, with its effects lagging the Southern Oscillation Index in the tropical Pacific by a couple of months. Ledley and Huang (1997) found a statistically significant relationship between SSTs in the Ross Sea and the ENSO cycle with a lag response time of 2 to 4 months based on observational data between 1982 and 1994. This is also supported by Klein et al. (1999) who showed that positive SST anomalies appeared in major ocean basins on average 3 to 6 months following ENSO-related peaks in SST in the tropical Pacific between 1952 and 1992. Similar to the results of Ledley and Huang (1997), Kwok and Comiso (2002) showed that the four ENSO events that took place between 1982 and 1998 led to record-breaking sea-ice retreat in the Bellingshausen and Amundsen Seas and strong climate anomalies over the ABS and the Weddell Sea sector with a delay of 2 to 3 months.

Lastly, Meredith et al. (2004) showed that the negative pattern in sea-ice cover over Antarctica was observed during the austral winter of 1998, a couple of months following the very strong 1997-98 El Niño. Their results indicate that during the mature phase of El Niño events, the low-pressure system in the Amundsen-Bellingshausen Sea weakens, resulting in a reduction in surface winds over the West Antarctic Peninsula which in turn leads to lower surface temperature and unusual sea ice expansion. According to Harangozo (2000), this pattern is reversed during cool La Niña periods and leads to the deepening of the ABSL and an increase in northerly surface winds. The changes to the ABSL ultimately result in higher surface temperature and lower sea-ice extent (Harangozo, 2000). More recently, Stuecker et al. (2017) showed that the presence of warm SST anomalies around Antarctica following the 2015 El Niño were partly responsible for the lowest Southern Hemisphere spring sea ice extent since the advent of the satellite era.

In this context, the occurrence of the very strong 2015-16 El Niño provides a unique opportunity to assess the effect of extreme ENSO events on the Antarctic Ice Sheet. To this end, and in combination with reanalysis datasets of atmospheric conditions, this study makes use of the GRACE Mascons solution from NASA's JPL to provide an assessment of the Surface Mass Balance of the Antarctic Ice Sheet in relation to the most recent El Niño event.

In particular, the mass balance signature and associated response of the ice sheet to the recent strong El Niño event of 2015-2016 are investigated and set within the context of the historical record. Observational datasets of Sea Surface Temperature and Sea Ice Extent are also analysed to assess changes in ocean conditions following El Niño events, with the aim to determine whether ENSO events can act as a proxy for previous and future estimates of sea ice behaviour. In turn, if a consistently strong relationship is found between El Niño events and sea ice changes, this could result in a better understanding of interannual influences on sea ice growth and thus improve our understanding of sea-ice behaviour in relation to interannual fluctuations.

3. Datasets and Methods

3.1. GRACE Dataset

Launched in 2002, the Gravity Recovery and Climate Experiment (GRACE) is a space mission partnership between the U.S. National Aeronautics and Space Administration (NASA) and the German Spatial Agency (DLR) to provide spatial and temporal gravity measurements of the Earth's gravity field (Wahr et al., 2002; Awange et al., 2011). Since its launch, the GRACE mission has revolutionised the field of gravimetry and provided valuable and accurate mass distribution and flux observations for the measurement of ice sheets and glaciers across the world (Velicogna and Wahr, 2006; Velicogna, 2009; King et al., 2012; Luthcke et al., 2013; Yi and Sun, 2014), as well as for observations of changes in ocean-mass distribution and currents (Wahr et al., 2002; Morison et al., 2007), and ground water storage (Swenson et al., 2003; Schmidt et al., 2006). The GRACE mission is composed of two near-polar (∼89.5° inclination) Earth-orbiting satellites flying on the same orbit at ∼460 km of altitude. With a high spatial resolution and a geoid height accuracy of 2-3 mm, the GRACE satellites provide highly accurate gravity measurements on a 30-day cycle (Wahr et al., 2002; Tapley *et al.,* 2004). The difference in distance between the front facing satellite and its counterpart is measured by a K-band range rate system (Awange et al., 2011).

In the first decade of the GRACE mission, the main technique used to estimate mass concentration variations in gravity fields came from unconstrained spherical harmonics basis functions (Watkins et al., 2015). However, the analysis of global gravity field from GRACE using spherical harmonics solutions have suffered from several correlated errors post-processing, mainly from the longitudinal stripes that require destriping filtering methods and errors associated with postglacial rebound estimates. Although the filtering and destriping techniques associated with the spherical harmonics method can be done using destriping algorithms or empirical smoothing, it often leads to leakages and the loss of geophysical signal between basins (Wouters and Schrama, 2007; Wiese et al., 2016a). Moreover, the lack of accurate estimates of Glacial Isostatic Adjustment (GIA) over certain regions of the world such as

Antarctica have increased further the uncertainties associated with the use of GRACE measurements (Thomas et al., 2011; Ivins et al., 2013).

More recently however, advancement in GRACE processing methods have led to a new processing approach known as global monthly mass concentration blocks (herein referred to as *Mascons*), which this study makes sole use of. The RL05M mascon solutions from NASA's Jet Propulsion Laboratory (JPL; http://grace.jpl.nasa.gov/data/get-data/jpl_global_Mascons) have been developed as an alternative to the spherical harmonics solutions by reducing noise and improving spatial resolution (Wiese et al., 2016b). As described by Watkins et al. (2015), the mascon solutions employ an analytic expression for the mass concentration function that have the advantage to directly estimate mass variations without the need to apply empirical post-processing filtering associated with the spherical harmonics solutions. More specifically, the JPL Mascons are expressed in terms of 4551 equal-area 3° spherical cap mass concentration functions and are coupled with a Coastline Resolution Improvement (CRI) filter that allows for an improved separation of land and ocean mass portions and a higher signal-to-noise ratio (Watkins et al., 2015; Wiese et al., 2016a). These Mascons differ from other Mascons solutions as they combine near-global geophysical models and altimetry data to remove the correlated errors associated with spherical harmonics solutions without the need to apply empirical destriping or smoothing algorithms (Luthcke et al., 2013; Watkins et al., 2015; Schlegel et al., 2016; Wiese et al., 2016b). Another difference is that the JPL Mascons include a newly-developed solid Earth Glacial Isostatic Adjustment (GIA) developed by Geruo et al. (2013). This specific GIA differs from previous GIA estimates as it incorporates a 3-D finite-element model to create a 3-D viscosity profile based on a realistic seismic tomography model, as opposed to the commonly used 1-D viscosity GIA models such as the W12a from Whitehouse et al. (2012) and the IJ05_R2 from Ivins et al. (2013).

3.1.1. GRACE Post-Processing Methods

In order to answer Research Question 2 and examine the response of the ice sheet at a sub-continental level, a basin-scale analysis was conducted by dividing the ice sheet into 27

drainage basins obtained from NASA's ICESat data (Zwally et al., 2012; http://icesat4.gsfc.nasa.gov/cryo_data/ant_grn_drainage_systems.php).

Figure 5. As Figure 3 but incorporating the basin IDs (numbers 1-27). The regions are color-coded and are as follows: Yellow: Antarctic Peninsula Ice Sheet (APIS), Red: West Antarctic Ice Sheet (WAIS), Green: Central Antarctic Ice Sheet (CAIS), Blue: East Antarctic Ice Sheet (EAIS).

This study follows a similar approach developed by Zwally et al. (2005) and Zwally and Giovinetto (2011) regarding the allocation of basin numbers and by separating the West and East sides of the Antarctic Ice Sheet along the TransAntarctic Moutain range (Figure 3-5). However, instead of separating the ice sheet into three regions, namely the Antarctic Peninsula, West Antarctica, and East Antarctica, this study divides the East Antarctic Ice Sheet (EAIS) into two sub-regions, resulting in four regions across the ice sheet (Figure 3-5). Thus, basins 2, 3, 10 and 17 are part of a separate region, herein referred to as the Central Antarctic Ice Sheet (CAIS), and the remaining basins (4-9 and 11-16) were assigned to the East Antarctic

Ice Sheet (Figure 5). The separation of East Antarctica into two sub-regions was done due to the large difference in altitude and atmospheric conditions over the Antarctic interior (CAIS) compared to the low-lying coastal basins of the EAIS, as previously shown by Lenaerts et al. (2012) and Palerme et al. (2014) (see Chapter 5.1). The other 11 basins are identical to previous studies, where basins 24-27 belong to the Antarctic Peninsula Ice Sheet (APIS), and basins 1 and 18-23 belong to the West Antarctic Ice Sheet (WAIS) (Figure 5).

The post-processing methods for the GRACE data were as follows: the GRACE Mascons were supplied on a 0.5 x 0.5-degree global grid in terms of equivalent water height.

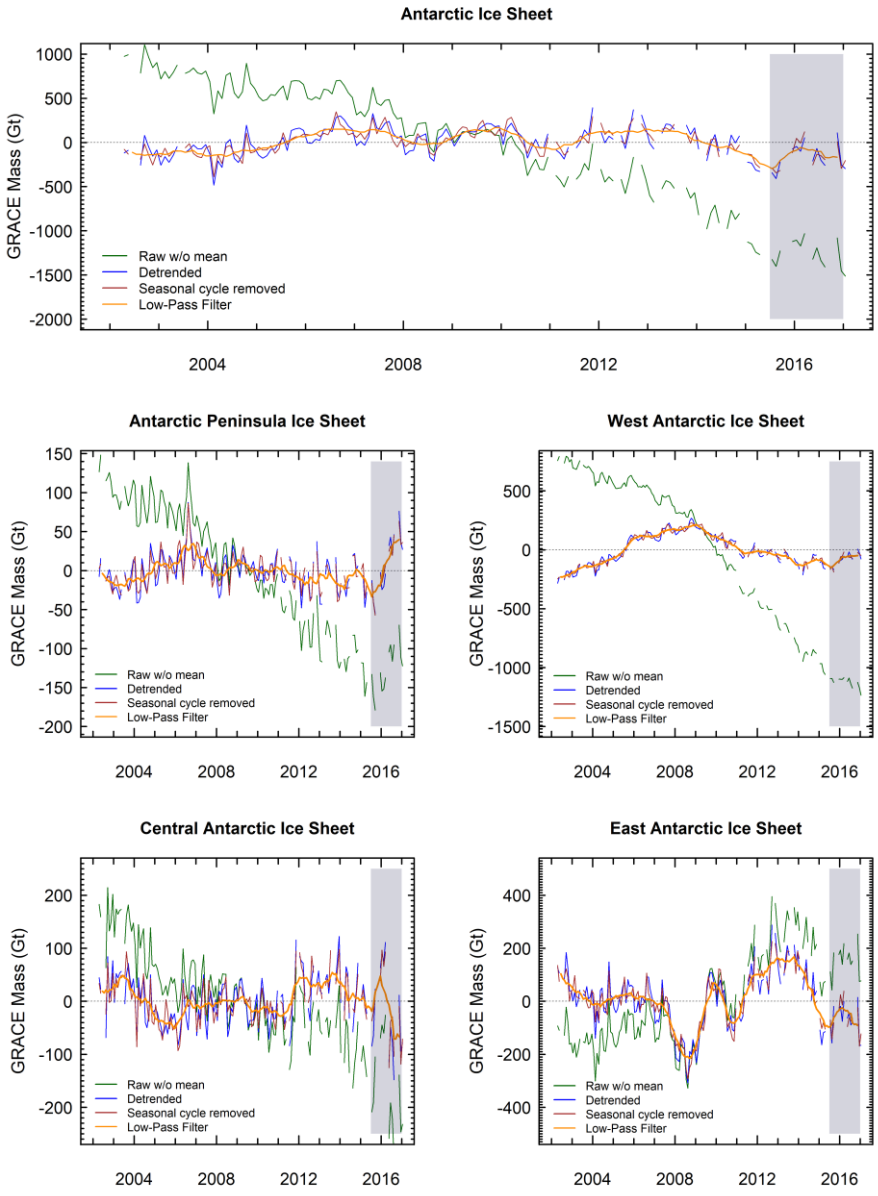

Figure 6. Sample dataset showing the impact of each post-processing methods used to obtain the GRACE time series for each of the four regions for 2002-2017. The grey box represents the 2015-16 El Niño period.

For each data point: (1) the mean was removed (Figure 6, green line), (2) the field was detrended using linear regression to obtain detrended mass anomalies (Figure 6, blue line); (3) the mean seasonal cycle was obtained by calculating the mean of all January months, February months, and so on until December, and then subtracting the mean January from all January months, the mean February from all February months, and so on until the December months (Figure 6, red line); and (4) the data was then filtered using a moving-window average (box-car) filter of length 13 months in order to better assess inter-annual variability in the data, since ENSO is an interannual phenomenon (Figure 6, orange line).

Unfortunately, due to recurrent battery management problems on the GRACE satellites, many data gaps are present in the data, restricting the analysis of data prior and post El Niño (see https://grace.jpl.nasa.gov/data/data-updates). In total, 24 out of 192 months were missing in the GRACE dataset (Supplementary Table 1). To counteract this issue, the missing months were accounted for during the detrending and the removal of the seasonal cycle, and any monthly gap in the data was filled by the box-car filter method (Figure 6).

The GRACE mass change anomaly maps in Figure 9 and 11 (Chapter 4.1) were created to represent mass change relative to the local trend at each point. They represent detrended mass change anomalies and are a visual representation of the time series in Figure 10 and 12. In certain cases, it is possible that the mass changes observed by GRACE on these maps are partly related to changes in ice dynamics, although we have minimised ice-dynamical influences by removing the secular trend in our datasets by means of linear regression. The reasoning behind comparing those with the Surface Mass Balance (SMB) precipitation time series in Figure 10 and 12 was to determine whether precipitation rates were at all dominant in the observed interannual fluctuations observed by GRACE, or whether other factors were responsible for the changes. The basin time series in Figure 12 were obtained by integrating the 27 drainage basin areas. These were obtained by creating a basin mask containing the longitude and latitude points for each basin. The data was then placed onto a perfect grid with regular spacing by incorporating the Earth authalic radius and transforming the latitudes from degrees to radians.

This is because projecting data onto a spherical grid can represent a source of error since not all area cells along the North/South meridian lines are of equal size, resulting in the grid cells decreasing in area towards the pole (Santini et al., 2010) (Figure 7). Indeed, as opposed to the parallels which remain constant from pole to pole, the meridians at the equator will be different from those at the poles, resulting in a change in the shape of cells from spherical quadrangles to spherical triangle where the meridians converge poleward (Figure 7).

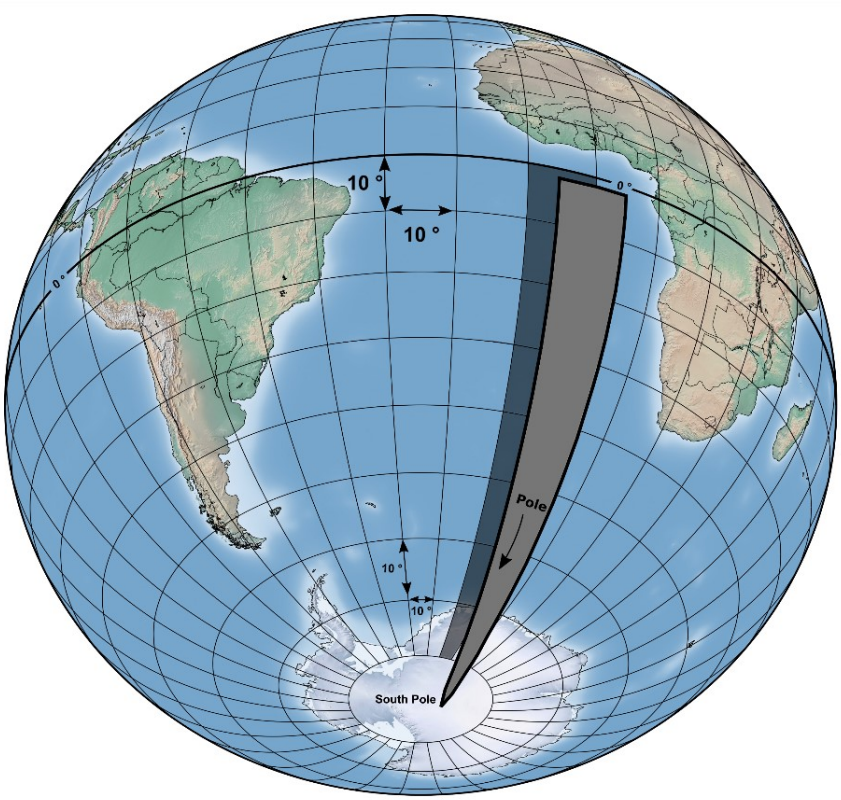

Figure 7. Example of a spherical grid with a cell size of 10° along the X (longitude) and Y (latitude) grid dimensions. As meridians converge towards the poles, the cells' shape extends poleward and becomes similar to the shape of a spherical triangle (see in dark grey on the image) whilst the distance between each parallel remains constant.

As previously mentioned in Chapter 2.7.2., previous research (Ledley and Huang, 1997; Klein et al., 1999; Kwok and Comiso 2002) has shown that the atmospheric and ocean responses in the high latitudes lags the ENSO signal in the Pacific by a few months. Therefore, in order to answer Research Question 3 and understand if the changes observed over the ice sheet are proportional to the strength of El Niño events and whether the signal is instantaneous (delayed) and homogenous (inhomogeneous), a lag analysis of the Antarctic response to the peak month of El Niño events was conducted on a monthly basis, where lag 0 represents the

peak month of ENSO in the Pacific, lag 1 represents a month following the peak month in the Pacific, lag 2 represents two months after, and so on until lag 12.

3.2. Surface Mass Balance Time Series

On the assumption that El Niño events primary influence mass balance changes as a result of changing precipitation rates, Surface Mass Balance (SMB) time series from the ERA gridded precipitation dataset (http://www.ecmwf.int) were derived by integrating the precipitation fields for each of the 27 drainage basin areas to create cumulative precipitation estimates. These SMB time series were integrated forward in time from the start of the dataset to provide El Niño-related mass change estimates. Since precipitation is positive (and thus cumulative), the resulting time series increase monotonically and can therefore be compared with the GRACE Mascons time series.

3.2.1. Surface Mass Balance Time Series Post-Processing Methods

Since the interest of this study is to assess interannual fluctuations relative to the long-term trend, a similar approach to the GRACE post-processing methods was used where, for each point in the time series, the mean was removed, the dataset detrended using linear regression, and the seasonal cycle was removed as described in the GRACE post-processing methods chapter (see Figure 6 for similar steps). A 13-month boxcar filter of the length of the GRACE period was also applied to obtain interannual fluctuations in mass due to fluctuations in precipitation rates. In order to make the two datasets as comparable to each other as possible, the missing months in the GRACE dataset were also masked in the ERA dataset in preparation for the box-car filtering process. Similar to the GRACE post-processing methods, it was necessary to place the ERA precipitation dataset onto a new generic cell area grid with regular spacing (Figure 7). The pointwise time series were then integrated per basin area to obtain basin mass change time series in gigatons. Lastly, since mass balance changes are given relative to the long-term mean field, the first data point in the starting month of the time series has a value that is either positive or negative, rather than starting from zero.

3.3. Meteorological and Ocean Datasets

In order to answer Research Question 1, composite maps of Mean Sea Level Pressure (MSLP) and Total Precipitation (TP) from the ERA-Interim products (http://www.ecmwf.int) were produced to observe the response of atmospheric conditions over Antarctica to El Niño events. The ERA-Interim mission is the latest global atmospheric reanalysis product produced by the European Centre for Medium-Range Weather Forecasts Reanalysis (ECMWF) and is one of the most reliable reanalysis datasets for assessing atmospheric conditions over Antarctica (Bromwich et al., 2011; Nicolas and Bromwich, 2011; Bracegirdle and Marshall, 2012). It uses a fixed version of numerical weather prediction systems to produce gridded datasets of reanalysed data without the influence of spurious trends associated with common versions of numerical weather prediction systems (Dee et al., 2011).

Similarly for ocean conditions, composite maps of Sea Surface Temperature (SST) and Sea Ice Extent (SIE) were produced using the National Oceanic and Atmospheric Administration's OISST V2 (NOAA; https://www.esrl.noaa.gov) one-degree grid dataset. This allowed for a more comprehensive understanding of El Niño's influence on ocean conditions around Antarctica and on the difference in timing between atmospheric and ocean conditions following interannual events. The OISST V2 Sea Ice concentration data was obtained from satellite-based passive microwave and infrared observations and a range of *in situ* and aircraft observations; whilst the OISST V2 Sea Surface Temperature data was obtained from *in situ* (ships and buoys) and high-resolution radiometer satellite, allowing to provide measurements for sea ice-covered areas (Reynolds et al., 2002). Sea Ice Extent values below 15% concentration were masked out for the final analysis in order to observe the total Antarctic sea ice extent (the cumulative area of ocean covered by sea ice) (Liu et al., 2004). The incentive behind the composite maps was to compare them directly to the GRACE Mascons and SMB time series in order to identify areas of high ENSO sensitivity, as well as to compare the composite maps from 2015-16 with composite maps from previous events to identify potentially similar patterns in ENSO's response over and around the Antarctic Ice Sheet.

3.3.1. Meteorological and Ocean Datasets Post-Processing Methods

All meteorological and ocean datasets were processed in a similar manner as for the GRACE mass change and SMB time series. First, the datasets were detrended using linear regression to obtain detrended anomalies. Then, following the methods from Chapter 3.1.1., the mean seasonal cycle was calculated for all 12 months of all the years of the study period and the mean removed from each dataset. Once the seasonal cycle and trend were excluded and the filtering was applied, composite maps were produced following similar methods to Fogt et al. (2011) and Welhouse et al. (2016) by calculating monthly means and standard deviations using the period 1979-2017 as the base period. The monthly means and standard deviations were then combined to include all months where El Niño anomalies were above the threshold of +0.5^{o}C (see Chapter 3.4). As for the GRACE processing (Chapter 3.1.1.), we also conducted a lag analysis for all the meteorological and ocean datasets to assess the time lag between the onset of ENSO in the Pacific and the first signs of El Niño anomalies around Antarctica.

3.4. Niño Index

ENSO events are categorised based on the definition of NOAA's Climate Prediction Centre (CPC; http://www.cpc.ncep.noaa.gov), where warm and cold ENSO events are defined as 5 consecutive overlapping months at or above the threshold of ± 0.5° C anomaly for the Niño 3.4 region (5^{o}N-5^{o} S, 120^{o}-170^{o} W). This anomaly threshold is further broken down into ENSO sub-categories: Weak (0.5 to 0.9 ^{o} C anomaly), Moderate (1.0 to 1.4 ^{o} C), Strong (1.5 to 1.9 ^{o} C), and Very Strong (> 2.0 ^{o} C) (Figure 8) (see Supplementary Table 2). Weak El Niño events were removed from the analysis due to their inability to project a Rossby wave strong enough to reach the Southern Ocean and result in strong enough anomalies in atmospheric conditions (Fogt et al., 2011). This results in seven El Niño intervals (three very strong, two strong and two moderate) corresponding to 84 months of El Niño anomalies for the period 1979-2017 (Figure 8, Supplementary Table 2). The analysis was then narrowed down to the peak month of El Niño event (Supplementary Table 2) and an estimate of the time it takes for the signal to reach Antarctica was given (i.e. for the 2015 El Niño, zero lag represents November 2015, herein referred to as *NOV15*).

Due to the little amount of change in atmospheric and ocean circulation observed over Antarctica following La Niña events, we narrowed the analysis down to El Niño events only. Moreover, only strong and very strong El Niño events were considered for the final analysis due to the little amount of change in atmospheric and ocean conditions around Antarctica following Moderate events. However, when necessary, some references to Moderate events are included in the text.

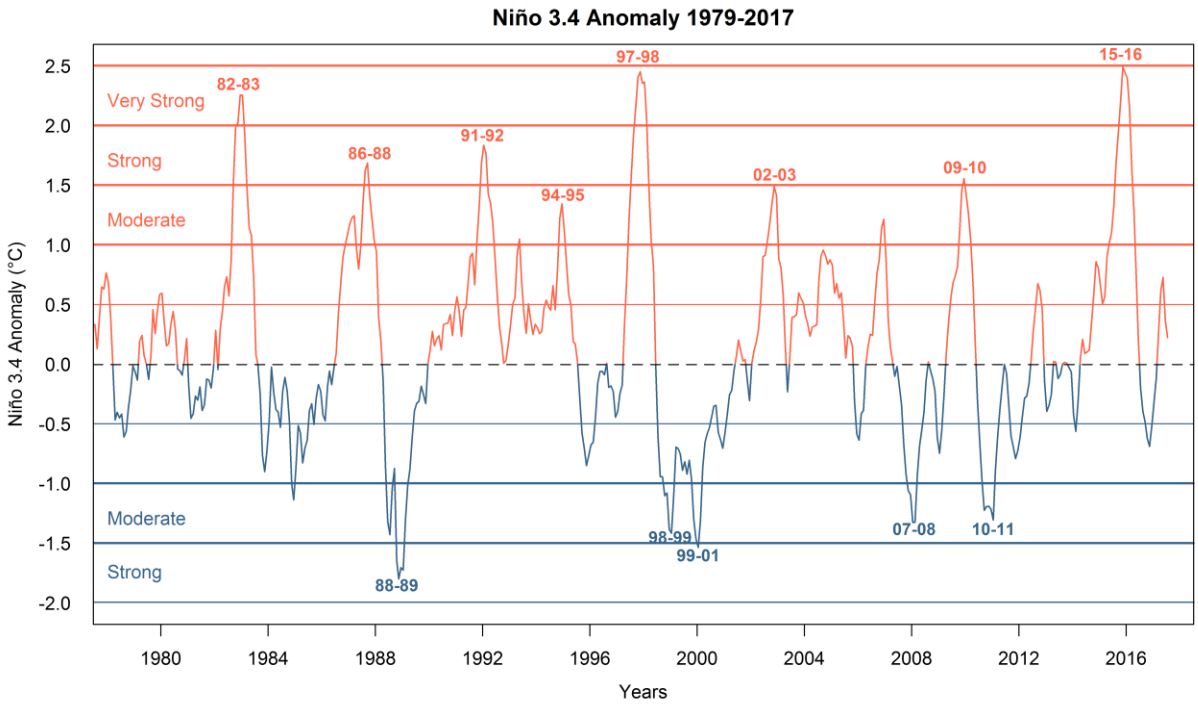

Figure 8. Monthly ENSO anomalies for the period 1979-2017 in degrees Celsius. Bold horizontal lines represent the different sub-categories (Moderate, Strong, and Very Strong). Red and blue colours show the El Niño and La Niña values respectively. See Supplementary Table 2 for more details.

Previous studies have highlighted the strong link between ENSO and the Southern Annular Mode (SAM), the second most important source of atmospheric variability over the AIS (Fogt and Bromwich, 2006; Stammerjohn et al., 2008; Pohl et al., 2010; Yeo and Kim, 2015; Welhouse et al., 2016). The Southern Annular Mode is a dominant mode of atmospheric conditions that can change from a positive to a negative state (Thompson and Wallace, 2000). This change in atmospheric conditions can impact air-sea ice interactions and Ekman flow by modifying the direction or the strength of surface westerly winds, driving Sea Surface Temperature anomalies (Stammerjohn et al., 2008). Whilst a lot of research has been conducted on the influence of

the SAM on Antarctica, less is known of the effects of El Niño on the Antarctic Ice Sheet. This study does not include any analysis of the SAM, therefore its influence on meteorological conditions over Antarctica on interannual timescales cannot be excluded. However, the SAM has been largely positive since the mid-1960s, owing partly to ozone depletion and carbon emissions following the industrial revolution (Thompson and Solomon, 2002, Marshall, 2003). Although seasonal changes in the strength and polarity of the SAM have been shown to affect ENSO's response over Antarctica (Stuecker et al., 2017), we followed the method of previous studies (Boening et al., 2012; Welhouse et al., 2016) and relied on the detrending of the data and the removal of the seasonal cycle as sufficient measures to exclude strong influences of the SAM on our results. This, at first can appear controversial, considering the importance of the SAM in shaping the atmospheric circulation of Antarctica and the complexity in separating the SAM and ENSO signals (Nicolas et al., 2017). However, this method has been successfully used elsewhere and has allowed for an in-depth analysis of ENSO's effect on Antarctica (i.e. Cullather et al., 1996; Renwick, 1998; Welhouse et al., 2016).

4. Results

4.1. Changes in Antarctica's Mass Balance following the 2015 El Niño

This study begins by considering the changes in mass over the Antarctic Ice Sheet as observed by GRACE. When analysing the GRACE anomaly maps following the 2015-16 El Niño, we observe a positive anomaly over the APIS region and the WAIS from lag 1 to lag 7 (Figure 9). Comparatively, we observe a negative anomaly over the Antarctic interior, and a more pronounced negative response over the East Antarctic sector, mainly over basins 12 and 13 (Figure 9 and Figure 11).

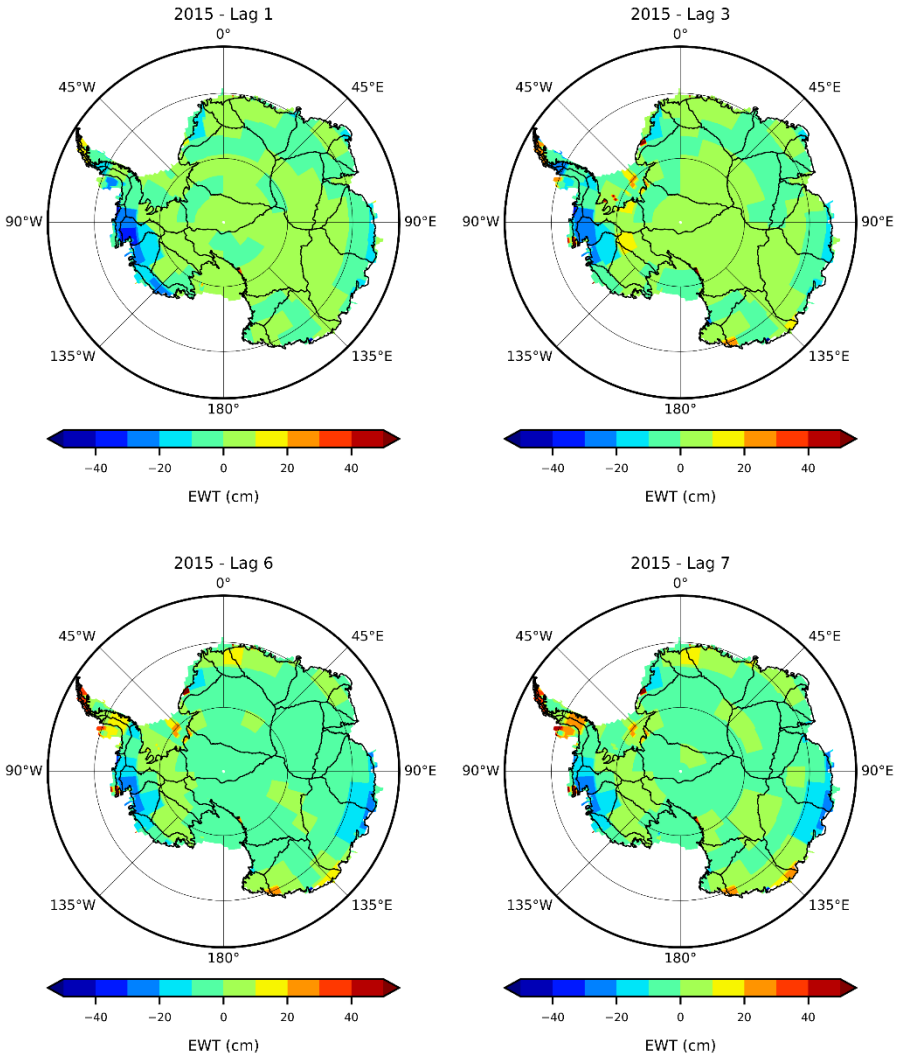

Figure 9. Detrended GRACE mass change anomalies at a continental level for the selected lags following the 2015-16 El Niño. Black lines represent the basin outlines. Refer to Figure 5 for details on basin IDs. Units are Equivalent Water Thickness (EWT) in centimetres.

Analysis of continent-wide estimates of mass changes from the GRACE Mascons shows an initial increase of +155 Gt over the AIS between mid-2015 and the beginning of 2016 to reach values of-75 Gt, followed by a delayed decrease of-100 Gt, to reach values of-175 Gt by the end of 2016 (Figure 10). Prior to the 2015 El Niño, a strong and consistent negative anomaly is observed over the entire AIS which was initiated at the beginning of 2013 and reached values of-230 Gt in 2015, its lowest value since the start of the first GRACE measurements in 2002.

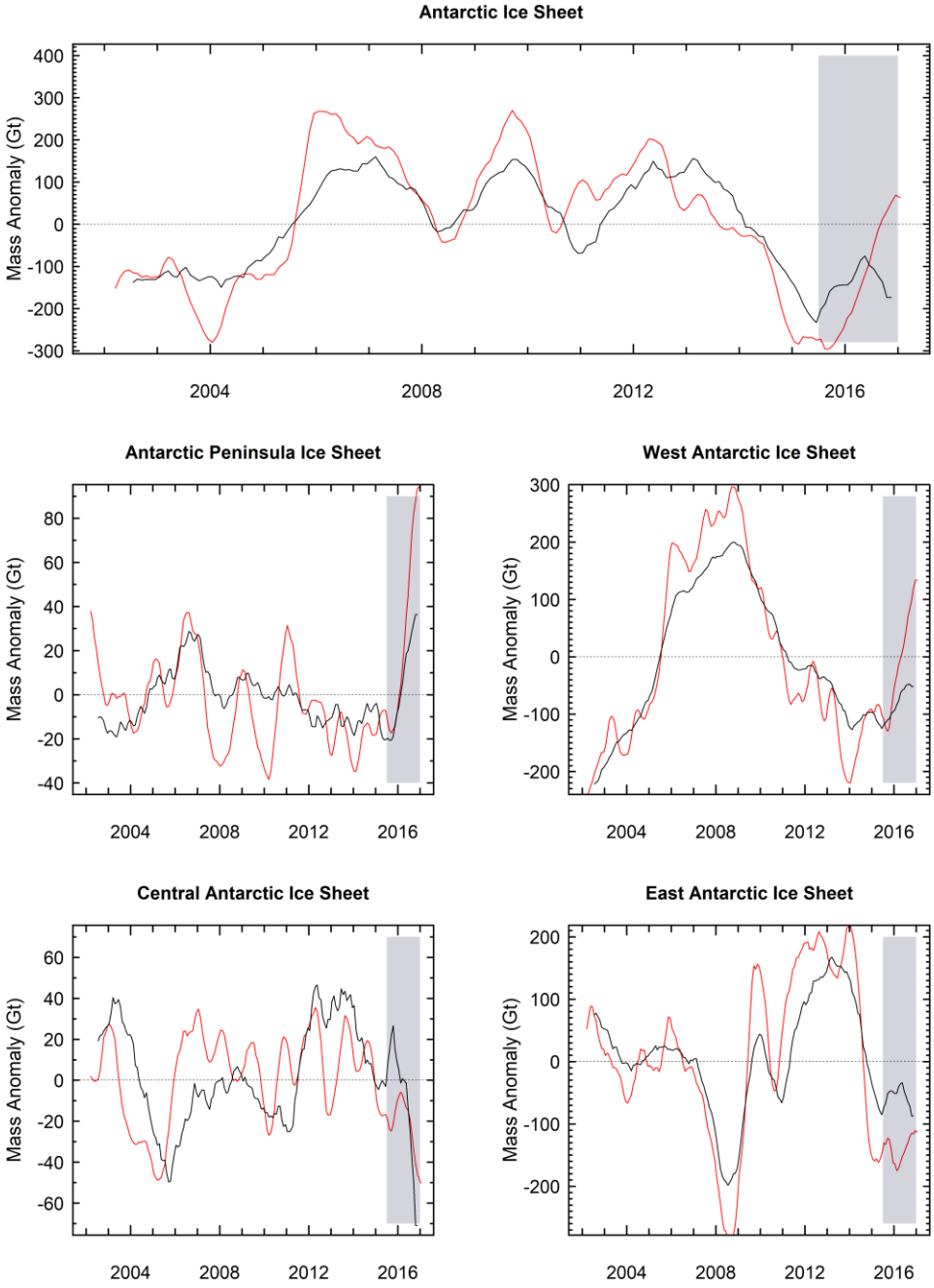

Figure 10. GRACE mass change (black) and Surface Mass Balance time series from integrated ERA precipitation (red) in gigatons for each of the four regions between 2002 and 2017. The grey box represents the 2015-16 El Niño period.

We attribute this initial increase and delayed decrease post-2015 to regional changes in mass. Firstly, the response of the Antarctic Peninsula Ice Sheet (APIS) and West Antarctic Ice Sheet (WAIS) to the 2015 El Niño is almost instantaneous and in line with the development and peak of El Niño in the Pacific. We observe a positive response over the APIS region, from-20 Gt prior to NOV15 to +35 Gt in December 2016, along with a positive anomaly over the WAIS, which appeared to gain from-125 Gt prior to NOV15 to-50 Gt post El Niño. This results in the APIS and WAIS gaining +55 Gt and +75 Gt respectively from NOV15 onwards, which corresponds to the initial increase in mass observed over the AIS. Secondly, we observe a delayed decrease in the Central Antarctic Ice Sheet (CAIS) from 0 Gt in early 2016 to-70 Gt post El Niño. This pattern is also observed over the East Antarctic Ice Sheet (EAIS) where we detect a delayed decrease in mass of-55 Gt, 3 to 4 months following NOV15. Although the delay in the post-Niño response is more obvious over the EAIS than over the CAIS, we observe a similar negative response on both regions following the 2015-16 El Niño. Thus, the initial positive response over the AIS appears to be dominated by the positive anomalies over the APIS and WAIS regions. This is then followed by a delayed negative response over the AIS when the negative anomalies over the CAIS and EAIS dominate, with a 3 to 4-month delay (Figure 10).

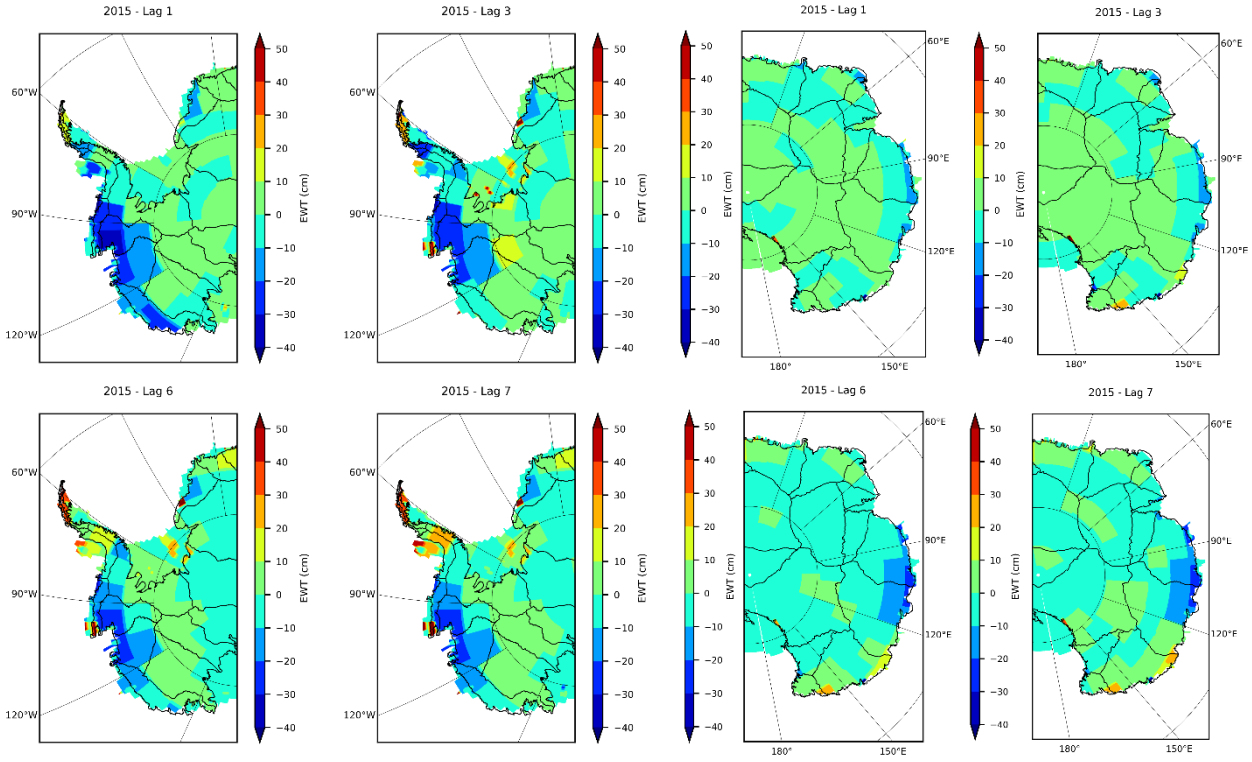

Figure 11. Detrended GRACE mass change anomalies at a regional level for the selected lags following the 2015 El Niño. The four panels on the left represent the APIS and WAIS, and the four panels on the right represent the CAIS and EAIS. Black lines represent the basin outlines. Refer to Figure 5 for details on basin IDs. Units are Equivalent Water Thickness (EWT) in centimetres.

When considering changes at a basin-scale level, we observe a large positive anomaly on the GRACE Mascons time series in the APIS basins post-El Niño (Figure 11), which resulted in a gain of +20 Gt in basin 24 and +10 to +15 Gt in basins 25-27 by the end of 2016 (Figure 12). A similar positive response is observed across all WAIS basins, although more pronounced in basins 1, 18, and 22-23 with a gain of between +10 and +20 Gt post-2016 (Figure 12).

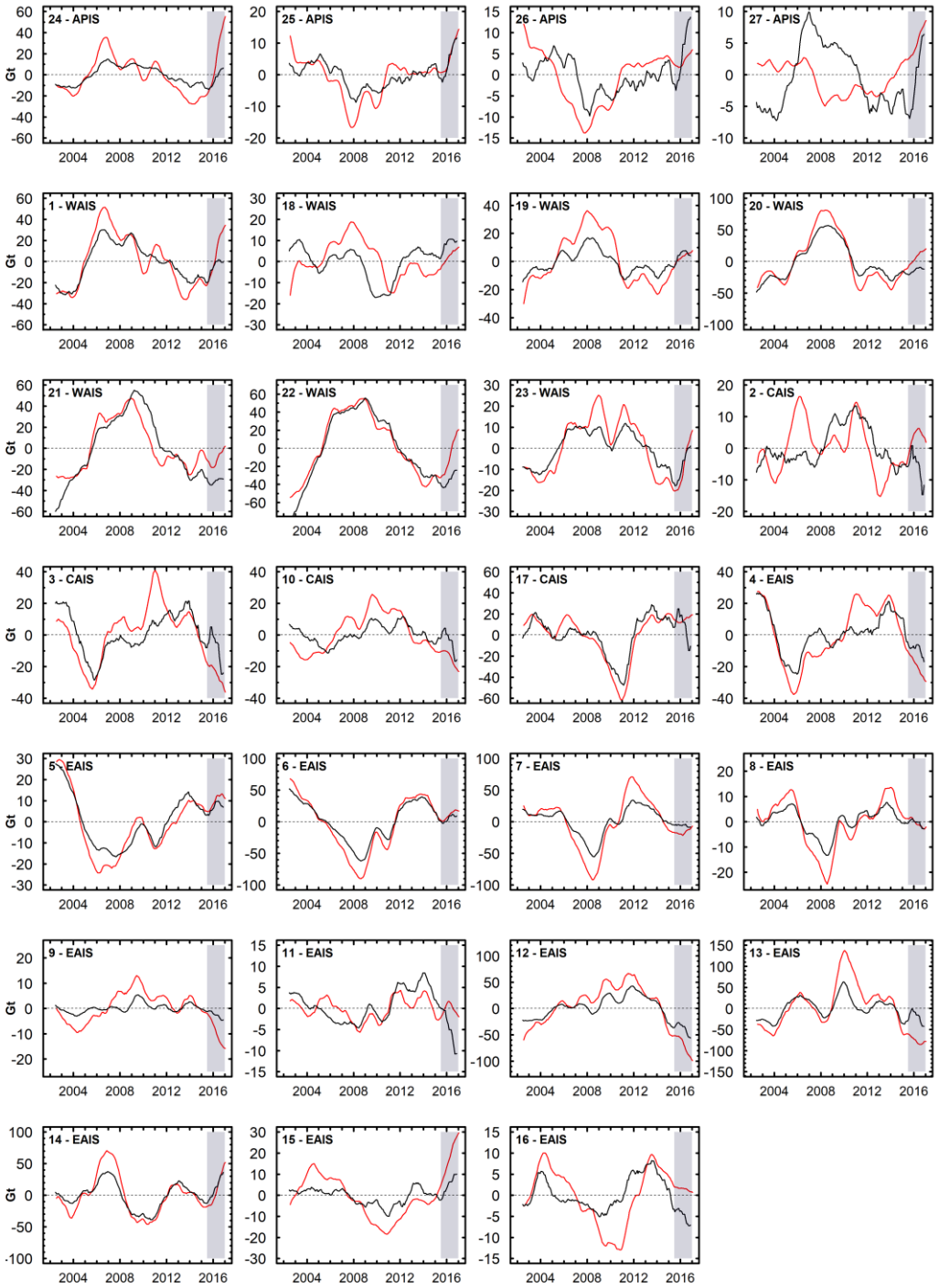

Figure 12. GRACE mass change (black) and Surface Mass Balance time series from integrated ERA precipitation (red) in gigatons for each of the 27 drainage basins per region between 2002 and 2017. The grey box represents the 2015-16 El Niño period.

For the CAIS, we observe a delayed decrease of-10 to-15 Gt for basins 2 and 10, and of-20 to -25 Gt in basins 3 and 17. The basins found in the EAIS region also experienced a delayed decrease in early 2016 of between-10 and-30 Gt, mainly for basins 4, 6, and 11-13. We also detect an increase of +25 and +10 Gt in basins 14 and 15 respectively, whilst other basins on the EAIS, namely basins 7-9 and 15, showed little or no change (Figure 12).

4.1.1. Comparison between GRACE and Surface Mass Balance Time Series

This study then considers how the changes observed by GRACE compared with the Surface Mass Balance time series from the ERA precipitation dataset. Although GRACE captures the entire mass signal over Antarctica, the SMB time series provide additional support to the GRACE results. Analysis of continent-wide estimates of cumulative precipitation shows a positive response post-El Niño, confirming the positive changes in mass over the APIS and WAIS observed by GRACE (Figure 10). Before the development of the 2015-2016 El Niño, we observe a large decrease in cumulative precipitation over the AIS, reaching values of-280 Gt. This is followed by an increase of +305 Gt post-Niño to reach +25 Gt by the end of 2016 (Figure 10). At a regional level, cumulative precipitation estimates increased significantly towards the end of 2015 for the APIS (+100 Gt) and WAIS (+200 Gt) to reach values of +85 and +100 Gt respectively post-Niño, whilst the CAIS experienced a decrease of-25 Gt to reach values of-40 Gt, and the EAIS experienced an increase of +30 Gt following a very strong decrease since 2014 (Figure 10, Table 1).

Comparison between GRACE and ERA time series post-2015							
APIS		**WAIS**		**CAIS**		**EAIS**	
GRACE	**ERA**	**GRACE**	**ERA**	**GRACE**	**ERA**	**GRACE**	**ERA**
+55 Gt	+100 Gt	+75 Gt	+200 Gt	-70 Gt	-25 Gt	-55 Gt	+30 Gt

Table 1. Comparison between the detrended GRACE Mascons and the ERA Surface Mass Balance time series following the 2015-16 El Niño in gigatons for each of the four regions.

At a basin-scale level, we observe a strong increase in precipitation of between +20 and +30 Gt in basins 6-7, 14-15, 21, and 23, and a more significant increase of between + 50 and +70 Gt in basins 1, 22, and 24 (Figure 12). We also observe a small decrease of up to-15 Gt in basin 11, and a stronger decrease of up to-50 Gt in basin 12. Other basins experienced little changes in precipitation, namely basins 2, 5, 8, 13, 16-18, and 25-26, whilst others experienced a continuous decrease (3-4 and 9) and increase (19-20, 27) initiated around 2014 (Figure 12). Overall, the most responsive basins to the 2015 El Niño appear to be in the APIS and WAIS regions, as well as basins 6 (Dronning Maud Land) and 12-14 (Wilkes Land) in the EAIS.

Although we find a good agreement between the ERA-Interim SMB and the GRACE time series for several regions and drainage basins, we also note that some disparities exist over all four regions. Indeed, although the cumulative precipitation estimates show the general increase over the APIS and WAIS, they strongly overestimate mass changes over those regions compared with the GRACE Mascons, from +100 Gt (ERA) to +55 Gt (GRACE) for the APIS, and from +200 Gt (ERA) to +75 Gt (GRACE) for the WAIS (Figure 10, Table 1). For the CAIS and EAIS, we observe an underestimation of mass changes for the cumulative precipitation estimates compared to the GRACE Mascons, from-25 Gt (ERA) to-70 Gt (GRACE), and we note that the SMB time series do not capture at all the decrease from the GRACE Mascons post-2015 (+30 Gt for ERA compared with-55 Gt for GRACE) (Figure 10, Table 1). The reasons for these differences are explored further in the Discussion section of this thesis.

4.2. Changes in Atmospheric Conditions following the 2015-16 El Niño

The following chapter discusses how the mass changes observed by GRACE and the SMB estimates relate to changes in atmospheric circulation over the Antarctic Ice Sheet following the 2015-16 El Niño. Analysis of atmospheric indices (Mean Sea Level Pressure and Total Precipitation) shows that strong anomalies in atmospheric conditions moved poleward during the event and peaked in intensity over Antarctica 6 months after the peak El Niño month in the Pacific. This is shown by the presence of a large high-pressure centre off the coast of the Antarctic Peninsula and over the Drake Passage (Figure 13-14). The pressure system over Drake

Passage is also accompanied by three low-pressure systems over Dronning Maud Land, off Wilkes Land and over the Amundsen Sea coast in 2015-16. The high-pressure system appears to develop slowly in lag 5 off the ABS sector, and subsequently gains in intensity and moves eastward towards the Antarctic Peninsula in lag 6 to reach values of +24 hectopascals (hPa) (Figure 13). In lag 7, the system has lost in intensity and moves northward over South America. This leaves space for two large low-pressure systems to develop over the Amundsen Sea and the Antarctic interior with values of up to -18 hPa (Figure 13). The high-pressure system observed in lag 6 in 2015-16 is by far the strongest high-pressure system observed in this study.

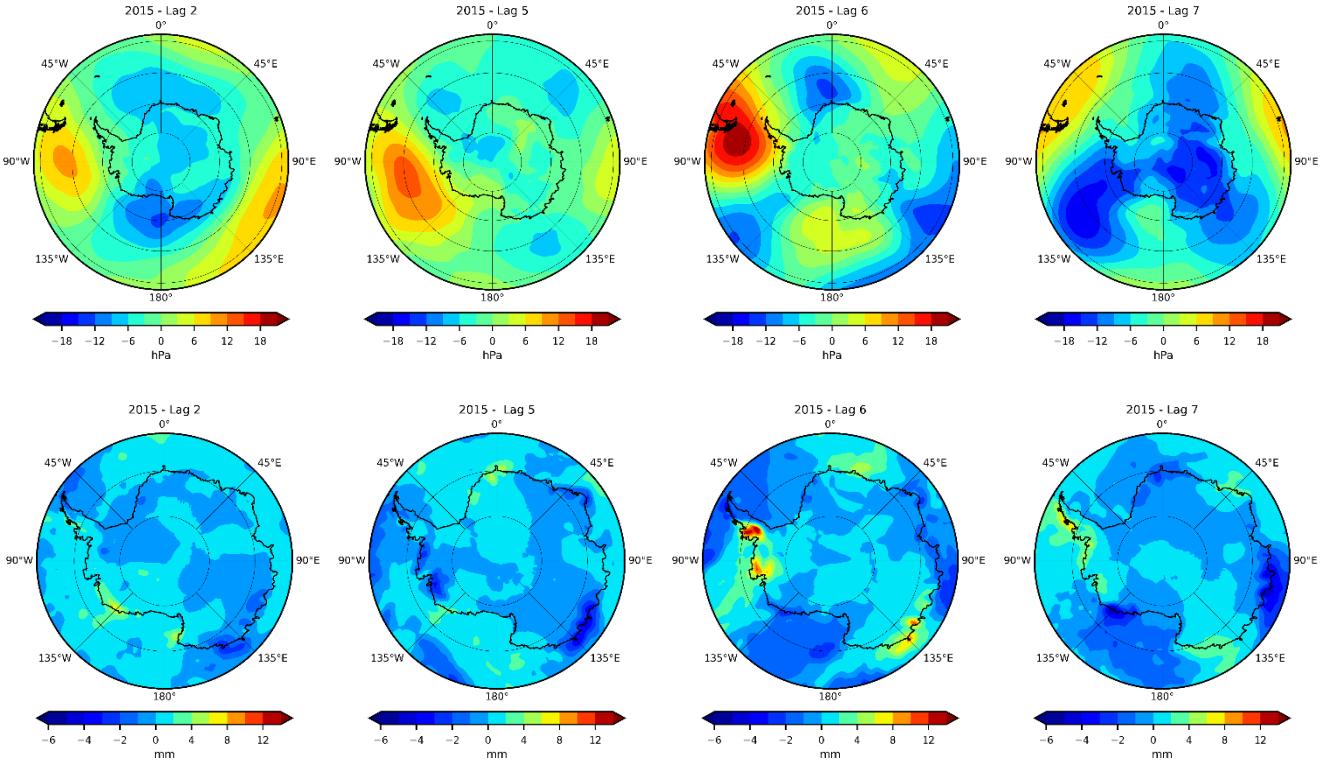

Figure 13. Mean Sea Level Pressure (top) and Total Precipitation (bottom) anomalies following the 2015-16 El Niño for the selected lags.

The formation of the high-pressure system in lag 5, and its subsequent peaks in lag 6 agrees well with changes in total precipitation over the continent. Particularly, the anti-clockwise (clockwise) motion of the high (low) pressure centres brings warm moist (cold dry) air from the ocean on the western flanks of the system, and cold dry (warm moist) Antarctic air from the interior to the sea on its eastern side. This is observed following the 2015 El Niño event where the strong high-pressure system over Drake Passage brings moist air to the Bellingshausen sector of the APIS as well as over Ellsworth Land, resulting in large accumulation rates of up to

+14 mm (Figure 13). Elsewhere, an increase in precipitation is visible over Dronning Maud Land (+6 mm) and Terre Adélie (+10 mm), both situated on the eastern flanks of the two low-pressure systems (Figure 13). East Antarctica is particularly affected by the low-pressure system in the Western Pacific Ocean which moves inland from lag 6 to lag 7 and leads to a decrease in precipitation of up to -6 mm in this sector in lag 7. The presence of the high (low) pressure systems and related precipitation anomalies over the APIS and WAIS (EAIS) regions agree well with the changes in mass observed over those basins in Figure 10 and 12. This suggests that the changes in mass observed by GRACE over those sectors are driven by changes in atmospheric conditions following the 2015-16 El Niño.

4.3. Changes in Atmospheric Conditions following Previous El Niño events

One of the remaining question is whether the patterns observed following the 2015-16 El Niño are reflective of previous very strong El Niño events. Determining an overall ENSO signature around Antarctica is difficult, mainly due to the availability and quality of reanalysis datasets prior to 1979 (see Chapter 5.1). However, when comparing atmospheric conditions following previous El Niño events since 1979, we observe strong similarities between the 2015-16 El Niño and the 1997-98 El Niño for both mean sea level pressure and precipitation datasets (Figure 13-14). Our analysis shows that precipitation rates following the 1997-98 event appear to increase in lag 5 and 6 in the ABS sector of the APIS, along with a decrease over Queen Mary Land and Wilkes Land (Figure 14).

These precipitation rates appear to be driven by the high-pressure system that develops in lag 5 and peaks in lag 6, although it is relatively weaker (up to 18 hPa) than the high-pressure system post-2015 conditions, and its position is much closer to the ABS coast (Figure 14). Over the East, a low-pressure system also develops over the interior in lag 5 but loses in strength and migrates poleward between 90° E and 120° E. Similar to post-2015 El Niño conditions, a low-pressure system develops in lag 7, which appears to correspond to the return of the Amundsen Sea Low (Figure 14).

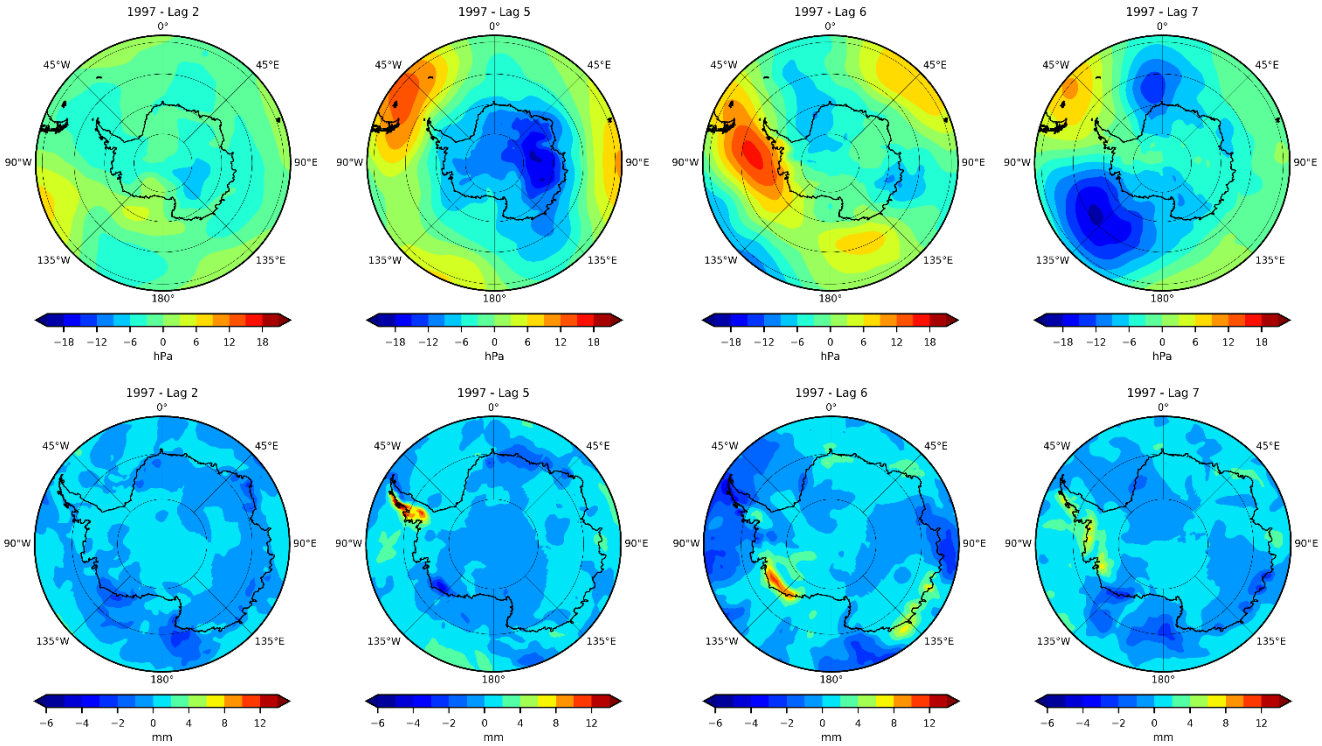

Figure 14. Mean Sea Level Pressure (top) and Total Precipitation (bottom) anomalies following the 1997-98 El Niño for the selected lags.

Due to the strong similarities in atmospheric conditions between the 1997-98 and the 2015-16 El Niño, SMB time series from the ERA dataset were computed for the period 1986-1999 to assess the difference in cumulative precipitation rates at a continental, regional and basin-scale level, and assess how those compared with the 2015-16 El Niño (Figure 15-16).

On a continental scale, we observe a small increase in cumulative precipitation post-1997 of +70 Gt, compared to an increase of +305 Gt post-2015 (Figure 15). On a regional scale, the APIS and WAIS appear to gain mass almost instantaneously, with an increase of +25 and +70 Gt respectively following the 1997-98 El Niño, compared with +100 and +200 Gt post-2015 (Figure 15, Table 2). Likewise, the CAIS the EAIS show similar patterns to the 2015-16 events, with a small decrease in the CAIS region of -20 Gt (as opposed to -25 Gt in 2015-16), and a small increase of up to +55 Gt (compared with +30 Gt in 2015-16) in the EAIS region (Figure 15, Table 2).

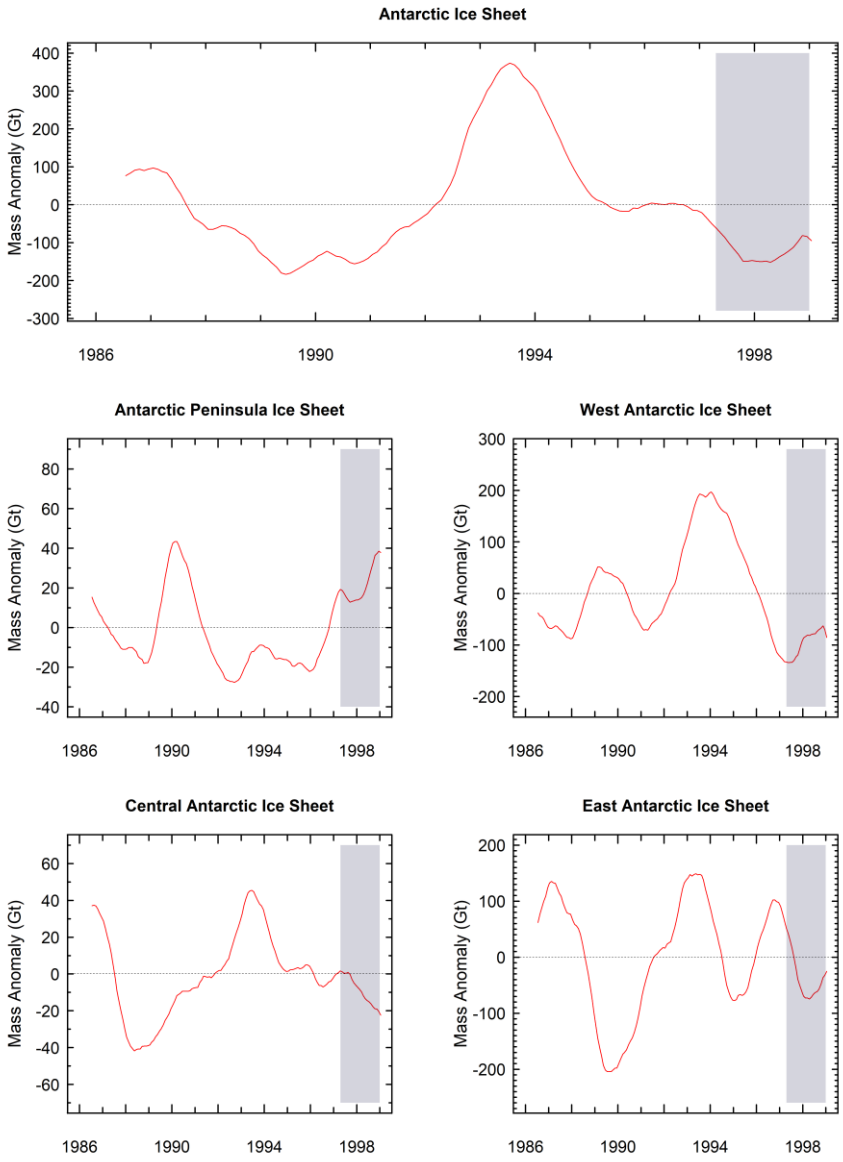

Figure 15. Surface Mass Balance time series from integrated ERA precipitation in gigatons for each of the four regions between 1986 and 1999. The grey box represents the 1997-98 El Niño period.

Overall, all regions show similar patterns to those observed post-2015 conditions but on much smaller scale for the AIS, APIS and WAIS, and on a similar scale for the CAIS and EAIS (Table 2).

Comparison of ERA time series between 2015-16 and 1997-1998							
APIS		**WAIS**		**CAIS**		**EAIS**	
2015	**1997**	**2015**	**1997**	**2015**	**1997**	**2015**	**1997**
+100 Gt	+25 Gt	+200 Gt	+70 Gt	-25 Gt	-20 Gt	+30 Gt	+35 Gt

Table 2. Comparison in ERA Surface Mass Balance time series estimates between the 2015-16 El Niño and the 1997-98 El Niño in gigatons for each of the four regions.

At a basin-scale level, we observe similarities between the 1997-98 and 2015-16 events, mainly for basins 21 to 25 where we observe a positive response following the 1997-98 El Niño, confirming further that these two regions are particularly sensitive to ENSO variability. Similar decreases are observed in basins 2-4, and similar increases but of smaller extents are observed in basins 6 and 7 (Figure 16).

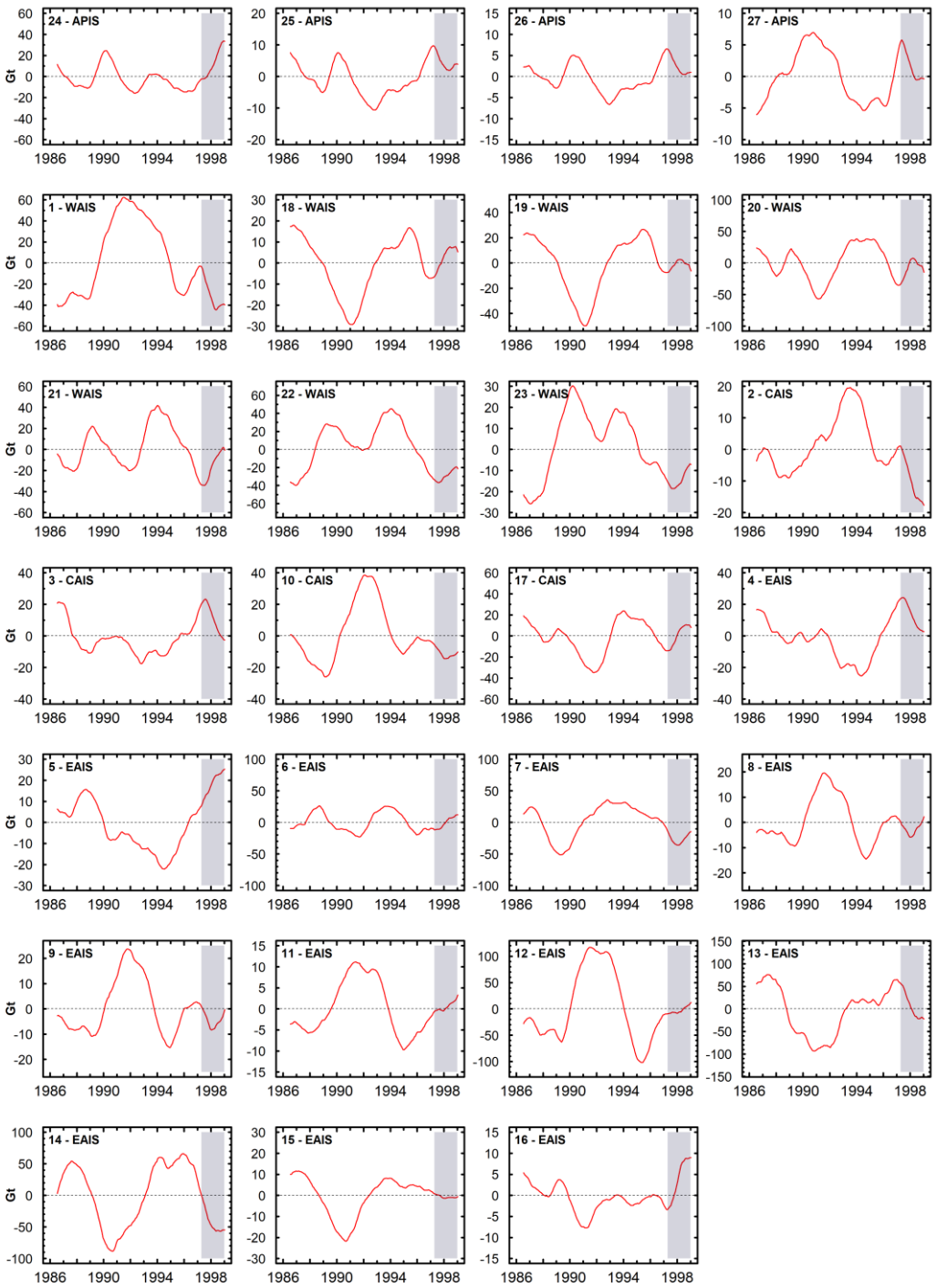

Figure 16. Surface Mass Balance time series from ERA Precipitation in gigatons for each of the 27 drainage basins per region between 1986 and 1999. The grey box represents the 1997-98 El Niño period.

The similarities between both very strong El Niño events over Dronning Maud Land and the Weddell Sea suggests that these sectors are highly sensitive to El Niño's influence. Other basins show little or no changes, such as basins 5, 10-11, 13-15, 19, and 26-27. Basins 5, 8-9, 12, and 16-18 show small increases of up to +20 Gt, whilst other basins, mainly basin 20, experienced a decrease of up to -25 Gt (Figure 16).

Although we observe similar results for the SMB time series post-1997 and post-2015, this does not indicate that it is the case for every El Niño event, nor that it is a general pattern observed after every very strong event. To understand how Antarctica is influenced by ENSO events regardless of their magnitude, we computed the standard deviation of the overall anomaly for every peak month of all El Niño events since 1979. Although we observe similar conditions between the overall anomaly and the 2015 El Niño, we also observe strong deviation in the signal for most coastal regions of Antarctica, specifically over the Antarctic Peninsula, ABS sector, and East Antarctica for both mean sea level pressure and precipitation rates (Figure 17).

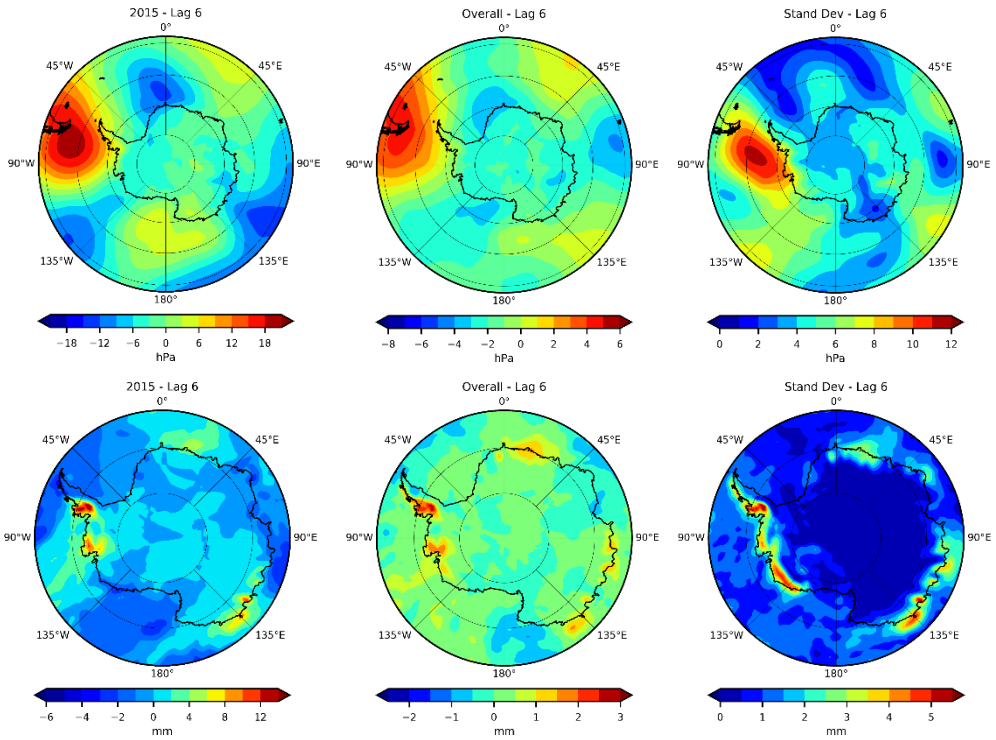

Figure 17. Mean Sea Level Pressure (top) and Total Precipitation (bottom) anomalies for the 2015-16 Lag 6 El Niño compared with the lagged anomaly for the peak month of all El Niño events since 1979 and the lagged standard deviation for both indices. Abbreviation: *Stand Dev* refers to Standard Deviation.

We suggest that the similarities observed between the 2015 El Niño and the overall anomaly might be related to the dominance of key atmospheric patterns following El Niño events of similar magnitude, such as the 1997-98 and 2015-16 events. Indeed, the strong level of variation in the signal, as shown by the standard deviation map, indicates that there does not appear to be a general response in atmospheric circulation over Antarctica following all El Niño events, despite the similarities between the overall anomaly and the 2015 anomaly maps. The lack of consistent patterns across events might results from a difference in the strength of El Niño events since 1979 which can ultimately affect the temporal and spatial response of atmospheric circulation over the ice sheet. Indeed, and with the exception of the 1982-83, 1997-98, and the 2015-16, the strength of previous El Niño events ranged from moderate to strong (although the maxima of all strong events are just above the 1.5° C anomaly, see Figure 8 and Supplementary Table 2). This indicates that aside from the two strongest El Niño events of 1997-98 and 2015-16, there does not appear to be a distinctive response of the ice sheet to changes in atmospheric conditions following El Niño events.

This becomes more apparent when comparing individual anomaly maps for previous El Niño events since 1979, where there is a lack of consistent similarities in atmospheric conditions over Antarctica between events (Supplementary Figures 1-2). Of special interest is the absence of similarities in atmospheric conditions between the 2015-16 El Niño and the 1982-83 El Niño, the second strongest El Niño event of the 20th Century after the 1997-98 event (Supplementary Figure 1-2). Analysis of MSLP does not show the distinctive high-pressure system observed over the ABS sector for the other two very strong events, and anomalies in precipitation rates characterised by an increase (decrease) in the ABS (East) sector are not apparent. This could suggest that little similarities are observed between El Niño events and that the response in atmospheric circulation over the Antarctic Ice Sheet might be influenced by other factors.

4.4. Changes in Ocean Conditions following the 2015-16 El Niño

We then analysed ocean indices of Sea Surface Temperature and Sea Ice Extent to assess the effect of the 2015-2016 El Niño event on ocean conditions around Antarctica. Conditions

following this recent event show a positive SST front moving inward towards the ABS coast between lag 0 and lag 3 and subsequently retreating northward in the following months (Figure 18). This is followed by the development and eastward expansion of a negative water front in the western Pacific Ocean, spreading from 90° E to 150° W. Positive SST anomalies are also present around the eastern flank of the Ross Sea/Amundsen Sea and east of Dronning Maud Land. From lag 0 to lag 6, an anomalous negative water front develops in Drake Passage and quickly extends to cover the Bellingshausen sector the APIS and the Weddell Sea region (Figure 18).

The presence of the anomalous negative SST in Drake Passage favours an abnormally large increase in Sea Ice Extent in the Bellingshausen sector of the APIS, which peaks in lag 6 with a +75 % increase (Figure 18). Elsewhere, there is a reduction in SIE of up to -75% in the Amundsen Sea, but no changes in the Ross Sea sector. The Weddell Sea sector experiences several decreases (up to -30%) and increases (up to +45%). Elsewhere, there is a general decrease near Dronning Maud Land, starting in lag 1 and reaching values of up to -60% in lag 6 and 7. We also observe a slow developing band of increasing SIE off the coast of Willem II Land between lag 1 but peaking in lag 5 and 6 with values of up to +75% (Figure 18).

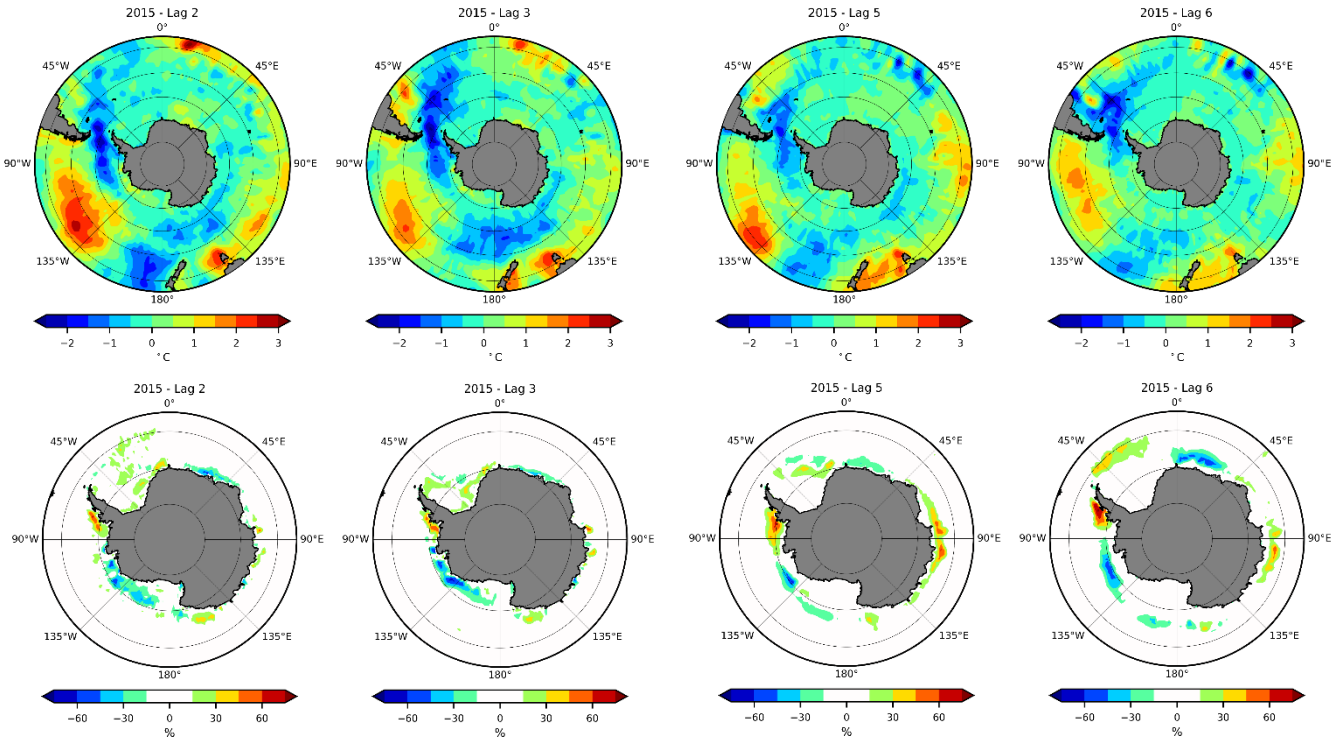

Figure 18. Sea Surface Temperature (top) and Sea Ice Extent (bottom) anomalies following the 2015-16 El Niño for the selected lags.

4.5. Changes in Ocean Conditions following Previous El Niño Events

The results observed following the recent El Niño are then compared with analysis of ocean datasets for previous El Niño events to assess the ENSO signature across various events. For all El Niño events except for the 1986-88, positive SSTs (between 0.5 and 3° C) appear to move poleward from the Pacific Ocean following ENSO conditions and retreat subsequently towards the Pacific side of South America once they reach the Amundsen Sea (Figure 19, Supplementary Figure 3).

However, the lack of positive SSTs off the Amundsen Coast and the presence of very positive SSTs off the coast of the Ronne Ice Shelf (up to +3 C) following the very strong 1997 El Niño is slightly anomalous compared with previous observations of SST anomalies for other El Niño events (Figure 19). In consequence, we also observe anomalous changes in sea ice conditions in 1997-98, with lower (higher) SIE in the Weddell Sea (Ross Sea) of up to -75 % (+75 %) (Figure 19).

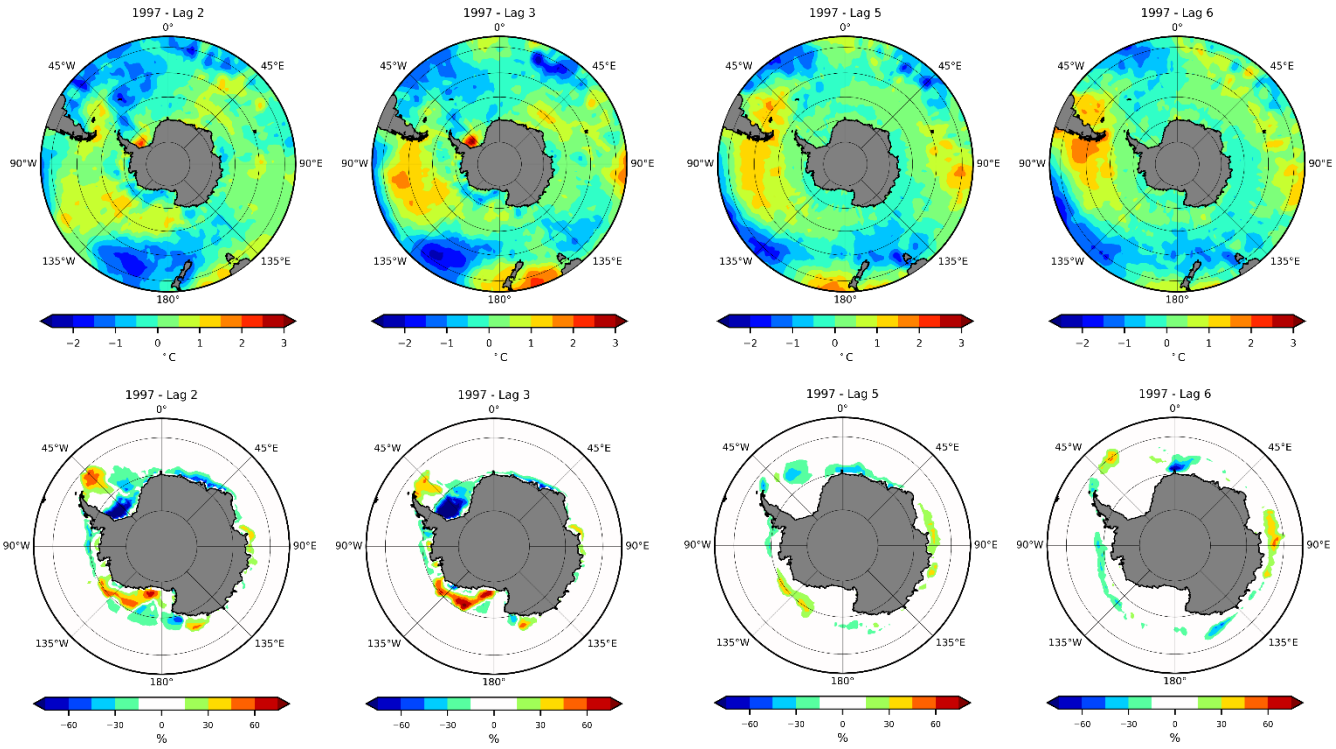

Figure 19. Sea Surface Temperature (top) and Sea Ice Extent (bottom) anomalies following the 1997-98 El Niño for the selected lags.

Analysis of Sea Ice Extent for previous El Niño events shows a contrasting response with an increase of up to +75% in the Bellingshausen Sea and a decrease of up to -75% in the Ross Sea following the 1982 El Niño (Supplementary Figure 4). SIE anomalies following the 1991 El Niño show a similar increase of up to +75% but to a smaller extent in the Bellingshausen sector, accompanied by strong increase (up to +75%) in the Weddell Sea and a moderate decrease (up to -60%) in the Amundsen and Ross Sea sectors. Almost no changes are observed following the 1986-88 and the 2009-10 El Niño events (Supplementary Figure 4).

5. Discussions

The results presented here show that the response of the Antarctic Ice Sheet to the 2015 El Niño event is dominated by an initial positive anomaly in the region of the Antarctic Peninsula and West Antarctica, and a delayed negative response in Central Antarctica and East Antarctica of 3 to 4 months following the peak El Niño month in the Pacific (Research Questions 1-3). Analysis of meteorological datasets shows the development of a high (low) pressure system over the Antarctic Peninsula (East Antarctica), which relates well with the increase (decrease) in precipitation over the APIS/WAIS (CAIS/EAIS). Comparison between the very strong 2015-16 and 1997-98 El Niño events show a similar response in atmospheric conditions and mass change estimates; however little similarity is found with other previous events (Research Question 1 and 3). Ocean indices show a contrasting response and do not appear to show a linear relationship across all El Niño events (Research Question 1 and 4). Overall, the APIS and WAIS regions appear to be highly responsive to El Niño variability, as well as Dronning Maud Land and Wilkes Land (East Antarctica).

5.1. Changes in Atmospheric Circulation as a Precursor for Post-El Niño Mass Changes

The increase (decrease) observed over the APIS and WAIS (CAIS/EAIS) following the 2015 El Niño reflects a contrasting response to Antarctica's long-term mass trend, which is normally characterised by a decrease (increase) over the West (East) (Thomas et al., 2004; Davis et al., 2005). As previously shown in Chapter 2, changes in the mass budget of the Antarctic Ice Sheet can result from flow-dynamics processes or changes in precipitation rates and/or snow drift. Previous studies (Payne et al., 2004) have shown that ice-dynamical processes such as ice sheet thinning and changes in flow dynamics affect the ice sheet on much longer timescales of years to decades, and therefore do not dominate mass changes on interannual timescales. Moreover, Lenaerts et al. (2012) showed that whilst snowfall appears to be greatly influencing surface mass balance on interannual timescales, snowdrift sublimation account for a very small part of interannual mass changes over Antarctica. Therefore, rapid changes in the mass

balance of the ice sheet must result from a change in atmospheric conditions, which drive changes in precipitation rates and lead to mass anomalies over the ice sheet on short timescales. We show this by comparing mass changes from gravimetry and SMB estimates with changes in atmospheric conditions over Antarctica following El Niño.

Previous studies have considered the influence of ENSO on changes in atmospheric circulation over the high southern latitudes, mainly categorised by intermittent atmospheric blocking activity (Renwick, 1998; Hirasawa et al., 2000; Boening et al., 2012). Cullather et al. (1996) analysed reanalyses precipitation fields from the ECMWF datasets over Antarctica and found a positive relationship between El Niño-Southern Oscillation and changes in atmospheric conditions over Antarctica. According to their study, the strong interannual variation in net precipitation rates led to a ± 1.2 – 1.5 mm/yr-1 maximum change in eustatic sea level contribution between 1980 and 1990. It has also been reported that changes in Antarctic precipitation rates on interannual and seasonal timescales are controlled by enhanced ridging due to changes in atmospheric pressure (Cullather et al., 1996; Marshall, 2009).

Boening et al. (2012) showed that changes in mass as observed by GRACE between 2009 and 2011 over Dronning Maud Land resulted in a positive anomaly totalling 350 Gt of cumulative mass gain, the equivalent of a decrease of 0.32 mm/yr in global mean sea level. The increase in moisture flux driven by a strong atmospheric pressure gradient are shown to increase precipitation rates over Dronning Maud Land, confirming that the observed mass changes are primarily the results of changes in precipitation on interannual timescales. These results are similar to ours, and to a previous study by Hirasawa et al. (2000) who observed an atmospheric blocking ridge forming as a result of tropical Rossby waves and brought heat and moisture over Dome Fuji in 1998. Both Hirasawa et al. (2000) and Boening et al. (2012) conclude that the sudden change in atmospheric conditions over these two sectors was likely the result of El Niño activity, whereby strong Rossby wave trains carry anomalies in atmospheric conditions over Antarctica and lead to changes in precipitation and surface air temperatures on interannual scales. This is shown by the strong high-low pressure systems following El Niño events which leads to anomalies in precipitation rates. Similar to these studies and others on past ENSO events, our results show the development of a high-pressure system over Drake Passage

following the 2015-16 El Niño events. This anomaly resulted in an anticyclonic wind circulation along the western flank of the high-pressure system which directed warm and moist air poleward towards the Bellingshausen sector of the Antarctic Peninsula. This resulted in increased cloud formation and precipitation over the Western side of the APIS, leading in turn to increased accumulation over the APIS and WAIS. Likewise, the low-pressure systems present over the Weddell and Ross Seas, and Wilkes Lands on the East Antarctic sector have resulted in lower precipitation rates in these sectors. This suggests that the primary factors for the observed changes in mass over the Antarctic continent post-2015 are changes in atmospheric circulation during and following the 2015 ENSO event in the Pacific. This provides an answer to Research Question 1 and 2 and suggests that changes in atmospheric conditions (mean sea level pressure and precipitation) are key factors influencing Antarctica's mass balance on interannual timescales following El Niño events.

Our results show a contrasting response to the long-term trend on the Antarctic Ice Sheet. As previously mentioned in Chapter 2, one of the most accurate estimate of ice sheet mass balance comes from the Shepherd et al. (2012) study, which combined a suite of altimetry, interferometry, and gravimetry data to improve and reduce the uncertainty range in estimates. Their research showed that between 1992 and 2011 the ice sheets of the Antarctic Peninsula, West Antarctica, and East Antarctica have experienced changes in mass of approximately -20 ± 14 Gt/yr^{-1}, -65 ± 26 Gt/yr^{-1}, and +14 ± 43 Gt/yr^{-1} respectively. Combining those estimates together bring an overall mass loss of 1350 ± 1010 Gt over the entire Antarctic Ice Sheet (Shepherd et al., 2012). These changes are predominantly dominated by ice-dynamical processes such as glacier flow acceleration and ice-shelf collapse amongst others, which can have significant and long-lasting impact on the mass budget of the Antarctic Ice Sheet (Payne et al., 2004; Rignot, 2006; Jenkins et al., 2010; King et al., 2012). However, ice-dynamical processes occur on much longer timescales of years to decades, as opposed to interannual events of the likes of ENSO, which are normally characterised by short but intense accumulation-derived mass changes (Rignot, 2006; Boening et al., 2012; Lenaerts et al., 2012).

The influence of the 2015-16 El Niño, as observed here, resulted in a contrasting response of the ice sheet to the long-term changes shown by Shepherd et al. (2012). These changes were

characterised by mass loss in the Antarctic Peninsula and West Antarctica, and a positive mass change in East Antarctica. In comparison, our results show that the Antarctic Peninsula and West Antarctica experienced positive anomalies following the 2015-16 El Niño event, whilst East Antarctica showed negative anomalies. This is confirmed by our Surface Mass Balance time series which show that changes in precipitation rates following the 2015-16 event primarily led to the positive anomalies over the Antarctic Peninsula and West Antarctica.

By removing the linear trend in their results for the period 2008-2010, Shepherd et al. (2012) were able to identify the anomalous event mentioned by Boening et al. (2012) over Dronning Maud Land (East Antarctic Ice Sheet) in 2009. According to Shepherd et al. (2012), this event led to +200 Gt of snow being deposited over the Dronning Maud Land sector between 2009 and 2010, an estimate much lower than the estimates of Boening et al. (2012) of +350 Gt. Our results also show this anomalous event, with an observed increase between 2009 and 2010 of similar magnitude to the Shepherd et al. (2012) study on drainage basins 5-8 (Figure 12). This anomaly is also reflected at a regional level on the East Antarctic Ice Sheet time series (Figure 10).

Unfortunately, the remaining part of our results cannot be directly compared to the Shepherd et al. (2012) study, as they consider crustal movements associated with the Glacial Isostatic Adjustment (GIA), whereas we exclude them. The GIA signal is an important factor influencing satellite gravimetry measurements and must be considered when assessing long-term mass balance changes on the Antarctic Ice Sheet (Shepherd et al. 2012). Indeed, and as previously mentioned in Chapter 3, the main source of errors between ice sheet mass balance estimates comes from corrections of the GIA (Velicogna and Wahr, 2013). The Glacial Isostatic Adjustment is the continuous viscoelastic response of the Earth's crust to past changes in surface loading, caused by the pressure of either ice or water onto the Earth's mantle since the end of the Last Glacial Maximum (Whitehouse et al., 2012; Velicogna and Wahr, 2013; LLovel et al., 2014). The work of Shepherd et al. (2012) intended to correct these uncertainties by combining a series of six different GIA models in their analysis. Whilst this was successful for assessing long-term changes in the ice sheet, the influence of the GIA is minimal when considering interannual fluctuations. Since our study focused on interannual changes on the

ice sheet, the removal of the trend by means of linear regression in the post-processing stages of the GRACE dataset reduced the long-term, secular uncertainty associated with the correction for crustal movements (Llovel et al., 2014). Our results are therefore not directly comparable with the Shepherd et al. (2012) study since GIA corrections would represent very little effect on our results.

An important aspect of this research showed that whilst the response of the APIS and WAIS were almost instantaneous, the response of the CAIS and EAIS appeared to be delayed by 3 to 4 months. This delay might be representative of a wider lag pattern between regions of the Southern Ocean, as ENSO-related anomalies are gradually transported via ocean and atmospheric processes to adjacent ocean basins (Peterson and White, 1998). Lag estimates for the reanalysis datasets also show a delay of 5 to 6 months following peak ENSO conditions in the Pacific, which is in line with previous lag estimates of 5 to 7 months (Sasgen et al., 2010). Therefore, the vulnerability of specific regions to El Niño might be dependent on their location, particularly those in the vicinity of the Pacific Ocean where El Niño develops.

When analysing the time series for the 2015-16 El Niño, we find that some disparities exist between the GRACE Mascons and the Surface Mass Balance time series. Whilst the increase in SMB in the APIS region appears to be of greater magnitude than the increase in the GRACE Mascons, the decrease in mass observed over the CAIS on the SMB time series is much lower than the GRACE Mascons. Similarly, the Surface Mass Balance estimates for the EAIS region plateaus and increases following the 2015 El Niño event, whereas the GRACE data shows a delayed decrease. Although the ERA-Interim dataset represents one of the most reliable reanalysis datasets for precipitation estimates over Antarctica (Bromwich et al*.,* 2011; Nicolas and Bromwich, 2011; Bracegirdle and Marshall, 2012), it has also been reported that it suffers from dry biases over the East Antarctic Plateau due, in part, to an underestimation of total accumulation rates at higher elevations (above 2,000 m a.s.l.) (Magand et al., 2007; Bromwich et al., 2011). In particular, snowfall tends to decrease from the coast to the interior of the Antarctic continent where arid, desert-like conditions tend to prevail (Lenaerts et al., 2012). The change in snowfall rates between peripheral areas and the East Antarctic Plateau can therefore add some uncertainties when interpreting the results for the reanalysis datasets

(Bromwich et al., 2000; Favier et al., 2013). Moreover, the reliability of in-situ observations of precipitation rates to validate the reanalysis datasets are sporadic and constrained in time and space over the Antarctic continent (Monaghan et al., 2006; Rignot et al., 2008). Therefore, the uncertainties associated with model reanalysis precipitation fields that rely on interpolated observations have restricted estimates of mass changes over the Antarctic continent (Davis et al., 2005).

In consequence, an underestimation of the overall trend in precipitation over the Antarctic Ice Sheet due to these dry biases could affect the interpretation of the relationship between the SMB and the GRACE Mascons time series. This is particularly obvious for the SMB estimate of the entire Antarctic Ice Sheet (Figure 10), which fails to show the delayed decrease observed by GRACE. Disparities between the two datasets is also observed on basins found in the Antarctic interior, mainly basins 2, 9, 11, 13, and 16 (Figure 12), which reinforces further the suggestion that reanalysis dataset are not completely reliable over more central basins.

On the contrary, the GRACE satellites have been used extensively to assess mass changes over Antarctica with a very high level of accuracy. More specifically, several studies have used the GRACE data to assess the mass balance of the Antarctic Ice Sheet and found very similar results to altimetry and synthetic aperture radar data (Chen et al., 2009; Horwath et al., 2012; Shepherd et al., 2012), whilst others found even more realistic results with GRACE than with other datasets (King et al., 2012).

Despite observing differences in magnitude between GRACE and cumulative precipitation estimates over the APIS and WAIS (mainly basin 18 and 26-27), the SMB estimates confirm most of the positive response observed by GRACE over these two regions. Indeed, previous studies have also found a good agreement between the ERA-Interim and other reanalysis datasets over the Antarctic Peninsula and West Antarctica, as well as with observations from the CloudSat and GRACE satellites (Davis et al., 2005; Sasgen et al., 2010; Bromwich et al., 2011; Boening et al., 2012). In particular, Palerme et al. (2014) found a good agreement between CloudSat and the ERA-Interim data in sectors where snowfall is high, mainly over the low-

altitude coastal areas as opposed to the high-altitude East Antarctic Plateau where snowfall tends to be weaker. Our results show that the ERA-Interim dataset can be a useful tool to identify mass changes over the APIS and WAIS, but more care should be applied when considering the CAIS and EAIS regions, and thus, the entire Antarctic Ice Sheet.

Recent studies have demonstrated the effects of the 2015-16 El Niño on the Antarctic Ice Sheet. Stuecker et al. (2017) showed that the presence of warm SST anomalies around Antarctica were partly responsible for the lowest Southern Hemisphere spring sea ice extent ever recorded, Walker and Gardner (2017) for the collapse of the Wordie Ice Shelf (APIS), and Aoki (2017) for the break-up of land-fast sea ice off the coast of East Antarctica, leading to the calving of the Shirase Glacier front. In the light of these recent studies and the results presented here, we suggest that the next step would be to conduct extensive small-scale analysis of individual outlet glaciers and sub-regions in response to the 2015 El Niño to determine potential areas particularly sensitive to external tropical forcing. One limitation to this is the recurrent problems of battery failure on the GRACE satellites and the recent announcement from the US/German space agencies to end the GRACE mission (NASA JPL, 2017). It is hoped that the new GRACE Follow-On (GRACE-FO) satellite mission will soon be launched to improve the record for gravitational measurements, which have proven useful both here and in previous studies to assess the vulnerability of the ice sheet to interannual events. This coupled with small-scale analysis of individual regions sensitive to El Niño variability could contribute to our understanding of El Niño's influence on the ice sheet and improve overall estimates of Antarctica's present and future sea level contribution.

5.2. Comparison between Post-2015 Atmospheric Conditions and Previous El Niño Events

The absence of consistent ENSO-related anomalies over Antarctica since 1979 suggests that it is not yet possible to determine a typical El Niño response over the ice sheet. Although we argue that strong similarities in atmospheric conditions exist between the very strong El Niño events of 1997-98 and 2015-16, the absence of those similarities with the other very strong El Niño event of 1982-83 is problematic. We suggest that a combination of different factors may

have resulted in this. In particular, the influence of external factors such as the SAM might have played a role in the response of Antarctica's atmospheric and ocean circulation post-1982. According to Stammerjohn et al. (2008), it is possible that a change in the mean state of Southern Annular Mode in the 1990s modulated the high-latitude response of ENSO during this event. Other studies suggest that a change in the modulation of Rossby wave propagation by the mean meridional circulation could have resulted in the variable response over Antarctica post-1982 (Renwick et al., 1998), whilst others suggest a change in tropical convection which affects the distribution and circulation of westerly winds (Mo and Higgings, 1997). A few studies (Trenberth and Stepaniak, 2001; Trenberth and Smith, 2006; Lee and McPhaden, 2010) have shown that a change in the response of the Southern latitudes could be reflective of variations in the flavour of El Niño events. Indeed, a change in the flavour of El Niño events impacts the location of the Rossby wave source region, which in turn affects the strength of atmospheric blocking over the High Latitudes and the response in atmospheric conditions over Antarctica (Wilson, 2014).

As previously mentioned, we suggest that the observed changes in mass balance following the 2015-16 El Niño could be similar to changes in mass conditions following the 1997-98 event, based on similarities in atmospheric conditions and SMB estimates. Indeed, for both events, we observe similar patterns for cumulative precipitation estimates in the APIS and WAIS regions, and to a smaller extent in the CAIS and the EAIS. Similarly, we also notice a delay in the response of the EAIS to the 1997-98 El Niño. Considering only those two events, this would suggest that changes in atmospheric conditions and surface mass balance of the Antarctic Ice Sheet are proportional to the strength of El Niño events (1997/98 and 2015/16) and the response is fairly symmetric on temporal and spatial scales across both very strong events (Research Question 3). However, although the SMB time series reproduced relatively well the general changes in mass observed by GRACE over coastal regions, they performed poorly over other more central regions. Therefore, inferring general patterns in surface mass balance post-1997, based solely on the results from the SMB time series would be inaccurate.

Generally speaking however, the results for both events indicate that the APIS and WAIS sectors are highly sensitive regions to ENSO variability, and the influence of El Niño on the CAIS and

EAIS appears to be very limited and constrained to key drainage basins along the coast of East Antarctica. This indicates that those two very strong events affected the surface mass balance of the ice sheet in similar locations, although we note that the 2015-16 event led to much stronger anomalies in atmospheric conditions and SMB than the 1997-98 event (Research Question 2). Unfortunately, the absence of GRACE data prior to 2002 does not allow for the same type of analysis, but a combination of laser and radar altimetry data (Davis et al., 2005; Shepherd et al., 2012) could provide an answer to this hypothesis. As suggested by previous studies (Timmermann et al., 1999; Cai et al., 2015), ENSO events will become stronger and more frequent over the course of the 21st Century. Therefore, understanding the potential for stronger El Niño events to alter Antarctica's surface mass balance and sea level rise contribution should become a priority for the future. This research lays the ground for such studies by identifying similarities in atmospheric conditions following very strong El Niño events.

5.3. Comparison between Post-2015 Ocean Conditions and Previous El Niño Events

An increase (decrease) in SIE anomalies in the Weddell Sea and ABS sector (Ross Sea) following El Niño conditions has been widely discussed in the literature and has been associated with the Antarctic Dipole (Zwally et al., 1983; Liu et al., 2002; Yuan and Li, 2008). The Antarctic Dipole, this wave pattern that forms in the western Amundsen Sea and with opposite polarity in the Weddell Sea responds strongly to ENSO by creating a complex set of interannual anomalies between Sea Ice Extent and Surface Air Temperature (Renwick, 2002; Yuan, 2004). This polarity typically brings positive (negative) Surface Air Temperature anomalies and negative (positive) SIE anomalies during El Niño events in the Pacific (Atlantic) sector of the ADP (Liu et al., 2002). The results for SST and SIE anomalies following the 2015-16 El Niño match the results of Stuecker et al. (2017) where El Niño-induced SST anomalies resulted in a decrease (increase) in SIE over the Ross Sea (Bellingshausen Sea). Similarly, sea ice conditions following the 1982-83 and the 1991-92 El Niño appear to match the typical footprint of El Niño on sea ice, with an increase (decrease) in the ABS (Ross Sea). However, little similarities are found following other El Niño events, especially following the very strong 1997-98 event. Similar to previous studies (Ledley and Huang, 1997; Klein et al., 1999; Kwok and Comiso, 2002), lag estimates of ocean conditions following El Niño events appear to peak on average 3 months following an El Niño

event in the Pacific, with some events showing peak conditions between 2 and 4 months. Overall, we find that sea ice conditions appear to be highly dependent on Sea Surface Temperature, especially in areas where SST anomalies migrate and remain for an extended period of time. This is the case for the 1997-98 El Niño where positive SST anomalies in the Weddell Sea resulted in sea ice decline in this sector. Likewise, the large band of negative SST anomalies in Drake Passage in 2015-16 resulted in sea ice growth in this region. However, the lack of strong and consistent patterns for both SST and SIE conditions following ENSO events prevents an overall conceptualisation of El Niño's influence on oceanic conditions around Antarctica (Research Question 4).

As previously shown, SST and SIE conditions are subject to numerous atmospheric and ocean influences, such as fluctuations in the position and strength of the Amundsen Sea Low (Purich et al., 2016), wind-forcing and sea ice drift (Holland and Kwok, 2012; Matear et al., 2015; Kwok et al., 2016), and Southern Annular Mode forcing (Stuecker et al., 2017) amongst others. Moreover, sea ice is influenced by a complex set of interactions between wind and Sea Surface Temperature, as well as being closely linked with Sea Air Temperature and the Antarctic Dipole (Liu et al., 2002; Turner, 2004). In this respect, many studies have shown that the complexity in understanding the various physical mechanisms influencing sea ice drift and growth around Antarctica can lead to significant errors in the interpretations of the results (Kwok et al., 2016; Purich et al., 2016; Pope et al., 2017). In particular, Pope et al. (2017) showed that the relationship between sea ice anomalies and atmospheric processes, especially in the case of ENSO, are highly nonlocal both spatially and temporally. Indeed, using a complex sea ice budget approach, they showed for the first time that regional changes in the sea ice budget of Antarctica following El Niño conditions is controlled by a set of thermodynamic feedback acting on inter-seasonal timescales. Their approach highlights the complexity of linking climate and sea ice anomalies and suggests that more care should be applied when interpreting sea ice changes as a result of natural variability. In the light of this recent study and previous studies that have intended to link ENSO and sea ice anomalies, we are not fully able to quantify the effect of the 2015-2016 El Niño on the sea ice budget of Antarctica, nor can we say with certainty that the anomalies observed post-El Niño are similar across all events. As a result, the

analysis presented here does not allow for a complete understanding of how El Niño influences ocean conditions around Antarctica (Research Question 4).

6. Conclusions

This study provides the first overall estimate of Antarctica's mass balance following an El Niño event using GRACE. We report a change in the secular trend of the Antarctic Ice Sheet on interannual timescales, which, for the last few decades has been characterised by a long-term mass loss over the West and a slight increase over the East. We show that the change in mass are influenced by the very strong 2015-16 El Niño event. The response of the AIS is characterised by an initial increase towards the end of 2015, dominated by a gain in mass of +55 Gt in the Antarctic Peninsula and +75 Gt in West Antarctica, and a subsequent decrease 3 to 4 months later, dominated by the negative signal over the Antarctic Interior (-70 Gt) and East Antarctica (- 55 Gt). We show that the development of a high (low) pressure system over the Antarctic Peninsula (East Antarctica) following the 2015-16 El Niño led to an increase (decrease) in precipitation in those sectors, which in turn resulted in the observed mass changes over the ice sheet. Cumulative precipitation estimates (SMB) confirm the positive trend over West Antarctica and the Antarctic Peninsula post-2015, but underestimate largely the GRACE observations over Central Antarctica, and do not reflect the negative response observed over East Antarctica.

A comparison of atmospheric and ocean conditions following the 2015 El Niño with previous El Niño events shows little resemblance, although similar atmospheric conditions are observed between the 2015-16 and the 1997-98 El Niño events. More specifically, we observe a similar pattern of increases in cumulative precipitation in the APIS and WAIS regions, but to a much lower extent than following 2015 conditions. We suggest that the observed variations in surface mass balance and atmospheric circulation following the 2015 El Niño event might be reflective of a more general pattern in Antarctica's response to very strong El Niño events, but the lack of gravimetry data pre-2002 does not allow for a similar comparison with the 1997-98 event. Overall, we find that the Antarctic Peninsula Ice Sheet, West Antarctic Ice Sheet, as well as Dronning Maud Land and Wilkes Land (East Antarctica) are highly sensitive regions to El Niño variability across both events.

Overall, this research confirms the vulnerability of certain regions to El Niño‘s influence and identifies further sub-regions and drainage basins where El Niño’s influence is particularly strong. We also conclude that special emphasis should be put on assessing the effect of future ENSO events on the Antarctic Ice Sheet, with the aim to determine whether future El Niño events lead to similar atmospheric conditions and whether this can be associated with a global ENSO response over Antarctica. If this can be established, it would represent a large step towards an improved understanding of extratropical anomalies on the Antarctic Ice Sheet and thus towards more accurate modelling of the ice sheet’s past and future behaviour.

As previously suggested, we advise that future work should focus on using altimetry data to compare surface mass balance changes following the 1997-98 El Niño and compare those with our results for the 2015-16 El Niño. This would provide additional support to our Surface Mass Balance estimates and allow for a more complete understanding of El Niño’s influence on the ice sheet following similar events. Moreover, a more comprehensive study on the effect of El Niño on Sea Ice Extent should be conducted, including a thorough analysis of surface air temperature and its relationship with atmospheric pressure, wind, and sea surface temperature. Combining those four datasets and conducting a seasonal and inter-seasonal analysis could provide a more complete understanding of how the 2015-16 El Niño impacted sea ice extent. Lastly, in the light of stronger and more frequent El Niño events in the future, we suggest that follow-up studies take advantage of the new GRACE-FO mission to assess the effect of future El Niño events on the Antarctic Ice Sheet.

References

Alley, R.B., Clark, P.U., Huybrechts, P. and Joughin, I., 2005. Ice-sheet and sea-level changes. science, 310(5747), pp.456-460. doi: 10.1126/science.1114613.

Arzeno, I.B., Beardsley, R.C., Limeburner, R., Owens, B., Padman, L., Springer, S.R., Stewart, C.L. and Williams, M.J., 2014. Ocean variability contributing to basal melt rate near the ice front of Ross Ice Shelf, Antarctica. Journal of Geophysical Research: Oceans, 119(7), pp.4214-4233. doi: 10.1002/2014JC009792.

Aoki, S., 2017. Breakup of land-fast sea ice in Lützow-Holm Bay, East Antarctica, and its teleconnection to tropical Pacific sea surface temperatures. *Geophysical Research Letters*, *44*(7), pp.3219-3227. doi:10.1002/2017GL072835.

Awange, J.L., Fleming, K.M., Kuhn, M., Featherstone, W.E., Heck, B. and Anjasmara, I., 2011. On the suitability of the 4× 4 GRACE mascon solutions for remote sensing Australian hydrology. *Remote Sensing of Environment*, 115(3), pp.864-875. doi: 10.1016/j.rse.2010.11.014.

Battisti, D.S., 1988. Dynamics and thermodynamics of a warming event in a coupled tropical atmosphere–ocean model. *Journal of the Atmospheric Sciences*, 45(20), pp.2889-2919. doi: 10.1175/1520-0469(1988)045<2889:DATOAW>2.0.CO;2.

Bell, G.D. and Halpert, M.S., 1998. Climate assessment for 1997. *Bulletin of the American Meteorological Society*, 79(5), pp.1014-1014. doi: 10.1175/1520-0477(1998)079<1014:CAF>2.0.CO;2.

Bindoff, N.L., J. Willebrand, V. Artale, A, Cazenave, J. Gregory, S. Gulev, K. Hanawa, C. Le Quéré, S. Levitus, Y. Nojiri, C.K. Shum, L.D. Talley and A. Unnikrishnan, 2007: *Observations: Oceanic Climate Change and Sea Level. In: Climate Change 2007: The Physical Science Basis. Contribution of Working Group I to the Fourth Assessment Report of the Intergovernmental Panel on Climate Change* [Solomon, S., D. Qin, M. Manning, Z. Chen, M. Marquis, K.B. Averyt, M. Tignor and H.L. Miller (eds.)]. Cambridge University Press, Cambridge, United Kingdom and New York, NY, USA.

Bjerknes, J., 1969. Atmospheric teleconnections from the equatorial pacific 1. *Monthly Weather Review*, 97(3), pp.163-172. doi: 10.1175/1520-0493(1969)097<0163:ATFTEP>2.3.CO;2.

Boening, C., Willis, J.K., Landerer, F.W., Nerem, R.S. and Fasullo, J., 2012. The 2011 La Niña: So strong, the oceans fell. *Geophysical Research Letters*, 39(19). doi: 10.1029/2012GL053055.

Boulanger, J.P. and Menkes, C., 1999. Long equatorial wave reflection in the Pacific Ocean from TOPEX/POSEIDON data during the 1992–1998 period. *Climate dynamics*, 15(3), pp.205-225. doi: 10.1007/s003820050277.

Bracegirdle, T.J. and Marshall, G.J., 2012. The reliability of Antarctic tropospheric pressure and temperature in the latest global reanalyses. *Journal of Climate*, 25(20), pp.7138-7146. doi: 10.1175/JCLI-D-11-00685.1.

Bromwich, D.H., Rogers, A.N., Kållberg, P., Cullather, R.I., White, J.W. and Kreutz, K.J., 2000. ECMWF analyses and reanalyses depiction of ENSO signal in Antarctic precipitation. *Journal of Climate*, 13(8), pp.1406-1420. doi: 10.1175/1520-0442(2000)013<1406:EAARDO>2.0.CO;2.

Bromwich, D.H., Nicolas, J.P. and Monaghan, A.J., 2011. An assessment of precipitation changes over Antarctica and the Southern Ocean since 1989 in contemporary global reanalyses. *Journal of Climate*, 24(16), pp.4189-4209. doi: 10.1175/2011JCLI4074.1.

Cai, W. and Baines, P.G., 2001. Forcing of the Antarctic Circumpolar Wave by El Niño-Southern Oscillation teleconnections. *Journal of Geophysical Research: Oceans,* 106(C5), pp.9019-9038. doi: 10.1029/2000JC000590.

Cai, W., Borlace, S., Lengaigne, M., Van Rensch, P., Collins, M., Vecchi, G., Timmermann, A., Santoso, A., McPhaden, M.J., Wu, L. and England, M.H., 2014. Increasing frequency of extreme El Niño events due to greenhouse warming. *Nature climate change*, 4(2), pp.111-116. doi: 10.1038/nclimate2100.

Cai, W., Santoso, A., Wang, G., Yeh, S.W., An, S.I., Cobb, K.M., Collins, M., Guilyardi, E., Jin, F.F., Kug, J.S. and Lengaigne, M., 2015. ENSO and greenhouse warming. *Nature Climate Change*, *5*(9), pp.849-859. doi: 10.1038/nclimate2743.

Cane, M.A., Zebiak, S.E. and Dolan, S.C., 1986. Experimental forecasts of El Niño. *Nature*, *321*, pp.827-832. doi: 10.1038/321827a0.

Cane, M.A., 2005. The evolution of El Niño, past and future. *Earth and Planetary Science Letters*, 230(3), pp.227-240. doi: 10.1016/j.epsl.2004.12.003.

Carleton, A.M., 1988. Sea ice–atmosphere signal of the Southern Oscillation in the Weddell Sea, Antarctica. *Journal of Climate*, *1*(4), pp.379-388. doi: 10.1175/1520-0442(1988)001<0379:SISOTS>2.0.CO;2.

Chen, J.L., Wilson, C.R., Blankenship, D. and Tapley, B.D., 2009. Accelerated Antarctic ice loss from satellite gravity measurements. *Nature Geoscience*, *2*(12), p.859. doi: 10.1038/ngeo694.

Chen, S., Wu, R., Chen, W., Yu, B. and Cao, X., 2016. Genesis of westerly wind bursts over the equatorial western Pacific during the onset of the strong 2015–2016 El Niño. *Atmospheric Science Letters*. doi: 10.1002/asl.669.

Christoph, M., Barnett, T.P. and Roeckner, E., 1998. The Antarctic Circumpolar Wave in a coupled ocean–atmosphere GCM. *Journal of Climate*, 11(7), pp.1659-1672. doi: 10.1175/1520-0442(1998)011<1659:TACWIA>2.0.CO;2.

Church, J. A. and Gregory, J. M., 2001. In Climate Change 2001: The Scientific Basis, Houghton, J.T., Ding, Y.D.J.G., Griggs, D.J., Noguer, M., van der Linden, P.J., Dai, X., Maskell, K. and Johnson, C.A., Eds. Cambridge Univ. Press, Cambridge, 2001, chap. 11, pp. 641–693.

Church, J.A. and White, N.J., 2006. A 20th century acceleration in global sea-level rise. *Geophysical research letters*, 33(1). doi: 10.1029/2005GL024826.

Church, J.A. and White, N.J., 2011. Sea-level rise from the late 19th to the early 21st century. *Surveys in Geophysics*, 32(4-5), pp.585-602. doi: 10.1007/s10712-011-9119-1.

Cullather, R. I., Bromwich, D. H., and Van Woert, M. L., 1996. Interannual variations in Antarctic precipitation related to El Niño-Southern Oscillation, *Journal of Geophysical Res*earch, 101(D14), 19109–19118. doi: 10.1029/96JD01769.

Davis, C.H., Li, Y., McConnell, J.R., Frey, M.M. and Hanna, E., 2005. Snowfall-driven growth in East Antarctic ice sheet mitigates recent sea-level rise. *Science*, *308*(5730), pp.1898-1901. doi: 10.1126/science.1110662.

DeConto, R.M. and Pollard, D., 2016. Contribution of Antarctica to past and future sea-level rise. *Nature*, 531(7596), pp.591-597. doi: 10.1038/nature17145.

Dee, D.P., Uppala, S.M., Simmons, A.J., Berrisford, P., Poli, P., Kobayashi, S., Andrae, U., Balmaseda, M.A., Balsamo, G., Bauer, D.P. and Bechtold, P., 2011. The ERA-Interim reanalysis:

Configuration and performance of the data assimilation system. Quarterly Journal of the royal meteorological society, 137(656), pp.553-597. doi: 10.1002/qj.828.

.Depoorter, M.A., Bamber, J.L., Griggs, J.A., Lenaerts, J.T.M., Ligtenberg, S.R.M., Van den Broeke, M.R. and Moholdt, G., 2013. Calving fluxes and basal melt rates of Antarctic ice shelves. *Nature*, 502(7469), pp.89-92. doi: 10.1038/nature12567.

Deser, C. and Wallace, J.M., 1990. Large-scale atmospheric circulation features of warm and cold episodes in the tropical Pacific. *Journal of Climate*, 3(11), pp.1254-1281. doi: 10.1175/1520-0442(1990)003<1254:LSACFO>2.0.CO;2.

Dupont, T.K. and Alley, R.B., 2005. Assessment of the importance of ice-shelf buttressing to ice-sheet flow. *Geophysical Research Letters,* 32(4). doi: 10.1029/2004GL022024.

Edwards, M.S., 2004. Estimating scale-dependency in disturbance impacts: El Niños and giant kelp forests in the northeast Pacific. *Oecologia*, 138(3), pp.436-447. doi: 10.1007/s00442-003-1452-8. doi: 10.1007/s00442-003-1452-8.

Enfield, D.B. and Allen, J.S., 1980. On the structure and dynamics of monthly mean sea level anomalies along the Pacific coast of North and South America. *Journal of Physical Oceanography*, 10(4), pp.557-578. doi: 10.1175/1520-0485(1980)010<0557:OTSADO>2.0.CO;2.

Favier, V., Agosta, C., Parouty, S., Durand, G., Delaygue, G., Gallée, H., Drouet, A.S., Trouvilliez, A. and Krinner, G., 2013. An updated and quality controlled surface mass balance dataset for Antarctica. *The Cryosphere*, 7(2), p.583. doi: 10.5194/tc-7-583-2013.

Favier, L., Durand, G., Cornford, S.L., Gudmundsson, G.H., Gagliardini, O., Gillet-Chaulet, F., Zwinger, T., Payne, A.J. and Le Brocq, A.M., 2014. Retreat of Pine Island Glacier controlled by marine ice-sheet instability. Nature Climate Change, 4(2), p.117. doi: 10.1038/nclimate2094.

Fogt, R.L. and Bromwich, D.H., 2006. Decadal variability of the ENSO teleconnection to the high-latitude South Pacific governed by coupling with the southern annular mode. *Journal of Climate*, *19*(6), pp.979-997. doi: 10.1175/JCLI3671.1.

Fogt, R.L., Bromwich, D.H. and Hines, K.M., 2011. Understanding the SAM influence on the South Pacific ENSO teleconnection. *Climate Dynamics*, 36(7-8), pp.1555-1576. doi: 10.1007/s00382-010-0905-0.

Francou, B., Vuille, M., Favier, V. and Cáceres, B., 2004. New evidence for an ENSO impact on low-latitude glaciers: Antizana 15, Andes of Ecuador, 0 28′ S. *Journal of Geophysical Research: Atmospheres*, 109(D18). doi: 10.1029/2003JD004484.

Gardner, A.S., Moholdt, G., Cogley, J.G., Wouters, B., Arendt, A.A., Wahr, J., Berthier, E., Hock, R., Pfeffer, W.T., Kaser, G. and Ligtenberg, S.R., 2013. A reconciled estimate of glacier contributions to sea level rise: 2003 to 2009. *Science*, 340(6134), pp.852-857. doi: 10.1126/science.1234532.

Garreaud, R. and Battisti, D.S., 1999. Interannual (ENSO) and interdecadal (ENSO-like) variability in the Southern Hemisphere tropospheric circulation. *Journal of Climate*, *12*(7), pp.2113-2123. doi: 10.1175/1520-0442(1999)012<2113:IEAIEL>2.0.CO;2.

Geruo, A., Wahr, J. and Zhong, S., 2013. Computations of the viscoelastic response of a 3-D compressible Earth to surface loading: an application to Glacial Isostatic Adjustment in Antarctica and Canada. *Geophysical Journal International*, 192, pp.557-572. doi: 10.1093/gji/ggs030.

Gloersen, P., 1995. Modulation of hemispheric sea-ice cover by ENSO events. *Nature*, 373(6514), p.503. doi: 10.1038/373503a0.

Glynn, P.W. and D'croz, L., 1990. Experimental evidence for high temperature stress as the cause of El Niño -coincident coral mortality. *Coral reefs,* 8(4), pp.181-191. doi: 10.1007/BF00265009.

Glynn, P.W. and De Weerdt, W.H., 1991. Elimination of Two Reef-Building Hydrocorals Following the 1982—83 El Niño Warming Event. *Science*, 253, pp.69-71. doi: 10.1126/science.253.5015.69.

Godfrey, J.S., 1975. On ocean spindown I: A linear experiment. *Journal of Physical Oceanography*, 5(3), pp.399-409. doi: 10.1175/1520-0485(1975)005<0399:OOSIAL>2.0.CO;2.

Graham, N.E. and White, W.B., 1988. The El Niño cycle: A natural oscillator of the Pacific ocean-atmosphere system. *Science*, 240(4857), p.1293. doi: 10.1126/science.240.4857.1293.

Grimm A., Barros V.R. and Doyle M.E., 2000. Climate variability in Southern South America associated with El Niño and La Niña events. *American Meteorological Society,* 13, pp. 35 - 58. doi: 10.1175/1520-0442(2000)013<0035:CVISSA>2.0.CO;2.

Hanna, E., Navarro, F.J., Pattyn, F., Domingues, C.M., Fettweis, X., Ivins, E.R., Nicholls, R.J., Ritz, C., Smith, B., Tulaczyk, S. and Whitehouse, P.L., 2013. Ice-sheet mass balance and climate change. *Nature*, 498(7452), pp.51-59. doi: 10.1038/nature12238.

Harangozo, S.A., 2000. A search for ENSO teleconnections in the west Antarctic Peninsula climate in austral winter. *International Journal of Climatology*, *20*(6), pp.663-679. doi: 10.1002/(SICI)1097-0088(200005)20:6<663::AID-JOC493>3.0.CO;2-I.

Harrison, D.E. and Schopf, P.S., 1984. Kelvin-wave-induced anomalous advection and the onset of surface warming in El Niño events. *Monthly weather review*, 112(5), pp.923-933. doi: 10.1175/1520-0493(1984)112<0923:KWIAAA>2.0.CO;2.

Harvell, C.D., Mitchell, C.E., Ward, J.R., Altizer, S., Dobson, A.P., Ostfeld, R.S. and Samuel, M.D., 2002. Climate warming and disease risks for terrestrial and marine biota. *Science*, 296(5576), pp.2158-2162. doi: 10.1126/science.1063699.

Hirasawa, N., Nakamura, H. and Yamanouchi, T., 2000. Abrupt changes in meteorological conditions observed at an inland Antarctic station in association with wintertime blocking. *Geophysical Research Letters*, 27(13), pp.1911-1914. doi: 10.1029/1999GL011039.

Hodder, J. and Graybill, M.R., 1985. Reproduction and survival of seabirds in Oregon during the 1982-1983 El Niño. *Condor*, pp.535-541. doi: 10.2307/1367954.

Holgate, S.J., 2007. On the decadal rates of sea level change during the twentieth century. *Geophysical Research Letters*, 34(1). doi: 10.1029/2006GL028492.

Holland, P.R., Jenkins, A. and Holland, D.M., 2010. Ice and ocean processes in the Bellingshausen Sea, Antarctica. *Journal of Geophysical Research: Oceans*, 115(C5). doi: 10.1029/2008JC005219.

Holland, P.R. and Kwok, R., 2012. Wind-driven trends in Antarctic sea-ice drift. *Nature Geoscience*, *5*(12), pp.872-875. doi: 10.1038/ngeo1627.

Hoskins, B.J. and Karoly, D.J., 1981. The steady linear response of a spherical atmosphere to thermal and orographic forcing. *Journal of the Atmospheric Sciences*, 38(6), pp.1179-1196. doi: 10.1175/1520-0469(1981)038<1179:TSLROA>2.0.CO;2.

Horwath, M., Legrésy, B., Rémy, R., Blarel, F. and Lemoine J., 2012. Consistent patterns of Antarctic ice sheet interannual variations from ENVISAT radar altimetry and GRACE satellite gravimetry. *Geophysical Journal International*, 189, pp. 863–876. doi: 10.1111/j.1365-246X.2012.05401.x

IPCC, 2013: Climate Change 2013: The Physical Science Basis. Contribution of Working Group I to the Fifth Assessment Report of the Intergovernmental Panel on Climate Change [Stocker, T.F., D. Qin, G.-K. Plattner, M. Tignor, S.K. Allen, J. Boschung, A. Nauels, Y. Xia, V. Bex and P.M. Midgley (eds.)]. Cambridge University Press, Cambridge, United Kingdom and New York, NY, USA, 1535 pp. doi:10.1017/CBO9781107415324.

Ivins, E.R., James, T.S., Wahr, J., Schrama, O., Ernst, J., Landerer, F.W. and Simon, K.M., 2013. Antarctic contribution to sea level rise observed by GRACE with improved GIA correction. *Journal of Geophysical Research: Solid Earth*, 118(6), pp.3126-3141. doi: 10.1002/jgrb.50208.

Jacobs, S.S., Helmer, H.H., Doake, C.S.M., Jenkins, A. and Frolich, R.M., 1992. Melting of ice shelves and the mass balance of Antarctica. Journal of Glaciology, 38(130), pp.375-387. doi: 10.3189/S0022143000002252.

Jacobs, S.S. and Comiso, J.C., 1993. A recent sea-ice retreat west of the Antarctic Peninsula. *Geophysical Research Letters*, 20(12), pp.1171-1174. doi: 10.1029/93GL01200.

Jenkins, A., Dutrieux, P., Jacobs, S.S., McPhail, S.D., Perrett, J.R., Webb, A.T. and White, D., 2010. Observations beneath Pine Island Glacier in West Antarctica and implications for its retreat. *Nature Geoscience*, *3*(7), p.468. doi: 10.1038/ngeo890.

Jin, F.F., 1996. Tropical ocean-atmosphere interaction, the Pacific cold tongue, and the El Niño-Southern Oscillation. *Science*, 274(5284), p.76. doi: 10.1126/science.274.5284.76.

Jin, F.F., 1997. An equatorial ocean recharge paradigm for ENSO. Part I: Conceptual model. *Journal of the Atmospheric Sciences,* 54(7), pp.811-829. doi: 10.1175/1520-0469(1997)054<0811:AEORPF>2.0.CO;2.

Julian, P.R. and Chervin, R.M., 1978. A study of the Southern Oscillation and Walker Circulation phenomenon. *Monthly Weather Review,* 106(10), pp.1433-1451. doi: 10.1175/1520-0493(1978)106<1433:ASOTSO>2.0.CO;2.

Kao, H.Y. and Yu, J.Y., 2009. Contrasting eastern-Pacific and central-Pacific types of ENSO. *Journal of Climate*, 22(3), pp.615-632. doi: 10.1175/2008JCLI2309.1.

Karoly, D.J., 1989. Southern hemisphere circulation features associated with El Niño-Southern Oscillation events. *Journal of Climate*, *2*(11), pp.1239-1252. doi: 10.1175/1520-0442(1989)002<1239:SHCFAW>2.0.CO;2.

Keen, R.A., 1982. The role of cross-equatorial tropical cyclone pairs in the Southern Oscillation. *Monthly Weather Review,* 110(10), pp.1405-1416. doi: 10.1175/1520-0493(1982)110<1405:TROCET>2.0.CO;2.

Kerr, R.A., 1998. Models win big in forecasting El Niño. *Science*, 280(5363), pp.522-523. doi: 10.1126/science.280.5363.522.

King, M.A., Bingham, R.J., Moore, P., Whitehouse, P.L., Bentley, M.J. and Milne, G.A., 2012. Lower satellite-gravimetry estimates of Antarctic sea-level contribution. *Nature*, 491(7425), pp.586-589. doi: 10.1038/nature11621.

Klein, S.A., Soden, B.J. and Lau, N.C., 1999. Remote sea surface temperature variations during ENSO: Evidence for a tropical atmospheric bridge. *Journal of Climate*, 12(4), pp.917-932. doi: 10.1175/1520-0442(1999)012<0917:RSSTVD>2.0.CO;2.

Kwok, R. and Comiso, J.C., 2002. Spatial patterns of variability in Antarctic surface temperature: Connections to the Southern Hemisphere Annular Mode and the Southern Oscillation. *Geophysical Research Letters*, 29(14). doi: 10.1029/2002GL015415.

Kwok, R., Comiso, J.C., Lee, T. and Holland, P.R., 2016. Linked trends in the South Pacific sea ice edge and Southern Oscillation Index. *Geophysical Research Letters*, 43(19). doi: 10.1002/2016GL070655.

Ladah, L.B., Zertuche-González, J.A. and Hernández-Carmona, G., 1999. Giant kelp (Macrocystis pyrifera, Phaeophyceae) recruitment near its southern limit in Baja California after mass disappearance during ENSO 1997–1998. *Journal of Phycology*, 35(6), pp.1106-1112. doi: 10.1046/j.1529-8817.1999.3561106.x.

Latif M. and Keenlyside N.S., 2009. El Niño/Southern Oscillation response to global warming. *PNAS,* 106, pp. 20578 - 20583. doi: 10.1073/pnas.0710860105.

Lau, K.M. and Chan, P.H., 1986. The 40-50 day oscillation and the El Niño/Southern Oscillation: A new perspective. *Bulletin of the American Meteorological Society*, 67, pp.533-533. doi: 10.1175/1520-0477(1986)067<0533:TDOATE>2.0.CO;2.

Lau, K.M. and Weng, H., 2001. Coherent modes of global SST and summer rainfall over China: An assessment of the regional impacts of the 1997-98 El Niño. *Journal of Climate,* 14(6), pp.1294-1308. doi: 10.1175/1520-0442(2001)014<1294:CMOGSA>2.0.CO;2.

Ledley, T.S. and Huang, Z., 1997. A possible ENSO signal in the Ross Sea. *Geophysical Research Letters*, *24*(24), pp.3253-3256. doi: 10.1029/97GL03315.

Lee, T. and McPhaden, M.J., 2010. Increasing intensity of El Niño in the central-equatorial Pacific. Geophysical Research Letters, 37(14). doi: 10.1029/2010GL044007.

Lenaerts, J.T.M., Den Broeke, M.R., Berg, W.J., Meijgaard, E.V. and Kuipers Munneke, P., 2012. A new, high-resolution surface mass balance map of Antarctica (1979–2010) based on regional atmospheric climate modeling. *Geophysical Research Letters,* 39(4). doi: 10.1029/2011GL050713.

Lengaigne, M., Guilyardi, E., Boulanger, J.P., Menkes, C., Delecluse, P., Inness, P., Cole, J. and Slingo, J., 2004. Triggering of El Niño by westerly wind events in a coupled general circulation model. *Climate Dynamics*, 23(6), pp.601-620. doi: 10.1007/s00382-004-0457-2.

Liu, J., Yuan, X., Rind, D. and Martinson, D.G., 2002. Mechanism study of the ENSO and southern high latitude climate teleconnections. *Geophysical Research Letters*, 29(14). doi: 10.1029/2002GL015143.

Liu, J., Curry, J.A. and Martinson, D.G., 2004. Interpretation of recent Antarctic sea ice variability. Geophysical Research Letters, 31(2). doi: 10.1029/2003GL018732.

Llovel, W., Willis, J.K., Landerer, F.W. and Fukumori, I., 2014. Deep-ocean contribution to sea level and energy budget not detectable over the past decade. Nature Climate Change, 4(11), p.1031. doi: 10.1038/nclimate2387.

Luthcke, S.B., Sabaka, T.J., Loomis, B.D., Arendt, A.A., McCarthy, J.J. and Camp, J., 2013. Antarctica, Greenland and Gulf of Alaska land-ice evolution from an iterated GRACE global mascon solution. *Journal of Glaciology*, 59(216), pp.613-631. doi: 10.3189/2013JoG12J147.

Luther, D.S., Harrison, D.E. and Knox, R.A., 1983. Zonal winds in the central equatorial Pacific and El Niño. *Science*, 222(4621), pp.327-330. doi: 10.1126/science.222.4621.327.

Magand, O., Genthon, C., Fily, M., Krinner, G., Picard, G., Frezzotti, M. and Ekaykin, A.A., 2007. An up-to-date quality-controlled surface mass balance data set for the 90–180 E Antarctica sector and 1950–2005 period. *Journal of Geophysical Research: Atmospheres*, 112(D12). doi: 10.1029/2006JD007691.

Marshall, G.J., 2003. Trends in the Southern Annular Mode from observations and reanalyses. *Journal of Climate*, *16*(24), pp.4134-4143. doi: 10.1175/1520-0442(2003)016<4134:TITSAM>2.0.CO;2.

Marshall, G.J., 2009. On the annual and semi-annual cycles of precipitation across Antarctica. *International Journal of Climatology*, *29*(15), pp.2298-2308. doi: 10.1002/joc.1810.

Matear, R.J., O'kane, T.J., Risbey, J.S. and Chamberlain, M., 2015. Sources of heterogeneous variability and trends in Antarctic sea-ice. *Nature communications,* 6, p.8656. doi: 10.1038/ncomms9656.

McPhaden, M.J., Busalacchi, A.J., Cheney, R., Donguy, J.R., Gage, K.S., Halpern, D., Ji, M., Julian, P., Meyers, G., Mitchum, G.T. and Niiler, P.P., 1998. The Tropical Ocean-Global Atmosphere observing system: A decade of progress. *Journal of Geophysical Research: Oceans*, 103(C7), pp.14169-14240. doi: 10.1029/97JC02906.

McPhaden, M.J., 1999. Genesis and evolution of the 1997-98 El Niño. *Science*, 283(5404), pp.950-954. doi: 10.1126/science.283.5404.950.

Meier, M.F., Dyurgerov, M.B., Rick, U.K., O'Neel, S., Pfeffer, W.T., Anderson, R.S., Anderson, S.P. and Glazovsky, A.F., 2007. Glaciers dominate eustatic sea-level rise in the 21st century. *Science*, 317(5841), pp.1064-1067. doi: 10.1126/science.1143906.

Meredith, M.P., Renfrew, I.A., Clarke, A., King, J.C. and Brandon, M.A., 2004. Impact of the 1997-98 ENSO on upper ocean characteristics in Marguerite Bay, western Antarctic Peninsula. *Journal of Geophysical Research: Oceans,* 109(C9). doi: 10.1029/2003JC001784.

Mo, K.C. and Higgins R.W. 1997. The Pacific–South American modes and tropical convection during the Southern Hemisphere winter. *Monthly Weather Review,* 126: 1581–1596. doi: 10.1175/1520-0493(1998)126<1581:TPSAMA>2.0.CO;2.

Monaghan, A.J., Bromwich, D.H., Fogt, R.L., Wang, S.H., Mayewski, P.A., Dixon, D.A., Ekaykin, A., Frezzotti, M., Goodwin, I., Isaksson, E. and Kaspari, S.D., 2006. Insignificant change in Antarctic snowfall since the International Geophysical Year. *Science*, 313(5788), pp.827-831. doi: 10.1126/science.1128243.

Morison, J., Wahr, J., Kwok, R. and Peralta-Ferriz, C., 2007. Recent trends in Arctic Ocean mass distribution revealed by GRACE. *Geophysical Research Letters*, 34(7). doi: 10.1029/2006GL029016.

NASA JPL, 2017. *Prolific Earth Gravity Satellites End Science Mission* [Press release]. 30 October 2017. Available at: <https://grace.jpl.nasa.gov/news/95/prolific-earth-gravity-satellites-end-science-mission> [Accessed on 01/01/2018].

Neelin, J.D., Battisti, D.S., Hirst, A.C., Jin, F.F., Wakata, Y., Yamagata, T. and Zebiak, S.E., 1998. ENSO theory. *Journal of Geophysical Research: Oceans*, 103(C7), pp.14261-14290. doi: 10.1029/97JC03424.

Nicholls, R.J. and Cazenave, A., 2010. Sea-level rise and its impact on coastal zones. *Science*, 328(5985), pp.1517-1520. doi: 10.1126/science.1185782.

Nicolas, J.P. and Bromwich, D.H., 2011. Precipitation changes in high southern latitudes from global reanalyses: A cautionary tale. *Surveys in geophysics*, *32* (4-5), pp.475-494. doi: 10.1007/s10712-011-9114-6.

NOAA., 2016. *Monthly Data for Niño 3.4 Index 1948-2016*. [Online]. Available at: <https://www.esrl.noaa.gov/psd/data/correlation/nina34.data> [Accessed on 23/12/2017].

Page, S.E., Siegert, F., Rieley, J.O., Boehm, H.D.V., Jaya, A. and Limin, S., 2002. The amount of carbon released from peat and forest fires in Indonesia during 1997. *Nature*, 420(6911), pp.61-65. doi: 10.1038/nature01131.

Palerme, C., Kay, J.E., Genthon, C., L'Ecuyer, T., Wood, N.B. and Claud, C., 2014. How much snow falls on the Antarctic ice sheet? *The Cryosphere,* 8(4), pp.1577-1587. doi: 10.5194/tc-8-1577-2014.

Park, Y.H., Roquet, F. and Vivier, F., 2004. Quasi-stationary ENSO wave signals versus the Antarctic Circumpolar Wave scenario. *Geophysical Research Letters*, 31(9). doi: 10.1029/2004GL019806.

Parkinson, C.L. and Cavalieri, D.J., 2012. Antarctic sea ice variability and trends, 1979-2010. *The Cryosphere*, 6(4), p.871. doi: 10.5194/tc-6-871-2012.

Paolo, F.S., Padman, L., Fricker, H.A., Adusumilli, S., Howard, S. and Siegfried, M.R., 2018. Response of Pacific-sector Antarctic ice shelves to the El Niño/Southern Oscillation. *Nature Geoscience*, p.1. doi: 10.1038/s41561-017-0033-0

Payne, A.J., Vieli, A., Shepherd, A.P., Wingham, D.J. and Rignot, E., 2004. Recent dramatic thinning of largest West Antarctic ice stream triggered by oceans. Geophysical Research Letters, 31(23). doi: 10.1029/2004GL021284.

Pearcy, W.G. and Schoener, A., 1987. Changes in the marine biota coincident with the 1982–1983 El Niño in the northeastern subarctic Pacific Ocean. *Journal of Geophysical Research: Oceans,* 92(C13), pp.14417-14428. doi: 10.1029/JC092iC13p14417.

Peterson, R.G. and White, W.B., 1998. Slow oceanic teleconnections linking the Antarctic Circumpolar Wave with the tropical El Niño-Southern Oscillation. *Journal of Geophysical Research: Oceans,* 103(C11), pp.24573-24583. doi: 10.1029/98JC01947.

Philander, S.G.H., 1983. El Niño southern oscillation phenomena. *Nature*, 302, pp. 295-301. doi: 10.1038/302295a0.

Philander, S.G.H. and Seigel, A.D., 1985. Simulation of El Niño of 1982–1983. *Elsevier oceanography series,* 40, pp.517-541. doi: 10.1016/S0422-9894(08)70729-3.

Philander, S.G. ed., 1989a. El Niño, La Niña, and the southern oscillation (Vol. 46). *Academic press*. doi: 10.1002/9781118015216.ch6.

Philander, G., 1989b. El Niño and La Niña. *American Scientist*, 77(5), pp.451-459. doi: 10.1175/1520-0469(1985)042<2652:ENALN>2.0.CO;2.

Pohl, B., Fauchereau, N., Reason, C.J.C. and Rouault, M., 2010. Relationships between the Antarctic Oscillation, the Madden–Julian Oscillation, and ENSO, and consequences for rainfall analysis. *Journal of Climate,* 23(2), pp.238-254. doi: 10.1175/2009JCLI2443.1.

Pope, J.O., Holland, P.R., Orr, A., Marshall, G.J. and Phillips, T., 2017. The impacts of El Niño on the observed sea ice budget of West Antarctica. *Geophysical Research Letters*. doi: 10.1002/2017GL073414.

Pritchard, H.D., Arthern, R.J., Vaughan, D.G. and Edwards, L.A., 2009. Extensive dynamic thinning on the margins of the Greenland and Antarctic ice sheets. *Nature*, *461*(7266), p.971. doi:10.1038/nature08471.

Pritchard, H.D., Ligtenberg, S.R.M., Fricker, H.A., Vaughan, D.G., Van den Broeke, M.R. and Padman, L., 2012. Antarctic ice-sheet loss driven by basal melting of ice shelves. Nature, 484(7395), pp.502-505. doi: 10.1038/nature10968.

Purich, A., England, M.H., Cai, W., Chikamoto, Y., Timmermann, A., Fyfe, J.C., Frankcombe, L., Meehl, G.A. and Arblaster, J.M., 2016. Tropical Pacific SST drivers of recent Antarctic sea ice trends. *Journal of Climate,* 29(24), pp.8931-8948. doi: 10.1175/JCLI-D-16-0440.1.

Quinn, W.H., 1974. Monitoring and predicting El Niño invasions. *Journal of Applied Meteorology*, 13(7), pp.825-830. doi: 10.1175/1520-0450(1974)013<0825:MAPENI>2.0.CO;2.

Rahmstorf, S., 2007. A semi-empirical approach to projective future sea-level rise. *Science*, 315 (5810), pp. 3058-3068. doi: 10.1126/science.1135456.

Rasmusson, E.M. and Carpenter, T.H., 1982. Variations in tropical sea surface temperature and surface wind fields associated with the Southern Oscillation/El Niño. *Monthly Weather Review*, *110*(5), pp.354-384. doi: 10.1175/1520-0493(1982)110<0354:VITSST>2.0.CO;2.

Rasmusson, E.M. and Wallace, J.M., 1983. Meteorological aspects of the El Niño/Southern Oscillation. *Science*, 222(1), pp.195-1202. doi: 10.1126/science.222.4629.1195.

Renwick, J.A., 1998. ENSO-related variability in the frequency of South Pacific blocking. *Monthly Weather Review,* 126(12), pp.3117-3123. doi: 10.1175/1520-0493(1998)126<3117:ERVITF>2.0.CO;2.

Renwick, J.A., 2002. Southern Hemisphere circulation and relations with sea ice and sea surface temperature. *Journal of Climate,* 15(21), pp.3058-3068. doi: 10.1175/1520-0442(2002)015<3058:SHCARW>2.0.CO;2.

Reynolds, R.W., Rayner, N.A., Smith, T.M., Stokes, D.C. and Wang, W., 2002. An improved in situ and satellite SST analysis for climate. *Journal of climate*, *15*(13), pp.1609-1625. doi: *10.1175/1520-0442(2002)015<1609:AIISAS>2.0.CO;2*.

Rignot, E., Vaughan, D.G., Schmeltz, M., Dupont, T. and MacAyeal, D., 2002. Acceleration of Pine island and Thwaites glaciers, west Antarctica. Annals of Glaciology, 34, pp.189-194. doi: 10.3189/172756402781817950.

Rignot, E., Casassa, G., Gogineni, P., Krabill, W., Rivera, A.U. and Thomas, R., 2004. Accelerated ice discharge from the Antarctic Peninsula following the collapse of Larsen B ice shelf. *Geophysical Research Letters,* 31(18). doi: 10.1029/2004GL020697.

Rignot, E., 2006. Changes in ice dynamics and mass balance of the Antarctic ice sheet. *Philosophical Transactions of the Royal Society of London A: Mathematical, Physical and Engineering Sciences*, *364*(1844), pp.1637-1655. doi: 10.1098/rsta.2006.1793.

Rignot, E. and Kanagaratnam, P., 2006. Changes in the velocity structure of the Greenland Ice Sheet. *Science*, 311(5763), pp.986-990. doi: 10.1126/science.1121381.

Rignot, E., Bamber, J.L., Van Den Broeke, M.R., Davis, C., Li, Y., Van De Berg, W.J. and Van Meijgaard, E., 2008. Recent Antarctic ice mass loss from radar interferometry and regional climate modelling. *Nature geoscience*, 1(2), pp.106-110. doi: 10.1038/ngeo102.

Rignot, E., Velicogna, I., van den Broeke, M.R., Monaghan, A. and Lenaerts, J.T., 2011. Acceleration of the contribution of the Greenland and Antarctic ice sheets to sea level rise. Geophysical Research Letters, 38(5). doi: 10.1029/2011GL046583.

Rignot, E., Jacobs, S., Mouginot, J. and Scheuchl, B., 2013. Ice-shelf melting around Antarctica. *Science*, 341(6143), pp.266-270. doi: 10.1126/science.1235798.

Rind, D., Chandler, M., Lerner, J., Martinson, D.G. and Yuan, X., 2001. Climate response to basin-specific changes in latitudinal temperature gradients and implications for sea ice variability. *Journal of Geophysical Research*, 106(20), pp.161-20. doi: 10.1029/2000JD900643.

Rott, H., Rack, W., Skvarca, P. and De Angelis, H., 2002. Northern Larsen ice shelf, Antarctica: further retreat after collapse. *Annals of Glaciology*, 34(1), pp.277-282. doi 10.3189/172756402781817716.

Santini, M., Taramelli, A. and Sorichetta, A., 2010. ASPHAA: A GIS-Based Algorithm to Calculate Cell Area on a Latitude-Longitude (Geographic) Regular Grid. *Transactions in GIS*, *14*(3), pp.351-377. doi: 10.1111/j.1467-9671.2010.01200.x.

Sasgen, I., Dobslaw, H., Martinec, Z. and Thomas, M., 2010. Satellite gravimetry observation of Antarctic snow accumulation related to ENSO. *Earth and Planetary Science Letters*, 299(3), pp.352-358. doi: 10.1016/j.epsl.2010.09.015.

Sasgen, I., Konrad, H., Ivins, E.R., Van den Broeke, M.R., Bamber, J.L., Martinec, Z. and Klemann, V., 2013. Antarctic ice-mass balance 2003 to 2012: regional reanalysis of GRACE satellite gravimetry measurements with improved estimate of glacial-isostatic adjustment based on GPS uplift rates. *The Cryosphere*, *7*, pp.1499-1512. doi: 10.5194/tc-7-1499-2013.

Schlegel, N.J., Wiese, D.N., Larour, E.Y., Watkins, M.M., Box, J.E. and van den Broeke, M.R., 2016. Application of GRACE to the assessment of model-based estimates of monthly Greenland Ice Sheet mass balance (2003-2012). *The Cryosphere,* 10(5), p.1965. doi: 10.5194/tc-10-1965-2016.

Schlosser, E., Manning, K.W., Powers, J.G., Duda, M.G., Birnbaum, G. and Fujita, K., 2010. Characteristics of high-precipitation events in Dronning Maud Land, Antarctica. *Journal of Geophysical Research: Atmospheres*, *115*(D14). doi: 10.1029/2009JD013410

Schmidt, R., Schwintzer, P., Flechtner, F., Reigber, C., Güntner, A., Döll, P., Ramillien, G., Cazenave, A., Petrovic, S., Jochmann, H. and Wünsch, J., 2006. GRACE observations of changes in continental water storage. *Global and Planetary Change*, 50(1), pp.112-126. doi: 10.1016/j.gloplacha.2004.11.018.

Shepherd, A. and Wingham, D., 2007. Recent sea-level contributions of the Antarctic and Greenland ice sheets. *Science*, 315(5818), pp.1529-1532. doi: 10.1126/science.1136776.

Shepherd, A., Ivins, E. R., Geruo, A., Barletta, V. R., Bentley, M. J., Bettadpur, S., Briggs, K. H., Bromwich, D. H., Forsberg, R., Galin, N., Horwath, M., Jacobs, S., Joughin, I., King, M. A., Lenaerts, J. T. M., Li, J. L., Ligtenberg, S. R. M., Luckman, A., Luthcke, S. B., McMillan, M., Meister, R., Milne, G., Mouginot, J., Muir, A., Nicolas, J. P., Paden, J., Payne, A. J., Pritchard, H., Rignot, E., Rott, H., Sorensen, L. S., Scambos, T. A., Scheuchl, B., Schrama, E. J. O., Smith, B., Sundal, A. V., van Angelen, J. H., van de Berg, W. J., van den Broeke, M. R., Vaughan, D. G., Velicogna, I., Wahr, J., Whitehouse, P. L., Wingham, D. J., Yi, D. H., Young, D., and Zwally, H. J., 2012. A reconciled estimate of ice-sheet mass balance. *Science*, *338*(6111), pp.1183-1189. doi: 10.1126/science.1228102.

Silva, T.A.M., Bigg, G.R. and Nicholls, K.W., 2006. Contribution of giant icebergs to the Southern Ocean freshwater flux. *Journal of Geophysical Research: Oceans,* 111(C3). doi: 10.1029/2004JC002843.

Simmonds, I. and Jacka, T.H., 1995. Relationships between the interannual variability of Antarctic sea ice and the Southern Oscillation. *Journal of Climate*, 8(3), pp.637-647. doi: 10.1175/1520-0442(1995)008<0637:RBTIVO>2.0.CO;2.

Smith, S.R. and Stearns, C.R., 1993. Antarctic pressure and temperature anomalies surrounding the minimum in the Southern Oscillation index. *Journal of Geophysical Research: Atmospheres,* 98(D7), pp.13071-13083. doi: 10.1029/92JD02157.

Stammerjohn, S.E., Martinson, D.G., Smith, R.C., Yuan, X. and Rind, D., 2008. Trends in Antarctic annual sea ice retreat and advance and their relation to El Niño–Southern Oscillation and Southern

Annular Mode variability. *Journal of Geophysical Research: Oceans*, *113*(C3). doi: 10.1029/2007JC004269.

Stenseth, N.C., Mysterud, A., Ottersen, G., Hurrell, J.W., Chan, K.S. and Lima, M., 2002. Ecological effects of climate fluctuations. *Science*, 297(5585), pp.1292-1296. doi: 10.1126/science.1071281.

Stenseth, N.C., Ottersen, G., Hurrell, J.W., Mysterud, A., Lima, M., Chan, K.S., Yoccoz, N.G. and Ådlandsvik, B., 2003. Studying climate effects on ecology through the use of climate indices: the North Atlantic Oscillation, El Niño Southern Oscillation and beyond. *Proceedings of the Royal Society of London B: Biological Sciences*, 270(1529), pp.2087-2096. doi: 10.1098/rspb.2003.2415.

Stuecker, M.F., Bitz, C.M. and Armour, K.C., 2017. Conditions leading to the unprecedented low Antarctic sea ice extent during the 2016 austral spring season. *Geophysical Research Letters*. doi: 10.1002/2017GL074691.

Swenson, S., Wahr, J. and Milly, P.C.D., 2003. Estimated accuracies of regional water storage variations inferred from the Gravity Recovery and Climate Experiment (GRACE). *Water Resources Research,* 39(8). doi: 10.1029/2002WR001808.

Tapley, B.D., Bettadpur, S., Ries, J.C., Thompson, P.F. and Watkins, M.M., 2004. GRACE measurements of mass variability in the Earth system. *Science*, 305(5683), pp.503-505. doi: 10.1126/science.1099192.

Tedesco, M. and Monaghan A. J., 2009. An updated Antarctic melt record through 2009 and its linkages to high-latitude and tropical climate variability, *Geophysical Research Letters*, 36, L18502. doi: 10.1029/2009GL039186.

Thomas, R.H., 1979. The dynamics of marine ice sheets. *Journal of Glaciology*, 24(90), pp.167-177. doi: 10.3189/S0022143000014726.

Thomas, R., Rignot, E., Casassa, G., Kanagaratnam, P., Acuña, C., Akins, T., Brecher, H., Frederick, E., Gogineni, P., Krabill, W. and Manizade, S., 2004. Accelerated sea-level rise from West Antarctica. *Science*, *306*(5694), pp.255-258. doi: 10.1126/science.1099650.

Thomas, I.D., King, M.A., Bentley, M.J., Whitehouse, P.L., Penna, N.T., Williams, S.D., Riva, R.E., Lavallee, D.A., Clarke, P.J., King, E.C. and Hindmarsh, R.C., 2011. Widespread low rates of

Antarctic glacial isostatic adjustment revealed by GPS observations. *Geophysical Research Letters,* 38(22). doi: 10.1029/2011GL049277.

Thompson, D.W. and Wallace, J.M., 2000. Annular modes in the extratropical circulation. Part I: month-to-month variability. *Journal of Climate*, *13*(5), pp.1000-1016. doi: 10.1175/1520-0442(2000)013<1000:AMITEC>2.0.CO;2.

Thompson, D.W. and Solomon, S., 2002. Interpretation of recent Southern Hemisphere climate change. *Science*, *296*(5569), pp.895-899. doi: 10.1126/science.1069270.

Timmermann, A., Oberhuber, J., Bacher, A., Esch, M., Latif, M. and Roeckner, E., 1999. Increased El Niño frequency in a climate model forced by future greenhouse warming. *Nature*, 398(6729), pp.694-697. doi: 10.1038/19505.

Tokinaga, H., Xie, S.P., Deser, C., Kosaka, Y. and Okumura, Y.M., 2012. Slowdown of the Walker circulation driven by tropical Indo-Pacific warming. Nature, 491(7424), pp.439-443. doi: 10.1038/nature11576

Trenberth, K.E., 1997. The definition of El Niño. *Bulletin of the American Meteorological Society* 78: 2771–2777. doi: 10.1175/1520-0477(1997)078<2771:TDOENO>2.0.CO;2.

Trenberth, K.E. and Stepaniak, D.P., 2001. Indices of el niño evolution. Journal of climate, 14(8), pp.1697-1701. doi: 10.1175/1520-0442(2001)014<1697:LIOENO>2.0.CO;2.

Trenberth, K.E. and Smith, L., 2006. The vertical structure of temperature in the tropics: Different flavors of El Nino. Journal of climate, 19(19), pp.4956-4973.

Turner, J., 2004. The El Niño–Southern Oscillation and Antarctica. *International Journal of Climatology*, *24*(1), pp.1-31. doi: 10.1002/joc.965.

Turner, J., Comiso, J.C., Marshall, G.J., Lachlan-Cope, T.A., Bracegirdle, T., Maksym, T., Meredith, M.P., Wang, Z. and Orr, A., 2009. Non-annular atmospheric circulation change induced by stratospheric ozone depletion and its role in the recent increase of Antarctic sea ice extent. *Geophysical Research Letters,* 36(8). doi: 10.1029/2009GL037524.

Turner, J., Hosking, J.S., Bracegirdle, T.J., Marshall, G.J. and Phillips, T., 2015. Recent changes in Antarctic sea ice. *Phil. Trans. R. Soc. A*, 373(2045), p.20140163. doi: 10.1098/rsta.2014.0163.

Tziperman, E., Stone, L., Cane, M.A. and Jarosh, H., 1994. El Niño chaos: Overlapping of resonances between the seasonal cycle and the Pacific Ocean-atmosphere oscillator. *Science*, 264(5155), pp.72-73. doi: 10.1126/science.264.5155.72.

Vargas, F.H., Lacy, R.C., Johnson, P.J., Steinfurth, A., Crawford, R.J., Boersma, P.D. and Macdonald, D.W., 2007. Modelling the effect of El Niño on the persistence of small populations: The Galápagos penguin as a case study. *Biological Conservation,* 137(1), pp.138-148. doi: 10.1016/j.biocon.2007.02.005.

Vaughan, D.G., 2006. Recent trends in melting conditions on the Antarctic Peninsula and their implications for ice-sheet mass balance and sea level. *Arctic, Antarctic, and Alpine Research*, *38*(1), pp.147-152. doi: 10.1657/1523-0430(2006)038[0147:RTIMCO]2.0.CO;2.

Vecchi, G.A. and Harrison, D.E., 2000. Tropical Pacific sea surface temperature anomalies, El Niño, and equatorial westerly wind events. *Journal of Climate*, 13(11), pp.1814-1830. doi: 10.1175/1520-0442(2000)013<1814:TPSSTA>2.0.CO;2.

Vecchi, G.A. and Wittenberg, A.T., 2010. El Niño and our future climate: where do we stand? *Wiley Interdisciplinary Reviews: Climate Change,* 1(2), pp.260-270. doi: 10.1002/wcc.33

Velicogna, I. and Wahr, J., 2006. Measurements of time-variable gravity show mass loss in Antarctica. *Science*, 311(5768), pp.1754-1756. doi: 10.1126/science.1123785.

Velicogna, I., 2009. Increasing rates of ice mass loss from the Greenland and Antarctic ice sheets revealed by GRACE. *Geophysical Research Letters*, 36(19). doi: 10.1029/2009GL040222.

Velicogna, I. and Wahr, J., 2013. Time-variable gravity observations of ice sheet mass balance: Precision and limitations of the GRACE satellite data. Geophysical Research Letters, 40(12), pp.3055-3063. doi: 10.1002/grl.50527.

Vimont, D.J., Wallace, J.M. and Battisti, D.S., 2003. The seasonal footprinting mechanism in the Pacific: implications for ENSO. *Journal of Climate*, 16(16), pp.2668-2675. doi: 10.1175/1520-0442(2003)016<2668:TSFMIT>2.0.CO;2

Wagnon, P., Ribstein, P., Francou, B. and Sicart, J.E., 2001. Anomalous heat and mass budget of Glaciar Zongo, Bolivia, during the 1997-98 El Niño year. *Journal of Glaciology*, 47(156), pp.21-28. doi: 10.3189/172756501781832593

Wahr, J.M., Jayne, S.R. and Bryan, F.O., 2002. A method of inferring changes in deep ocean currents from satellite measurements of time-variable gravity. *Journal of Geophysical Research*: Oceans, 107(C12). doi: 10.1029/2001JC001274.

Wakata, Y. and Sarachik, E.S., 1991. On the role of equatorial ocean modes in the ENSO cycle. *Journal of physical oceanography*, 21(3), pp.434-443. doi: 10.1175/1520-0485(1991)021<0434:OTROEO>2.0.CO;2.

Walker, G.T., 1924. Correlation in seasonal variations of weather, IX. A further study of world weather. *Memoirs of the India Meteorological Department*, 24, (9), pp. 275-333.

Walker, D.P., Brandon, M.A., Jenkins, A., Allen, J.T., Dowdeswell, J.A. and Evans, J., 2007. Oceanic heat transport onto the Amundsen Sea shelf through a submarine glacial trough. Geophysical Research Letters, 34(2). doi: 10.1029/2006GL028154.

Walker, C.C. and Gardner, A.S., 2017. Rapid drawdown of Antarctica's Wordie Ice Shelf glaciers in response to ENSO/Southern Annular Mode-driven warming in the Southern Ocean. *Earth and Planetary Science Letters*, *476*, pp.100-110. doi: 10.1016/j.epsl.2017.08.005.

Watkins, M.M., Wiese, D.N., Yuan, D.N., Boening, C. and Landerer, F.W., 2015. Improved methods for observing Earth's time variable mass distribution with GRACE using spherical cap Mascons. *Journal of Geophysical Research: Solid Earth*, *120*(4), pp.2648-2671. doi: 10.1002/2014JB011547.

Wang, C., 2002. Atmospheric circulation cells associated with the El Niño–Southern Oscillation. *Journal of Climate*, 15(4), pp.399-419. doi: 10.1175/1520-0442(2002)015<0399:ACCAWT>2.0.CO;2.

Wang, C. and Picaut, J., 2004. Understanding ENSO physics — a review. *Earth's Climate*, pp.21-48. doi: 10.1029/147GM02.

Weisberg, R.H. and Wang, C., 1997. A western Pacific oscillator paradigm for the El Niño-Southern Oscillation. *Geophysical research letters*, 24(7), pp.779-782. doi: 10.1029/97GL00689.

Welhouse, L.J., Lazzara, M.A., Keller, L.M., Tripoli, G.J. and Hitchman, M.H., 2016. Composite analysis of the effects of ENSO events on Antarctica. *Journal of Climate,* 29(5), pp.1797-1808. doi: 10.1175/JCLI-D-15-0108.1.

van der Werf, G.R., Randerson, J.T., Collatz, G.J., Giglio, L., Kasibhatla, P.S., Arellano, A.F., Olsen, S.C. and Kasischke, E.S., 2004. Continental-scale partitioning of fire emissions during the 1997 to 2001 El Niño /La Niña period. *Science*, 303(5654), pp.73-76. doi: 10.1126/science.1090753.

White, W.B. and Peterson, R.G., 1996. An Antarctic circumpolar wave in surface pressure, wind, temperature and sea-ice extent. *Nature*, 380(6576), pp.699 -702. doi: 10.1038/380699a0.

Whitehouse, P.L., Bentley, M.J., Milne, G.A., King, M.A. and Thomas, I.D., 2012. A new glacial isostatic adjustment model for Antarctica: calibrated and tested using observations of relative sea-level change and present-day uplift rates. *Geophysical Journal International*, 190(3), pp.1464-1482. doi: 10.1111/j.1365-246X.2012.05557.x.

Wiese, D.N., Landerer, F.W. and Watkins, M.M., 2016a. Quantifying and reducing leakage errors in the JPL RL05M GRACE mascon solution. *Water Resources Research*, 52(9), pp.7490-7502. doi: 10.1002/2016WR019344.

Wiese, D.N., Larour, E.Y., Watkins, M.M., Box, J.E. and van den Broeke, M.R., 2016b. Application of GRACE to the assessment of model-based estimates of monthly Greenland Ice Sheet mass balance (2003-2012). *The Cryosphere,* 10(5), p.1965. doi: 10.5194/tc-10-1965-2016.

Wouters, B. and Schrama, E.J.O., 2007. Improved accuracy of GRACE gravity solutions through empirical orthogonal function filtering of spherical harmonics. *Geophysical Research Letters*, 34(23). doi: 10.1029/2007GL032098.

Wyrtki, K., 1975. El Niño—the dynamic response of the equatorial Pacific Ocean to atmospheric forcing. *Journal of Physical Oceanography,* 5(4), pp.572-584. doi: 10.1175/1520-0485(1975)005<0572:ENTDRO>2.0.CO;2.

Wyrtki, K., 1985. Water displacements in the Pacific and the genesis of El Niño cycles. *Journal of Geophysical Research: Oceans,* 90(C4), pp.7129-7132. doi: 10.1029/JC090iC04p07129.

Yeo, S.R. and Kim, K.Y., 2015. Decadal changes in the Southern Hemisphere Sea Surface Temperature in association with El Niño–Southern Oscillation and Southern Annular Mode. *Climate Dynamics*, *45*(11-12), pp.3227-3242. doi: 10.1007/s00382-015-2535-z.

Yi, S. and Sun, W., 2014. Evaluation of glacier changes in high-mountain Asia based on 10 year GRACE RL05 models. *Journal of Geophysical Research: Solid Earth*, 119(3), pp.2504-2517. doi: 10.1002/2013JB010860.

Yu, L. and Rienecker, M.M., 1998. Evidence of an extratropical atmospheric influence during the onset of the 1997–98 El Niño. *Geophysical Research Letters,* 25(18), pp.3537-3540. doi: 10.1029/98GL02628.

Yuan, X. and Martinson, D.G., 2000. Antarctic sea ice extent variability and its global connectivity. *Journal of Climate,* 13(10), pp.1697-1717. doi: 10.1175/1520-0442(2000)013<1697:ASIEVA>2.0.CO;2.

Yuan, X.I. and Martinson, D.G., 2001. The Antarctic dipole and its predictability. *Geophysical Research Letters,* 28(18), pp.3609-3612. doi: 10.1029/2001GL012969.

Yuan, X.I., 2004. ENSO-related impacts on Antarctic sea ice: a synthesis of phenomenon and mechanisms. *Antarctic Science*, 16(04), pp.415-425. doi: 10.1017/S0954102004002238.

Yuan, X.I. and Li, C., 2008. Climate modes in southern high latitudes and their impacts on Antarctic sea ice. *Journal of Geophysical Research: Oceans,* 113(C6). doi: 10.1029/2006JC004067.

Zebiak, S.E. and Cane, M.A., 1987. A Model El Niño–Southern Oscillation. *Monthly Weather Review,* 115(10), pp.2262-2278. doi: 10.1175/1520-0493(1987)115<2262:AMENO>2.0.CO;2.

Zebiak, S.E., 1989. Oceanic heat content variability and El Niño cycles. *Journal of Physical Oceanography,* 19(4), pp.475-486. doi: 10.1175/1520-0485(1989)019<0475:OHCVAE>2.0.CO;2.

Zhai, P., Yu, R., Guo, Y., Li, Q., Ren, X., Wang, Y., Xu, W., Liu, Y. and Ding, Y., 2016. The strong El Niño of 2015-16 and its dominant impacts on global and China's climate. *Journal of Meteorological Research,* 30(3), pp.283-297. doi: 10.1007/s13351-016-6101-3.

Zwally, H.J., Comiso, J.C., Parkinson, C.L., Campbell, W.J. and Carsey, F.D., 1983. *Antarctic sea ice, 1973-1976: Satellite passive-microwave observations* (No. NASA-SP-459). NATIONAL AERONAUTICS AND SPACE ADMINISTRATION: WASHINGTON DC.

Zwally, H.J., Giovinetto, M.B., Li, J., Cornejo, H.G., Beckley, M.A., Brenner, A.C., Saba, J.L. and Yi, D., 2005. Mass changes of the Greenland and Antarctic ice sheets and shelves and contributions to sea-level rise: 1992–2002. *Journal of Glaciology*, *51*(175), pp.509-527. doi: 10.3189/172756505781829007.

Zwally, H.J. and Giovinetto, M.B., 2011. Overview and assessment of Antarctic ice-sheet mass balance estimates: 1992–2009. *Surveys in Geophysics,* 32(4-5), pp.351-376. doi: 10.1007/s10712-011-9123-5.

Zwally, H. Jay, Mario B. Giovinetto, Matthew A. Beckley, and Jack L. Saba, 2012. *Antarctic and Greenland Drainage Systems, GSFC Cryospheric Sciences Laboratory*. Available at: https://icesat4.gsfc.nasa.gov/cryo_data/ant_grn_drainage_systems.php.

Supplementary Material

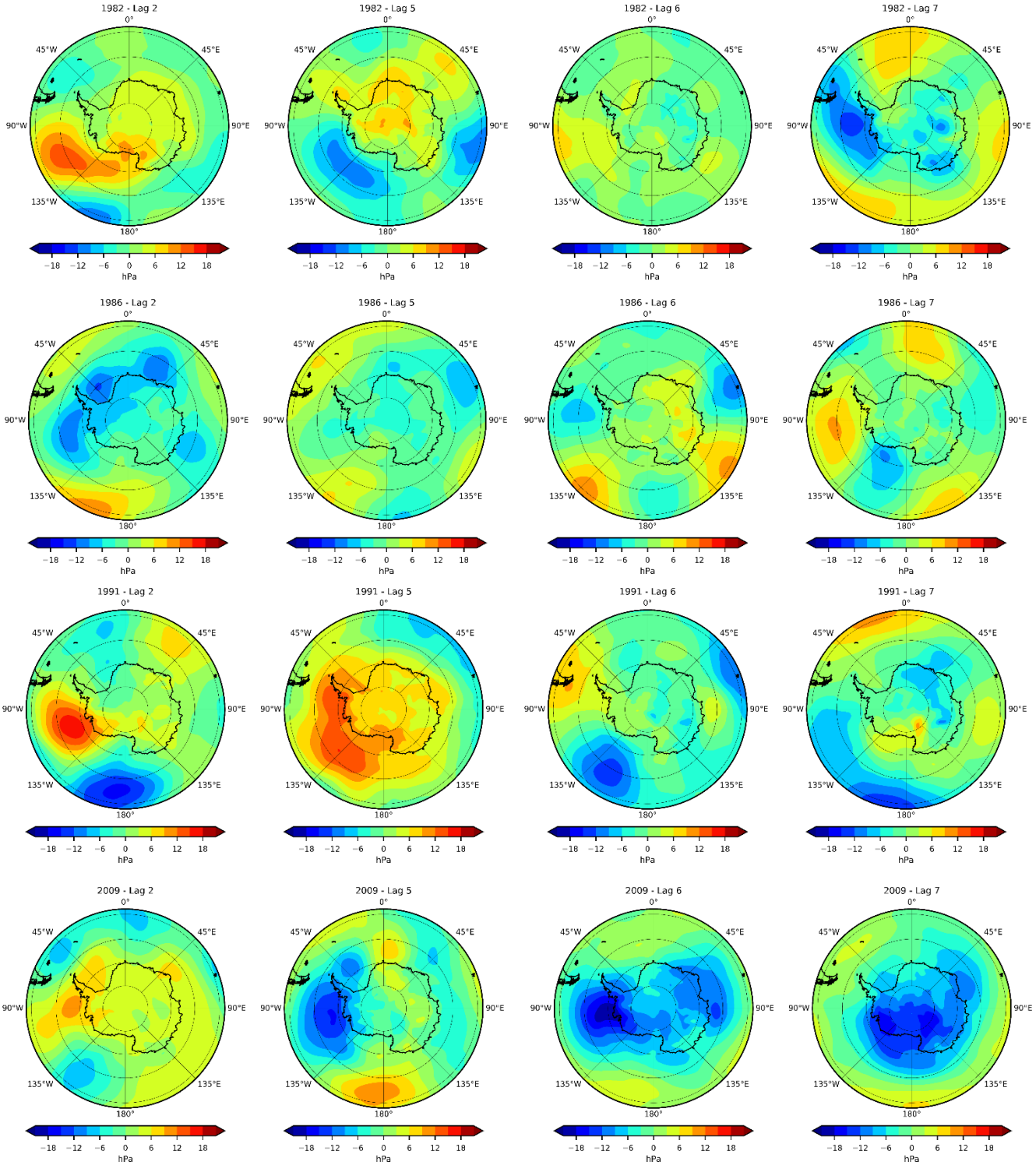

Supplementary Figure 1. Mean Sea Level Pressure anomalies following the 1982, 1986, 1991 and 2009 El Niño events for the selected lags.

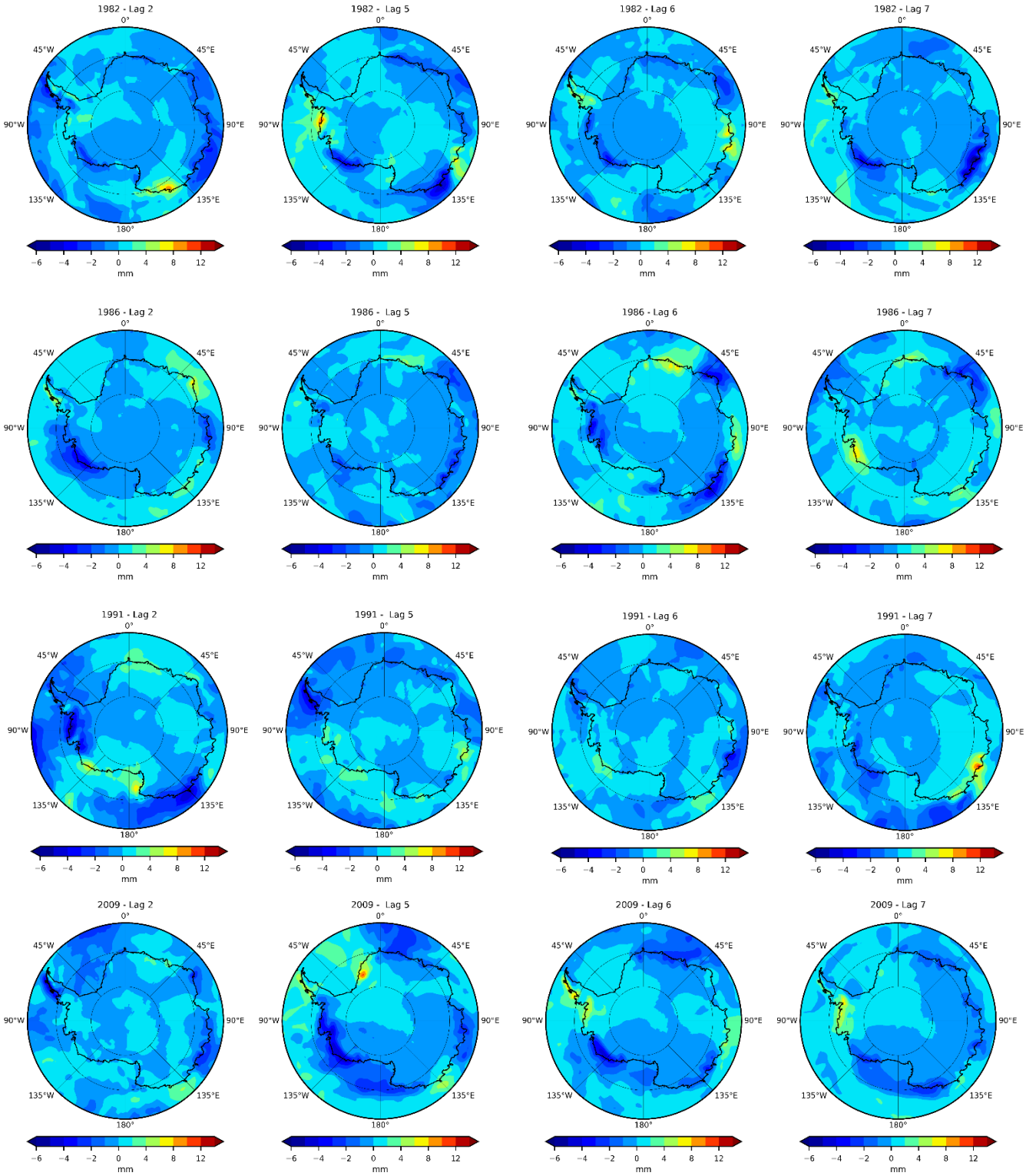

Supplementary Figure 2. Total Precipitation anomalies following the 1982, 1986, 1991 and 2009 El Niño events for the selected lags.

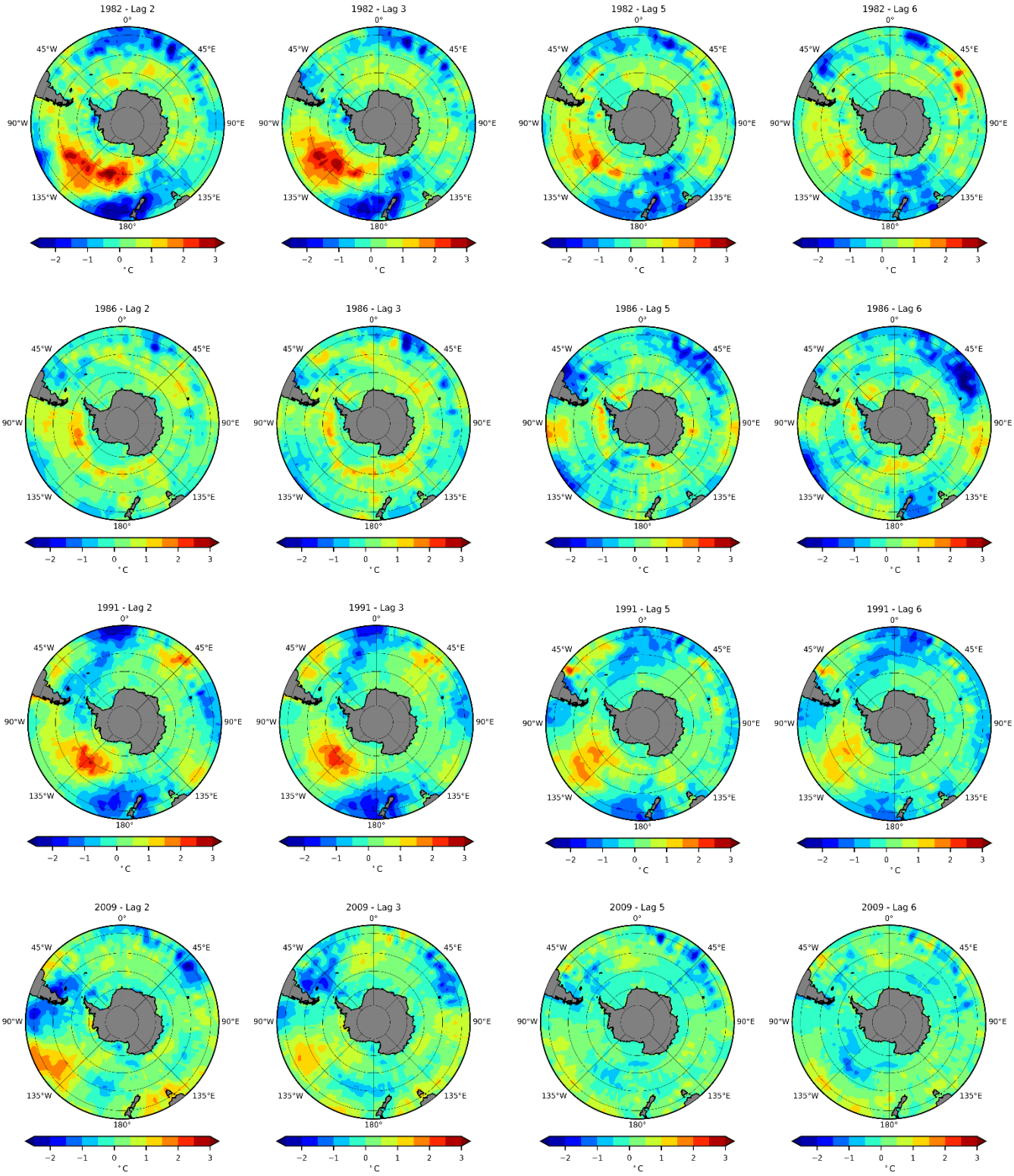

Supplementary Figure 3. Sea Surface Temperature anomalies following the 1982, 1986, 1991 and 2009 El Niño events for the selected lags.

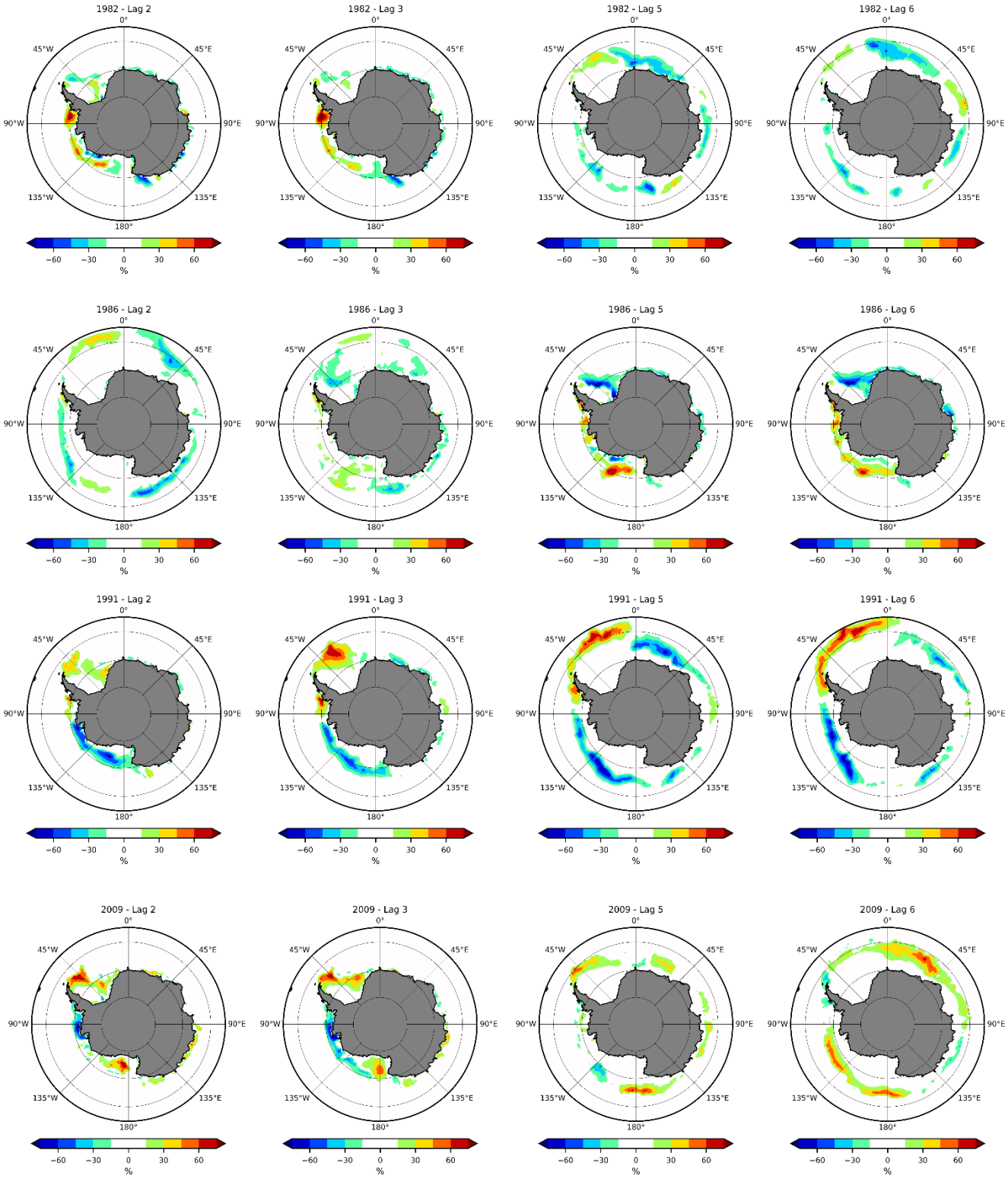

Supplementary Figure 4. Sea Ice Extent anomalies following the 1982, 1986, 1991 and 2009 El Niño events for the selected lags.

GRACE Months Table (2002-2017)						
Missing Month	Missing Month	Missing Month	2002-04-16	2002-05-10	Missing Month	Missing Month
2002-08-16	2002-09-16	2002-10-16	2002-11-16	2002-12-16	2003-01-16	2003-02-15
2003-03-16	2003-04-16	2003-05-11	Missing Month	2003-07-16	2003-08-16	2003-09-16
2003-10-16	2003-11-16	2003-12-16	2004-01-07	2004-02-17	2004-03-16	2004-04-16
2004-05-16	2004-06-16	2004-07-16	2004-08-16	2004-09-16	2004-10-16	2004-11-16
2004-12-16	2005-01-16	2005-02-15	2005-03-16	2005-04-16	2005-05-16	2005-06-16
2005-07-16	2005-08-16	2005-09-16	2005-10-16	2005-11-16	2005-12-16	2006-01-16
2006-02-15	2006-03-16	2006-04-16	2006-05-16	2006-06-16	2006-07-16	2006-08-16
2006-09-16	2006-10-16	2006-11-16	2006-12-16	2007-01-16	2007-02-15	2007-03-16
2007-04-16	2007-05-16	2007-06-16	2007-07-16	2007-08-16	2007-09-16	2007-10-16
2007-11-16	2007-12-16	2008-01-16	2008-02-15	2008-03-16	2008-04-16	2008-05-16
2008-06-16	2008-07-16	2008-08-16	2008-09-16	2008-10-16	2008-11-16	2008-12-16
2009-01-16	2009-02-15	2009-03-16	2009-04-16	2009-05-16	2009-06-16	2009-07-16
2009-08-16	2009-09-16	2009-10-16	2009-11-16	2009-12-16	2010-01-16	2010-02-15
2010-03-16	2010-04-16	2010-05-16	2010-06-16	2010-07-16	2010-08-16	2010-09-16
2010-10-16	2010-11-16	2010-12-16	Missing Month	2011-02-18	2011-03-16	2011-04-16
2011-05-16	Missing Month	2011-07-19	2011-08-16	2011-09-16	2011-10-16	2011-11-01
Missing Month	2012-01-02	2012-02-15	2012-03-16	2012-04-10	Missing Month	2012-06-16
2012-07-16	2012-08-16	2012-09-13	Missing Month	2012-11-20	2012-12-16	2013-01-16
2013-02-14	Missing Month	2013-04-21	2013-05-16	2013-06-16	2013-07-16	Missing Month
Missing Month	2013-10-16	2013-11-16	2013-12-16	2014-01-09	Missing Month	2014-03-17
2014-04-16	2014-05-16	2014-06-13	Missing Month	2014-08-16	2014-09-16	2014-10-16
2014-11-17	Missing Month	2015-01-22	2015-02-15	2015-03-16	2015-04-16	Missing Month
Missing Month	2015-07-15	2015-08-16	2015-09-14	Missing Month	Missing Month	2015-12-23
2016-01-16	2016-02-14	2016-03-16	Missing Month	2016-05-20	2016-06-16	2016-07-15
2016-08-21	Missing Month	Missing Month	2016-11-27	2016-12-24	2017-01-21	Missing Month
Missing Month	Missing Month	Missing Month	Missing Month	Missing Month	Missing Month	Missing Month
Missing Month	Missing Month	Missing Month				

Supplementary Table 1. Table showing GRACE data days and missing months due to battery management and other technical issues.

Monthly ENSO Absolute Anomaly values 1979-2017													
	January	February	March	April	May	June	July	August	September	October	November	December	Intensities
1979	-0.07	-0.13	0.19	0.24	0.07	0.00	-0.13	0.07	0.46	0.26	0.45	0.58	
1980	0.59	0.36	0.15	0.17	0.34	0.44	0.28	-0.04	-0.05	-0.09	0.04	0.21	
1981	-0.18	-0.45	-0.42	-0.27	-0.30	-0.19	-0.39	-0.34	-0.12	-0.13	-0.20	-0.04	
1982	0.28	-0.04	0.29	0.44	0.65	0.73	0.57	0.88	1.54	2.00	2.02	2.25	VERY STRONG (82-83)
1983	2.25	1.93	1.48	1.14	1.08	0.73	0.08	-0.01	-0.25	-0.76	-0.90	-0.73	
1984	-0.48	-0.02	-0.24	-0.38	-0.40	-0.53	-0.23	-0.11	-0.22	-0.48	-1.00	-1.14	WEAK (84-85)
1985	-0.87	-0.51	-0.58	-0.83	-0.70	-0.64	-0.39	-0.33	-0.50	-0.28	-0.17	-0.23	
1986	-0.43	-0.47	-0.20	-0.06	-0.17	-0.03	0.09	0.43	0.68	0.90	1.00	1.08	MODERATE (86-88)
1987	1.17	1.23	1.24	0.97	0.80	1.01	1.35	1.63	1.69	1.41	1.22	1.03	
1988	0.94	0.39	0.18	-0.15	-0.85	-1.32	-1.43	-1.04	-0.87	-1.64	-1.80	-1.71	STRONG (88-89)
1989	-1.73	-1.30	-1.02	-0.88	-0.61	-0.39	-0.33	-0.31	-0.18	-0.25	-0.33	0.00	
1990	0.12	0.28	0.15	0.21	0.24	0.12	0.33	0.34	0.35	0.42	0.24	0.44	
1991	0.56	0.45	0.23	0.45	0.48	0.67	0.90	0.93	0.67	1.04	1.32	1.68	STRONG (91-92)
1992	1.83	1.77	1.42	1.35	1.19	0.90	0.58	0.32	0.18	0.01	0.03	0.16	
1993	0.32	0.51	0.55	0.93	1.05	0.68	0.42	0.26	0.51	0.37	0.25	0.33	WEAK (93)
1994	0.30	0.26	0.27	0.47	0.54	0.48	0.45	0.66	0.46	0.79	1.22	1.34	MODERATE (94-95)
1995	1.12	0.85	0.58	0.49	0.19	0.17	0.02	-0.28	-0.57	-0.70	-0.85	-0.77	WEAK (95-96)
1996	-0.68	-0.65	-0.45	-0.16	-0.06	-0.06	-0.09	0.01	-0.19	-0.18	-0.23	-0.45	
1997	-0.40	-0.24	-0.18	0.33	0.72	1.21	1.57	1.92	2.16	2.41	2.45	2.35	VERY STRONG (97-98)
1998	2.36	2.04	1.46	1.03	0.82	-0.02	-0.61	-0.94	-0.94	-1.10	-1.08	-1.39	MODERATE (98-99)
1999	-1.42	-1.09	-0.70	-0.71	-0.75	-0.89	-0.82	-0.92	-0.80	-0.96	-1.30	-1.47	MODERATE (99-00)
2000	-1.54	-1.30	-0.87	-0.66	-0.58	-0.53	-0.44	-0.35	-0.34	-0.57	-0.63	-0.71	
2001	-0.58	-0.42	-0.26	-0.22	-0.05	0.06	0.20	0.11	0.03	0.04	-0.15	-0.31	
2002	0.00	0.12	0.18	0.29	0.55	0.90	0.91	1.04	1.18	1.35	1.49	1.41	MODERATE (02-03)
2003	0.88	0.81	0.57	0.15	-0.23	0.05	0.39	0.40	0.42	0.60	0.55	0.51	
2004	0.40	0.34	0.23	0.31	0.32	0.33	0.71	0.91	0.96	0.91	0.84	0.87	WEAK (04-05)
2005	0.83	0.60	0.67	0.55	0.60	0.37	0.05	0.24	0.22	0.15	-0.31	-0.59	
2006	-0.64	-0.41	-0.39	-0.01	0.15	0.25	0.24	0.52	0.77	0.88	1.14	1.21	WEAK (06-07)
2007	0.88	0.37	0.15	0.02	-0.10	-0.02	-0.18	-0.34	-0.67	-0.92	-1.06	-1.10	MODERATE (07-08)
2008	-1.33	-1.32	-0.94	-0.69	-0.55	-0.40	-0.14	0.02	-0.05	-0.12	-0.23	-0.62	

	January	February	March	April	May	June	July	August	September	October	November	December	Intensities
2009	-0.75	-0.55	-0.26	0.09	0.35	0.55	0.68	0.74	0.82	1.10	1.46	1.55	MODERATE (09-10)
2010	1.41	1.26	1.02	0.67	0.17	-0.32	-0.66	-0.98	-1.22	-1.19	-1.19	-1.22	MODERATE (10-11)
2011	-1.31	-0.90	-0.62	-0.39	-0.19	0.00	-0.08	-0.34	-0.60	-0.69	-0.79	-0.73	WEAK (11-12)
2012	-0.62	-0.44	-0.29	-0.27	-0.16	0.03	0.28	0.47	0.68	0.62	0.45	-0.15	
2013	-0.40	-0.34	-0.26	0.02	0.02	-0.12	-0.09	0.00	0.02	0.01	-0.03	-0.07	
2014	-0.43	-0.56	-0.32	0.04	0.21	0.09	0.10	0.12	0.35	0.59	0.86	0.80	VERY STRONG (14-16)
2015	0.66	0.51	0.56	0.90	1.02	1.10	1.32	1.69	1.94	2.20	2.49	2.44	
2016	2.39	2.15	1.63	1.27	0.78	0.21	-0.20	-0.39	-0.48	-0.62	-0.69	-0.52	
2017	-0.32	-0.11	0.26	0.61	0.73	0.37	0.22	NA	NA	NA	NA	NA	

Supplementary Table 2. ENSO warm (red) and cold (blue) anomalies per months since 1979. The right-hand side column shows the intensity and period of each ENSO event.